UNIVERSITÀ DEGLI STUDI DI MESSINA

DIPARTIMENTO DI SCIENZE CHIMICHE, BIOLOGICHE, FARMACEUTICHE ED AMBIENTALI

DOCTOR OF PHILOSOPHY IN CHEMICAL SCIENCES

INNOVATIVE INSTRUMENTAL APPROACHES COUPLING MULTIDIMENSIONAL GAS CHROMATOGRAPHY WITH SPECTROSCOPIC TECHNIQUES IN THE FIELD OF FLAVOURS AND FRAGRANCES

Ph.D. Thesis of:

Gemma De Grazia

Tutor:

Professor Paola Dugo

Coordinator:

Professor Concetta De Stefano

CICLO XXXV – a. a. 2021/2022 – SSD CHIM/10

“L’essentiel est invisible pour les yeux.”

Antoine de Saint-Exupéry

Acknowledgements

I am deeply grateful to Professor Luigi Mondello for imparting his vast knowledge in the field of Analytical Chemistry and providing me with the opportunity to learn.

I also extend my appreciation to Professor Paola Dugo for her support and guidance throughout my three-year PhD course.

Additionally, I would like to express my gratitude to CAPUA 1880 S.r.l. for their funding and collaboration opportunities.

My sincere thanks to Professor Danilo Sciarrone for his constant encouragement and teachings.

Lastly, I am forever indebted to my admirable parents, Antonino and Mariella, for their love and support, which has always been my source of strength throughout my journey.

Table of Contents

Abstract

The research work was mainly focused on the development of analytical approaches based on multidimensional gas chromatography for authenticity assessment, preparative purpose, and sensory evaluation of complex matrices containing molecules of flavour and fragrance interest. Part of the studies were focused on the evaluation of analytical methods applied to the authenticity assessment of valuable products by isotopic ratio measurements. For such a purpose, multidimensional gas chromatography (MDGC) coupled to a simultaneous quadrupole mass spectrometry (qMS) and an isotope ratio mass spectrometry (IRMS) were exploited for obtaining reliable $\delta^{13}C$ measurements, even in the case of complex matrices. Furthermore, scientific efforts were put into the development of multi-technique analytical approaches including both preparative gas chromatography and spectroscopy for the efficient isolation and structure elucidation of target molecules. Aiming to expand the knowledge in flavour and fragrance field, the investigation of less conventional matrices allowed to improve the mass spectral laboratory-constructed database; in detail, a contribution was provided through the definite structural elucidation by NMR experiments. In addition, evolved trapping technologies were exploited in order to maximise the recovery of pure analytes with different physicochemical properties. Finally, particular emphasis was dedicated to the study of odour-active compounds through the development of a panellist-friendly system. Specifically, combining the heart-cut MDGC and the use of mega bore columns with an olfactometric detection, extremely enhanced performances over conventional approaches were obtained. Thus, all the research activities have been focused on a modern purpose of flavour and fragrance analysis, aiming to characterise key fractions of complex matrices, as also to recognise interesting odour active molecules.

Chapter 1: Overview of Multidimensional Gas Chromatography and hyphenated techniques in the field of flavours and fragrances.

1.1 Brief introduction to Gas Chromatography.

Chromatography has been defined from the International Union of Pure and Applied Chemistry (IUPAC) as "A physical method of separation in which the components to be separated are distributed between two phases, one of which is stationary (stationary phase) while the other (the mobile phase) moves in a definite direction". The principle of chromatography is based on the distribution of the constituents to be separated between two immiscible phases; one of these is a stationary bed (stationary phase) with a large surface area, while the other is a mobile phase which percolates through that stationary bed in a definite direction [1]. The technique was first introduced in 1903 by the Russian botanist, Michael Tswett, who used a packed column containing finely dispersed calcium carbonate to separate extracts of leaf pigments, attaining a series of coloured bands by allowing a solvent to percolate through the column bed [2]. The process was then described as chromatography, from the Greek *chroma* (colour) and *graphein* (writing). Although many scientists made substantial contributions to the evolution of modern chromatography, one of the most significant ones was certainly made by A. J. P. Martin, who along with R. L. M. Synge, first introduced the concept of liquid-liquid chromatography (LLC) in 1941. Furthermore, they were awarded the Nobel Prize for the invention of partition chromatography in 1952 [3]. The novelty consisted of exploiting the higher diffusivity of solutes in gases, suitably used as mobile phase. The latter make the equilibrium steps involved in a chromatographic process faster and thus, the columns much more efficient. In 1952 A. T. James and A. J. P. Martin [4] described the gas-liquid chromatography (GLC) technique, commonly referred to as gas chromatography (GC), representing a milestone in the evolution of separation sciences. In its beginnings gas chromatographic techniques were usually performed on packed columns, which low permeability prohibitively required high pressures to significantly improve the resolution. The proposal of M. J. E. Golay, made in 1957, that packed columns could be replaced by a narrow open tube with a thin film of stationary phase on the inner wall (open-tubular column), has proved to be truly significant [5]. Open-tubular columns present enhanced permeability when compared to packed columns and its separation power may be increased using longer columns, permitting high resolution gas chromatography. The almost complete replacement of metal columns by those fabricated from glass during the 1970s, as the chemistry of the glass surface became better understood [6], contributed

particularly to the expansion of open tubular column gas chromatography over the past decades. Considerable progress was made, particularly, by refinement of techniques in the areas of column technology, derivatization of samples prior to GC analysis to increase volatility, and detection [7]. Typically, a gas chromatograph is equipped with three controlled thermal zones: the injector unit which ensures rapid volatilization of the introduced sample; the column oven where the separation process occurs, and the detector by which the individual sample components are measured in the vapor phase. The analytes are separated based on their relative vapor pressures and affinities for the stationary bed, and the detector, together with auxiliary electronic and recording devices, generates the chromatogram which is a signal *vs* time graphic. Ideally, the individual component chromatographic band could be very closely approximated by the Gaussian distribution curve. The area and height of the peak are function of the analyte amount, while the peak width depends on the band spreading into the column [8]. The complete resolution of the compounds of interest, in the minimum time, is always the primary objective in any chromatographic separation. To achieve this task the most suitable analytical column (dimension and stationary phase type) must be used, and adequate chromatographic parameters applied to limit peak broadening phenomena. A good knowledge of chromatographic theory is, indeed, of great support for the method optimization process, as well as for the development of innovative techniques.

1.1.1 Retention parameters.

As well-known, the retention of analytes in gas chromatographic capillary columns results from the differential distribution (partition) of the solutes between the stationary liquid and the mobile gas phases [1]. Solutes retention in the column, as also its resolution, is attained because of the solution and dissolution process of the solute molecules into and out of the stationary liquid phase. When considering the average gas linear velocity as constant throughout an analysis, the solutes should spend an identical period in the mobile phase to elute from the column. To this extent, only the differences in the time spent in the stationary phase are responsible for the solute's distinct retention time values. The time that any solute spends in the mobile phase, that is the unretained peak time (t_M) summed with the so-called adjusted retention time (t'_R), which corresponds to the time the solute spends distributed in the stationary phase, is equivalent to the retention time (t_R) [see *Eq. (1.1)*].

$$t'_R = t_R - t_M$$

Eq. (1.1)

The magnitude of retention depends on the partition coefficient, or distribution constant, (K_D) which is defined as the ratio of the equilibrium concentrations of solute in the stationary (C_S) and mobile phase (C_M) during partitioning in the column [refer to *Eq. (1.2)*].

$$K_D = C_S \ / C_M$$

Eq. (1.2)

Hence the greater is the K_D value for a sample component, the higher is its solubility and the longer its retention in the stationary phase.

The retention time in GC is also related to the phase ratio (β), expressed as the ratio of the phase volumes in the capillary column [see *Eq. (1.3)*].

$$\beta = V_S \ / V_M$$

Eq. (1.3)

V_S is the volume of the stationary phase, and V_M is the volume of the mobile phase in a chromatographic column.

In general, the affinity of a solute for the stationary phase depends on its vapor pressure and the activity coefficient of the solute in that phase. Differences between those two properties result in the column's ability to differentiate two solutes, eluting them with different retention times. Solute retention can also be expressed in terms of retention factor, k, which quantifies the ratio of the time spent in the stationary phase to that spent in the mobile phase, as presented in *Eq. (1.4)*.

$$k = t'_R \ / t_M$$

Eq. (1.4)

A further parameter is the relative retention (r), which expresses the degree of separation between two peaks, not necessarily in adjacent positions; one represents a standard (st) and the other the solute of interest. Relative retention can be expressed using standard solute retention factors or adjusted retention times. The latter are used in *Eq.* (1.5), where "i" refers to an

individual solute. The relative retention of solutes eluting after the standard will be greater than 1, while that of compounds eluting prior to the standard less than 1.

$$r = t'_{R_i}/t'_{R_{st}}$$

Eq. (1.5)

Additionally, a useful measure of relative peak position in the chromatogram is the selectivity factor α, also denominated as separation factor; the latter describes the relative retention of two peaks in a chromatogram, and it is calculated by the following equation:

$$\alpha = k_2/k_1 = (t_{R2} - t_M)/(t_{R1} - t_M)$$

Eq. (1.6)

where k_1 and k_2 are the retention factors, while t_{R1} and t_{R2} are the retention times of the two components. However, since it does not contain any information about peak widths, it is not adequate to describe peak separations [1].

1.1.2 Separation mechanisms and Resolution.

The separation of two peaks in a chromatogram is defined by their resolution, R_S, which is a quantitative measure of separation degree between two chromatographic Gaussian peaks, and it is defined as:

$$R_S = \frac{\Delta t}{\frac{1}{2} \times (w_{b1} + w_{b2})}$$

Eq. (1.7)

where w_{b1} and w_{b2} are the peak widths of the two compounds at the baseline. The degree of separation between two chromatographic peaks improves with an increase in R_S. Satisfactory resolution requires $R_S \geq 1$, and baseline resolution is obtained when $R_S \geq 1.5$ [9].

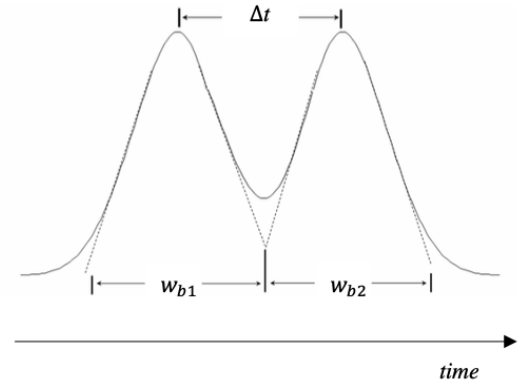

Figure 1.1.1. **Two chromatographic Gaussian peaks: w_{b1} and w_{b2} are the peak widths of the two compounds at the baseline.**

The length of a chromatographic column L is considered as divisible into imaginary volume units (plates) in which a complete equilibrium of the solute between the two phases is attained. Obviously, for a given value of t_R, narrower peaks provide greater numbers of theoretical plates than broader peaks. The length element of a chromatographic column occupied by a theoretical plate is the plate height (H)

$$H = L/N$$

Eq. (1.8)

An arbitrary, but the most widely used, criterion of the column efficiency is the number of theoretical plates (N). This can be achieved by using the Purnell equation, *Eq. (1.9)*:

$$N = 16 \times R_S^2 \left(\frac{\alpha}{\alpha - 1}\right)^2 \left(\frac{k+1}{k}\right)^2$$

Eq. (1.9)

The column efficiency N can be dependent on several variables. Most importantly, the plate height is shown to be a function of the linear gas velocity $\bar{u}$ according to the van Deemter equation:

$$H = A + \frac{B}{\bar{u}} + C\bar{u}$$

Eq. (1.10)

where, the constant A describes the chromatographic band dispersion caused by the gas-flow irregularities in the column. The B term represents the peak dispersion due to the diffusion processes occurring longitudinally inside the column, and the C term is due to a flow-dependent lack of the instantaneous equilibrium of solute molecules between the gas and the stationary phase. The mass transfer between the two phases occurs due to a radial diffusion of the solute molecules. *Eq. (1.10)* is represented graphically by a hyperbolic plot, the van Deemter curve, in Figure 1.2.

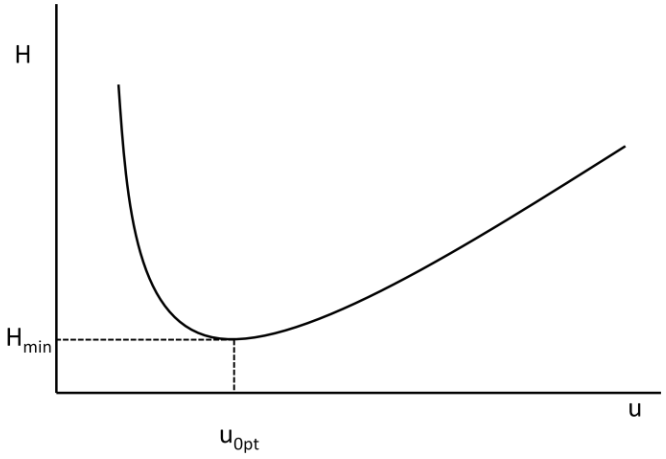

Figure 1.1.2. **Relationship of the plate height and linear gas velocity (van Deemter curve).**

The curve shows the existence of an optimum velocity at which a given column exhibits its highest number of theoretical plates. Shapes of the van Deemter curves are further dependent on several variables: solute diffusion rates in both phases, column dimensions and various geometrical constants, the phase ratio, and retention times. Highly effective GC separations often depend on thorough understanding and optimization of such variables [10].

Since open tubular or capillary columns were introduced in GC, the absence of any packing material inside the column modified the van Deemter equation because their rate equation does not have the A-term. This conclusion was pointed out by Golay [11], who also proposed a new term to deal with the diffusion process in the gas phase of open tubular columns. His equation had two C-terms, one for the mass transfer in the stationary phase, C_S (similar to van Deemter), and one for mass transfer in the mobile phase, C_M. Thus, the Golay equation is:

$$H = \frac{B}{\bar{u}} + (C_S + C_M) \times \bar{u}$$

Eq. (1.11)

The B-term of *Eq. (1.11)* accounts for the well-known molecular diffusion. The equation tells us that a small value for the diffusion coefficient is desirable so that diffusion is minimized, yielding a small value for B and for H. In general, a low diffusion coefficient can be achieved by using carrier gas with larger molecular weights like nitrogen or argon. In the Golay equation (*Eq. 1.11*), this term is divided by the linear velocity, so a large velocity or flow rate will also minimize the contribution of the B-term to the overall peak broadening. That is, a high velocity will decrease the time a solute spends in the column and thus decrease the time available for molecular diffusion. The C-terms in the Golay equation relate to mass transfer of the solute, either in the stationary phase or in the mobile phase [9]. The relative importance of the two C-terms in the rate equation depends primarily on the film thickness and the column radius. Considering the case of thin films (< 0.2 μm), the C-term results controlled by mass transfer in the mobile phase; on the contrary, for thick films (2-5 μm), it is controlled by mass transfer in the stationary phase. Additionally, the significance of the mass transfer in the mobile phase is considerably greater for wide bore columns than the narrow ones.

1.1.3 Retention Indices.

A peak's retention behavior on a specific column is characterized by the three parameters: retention time, retention factor and relative retention. The retention time is usually influenced by the applied linear velocity, temperature, phase ratio, and column length. As a consequence, retention time is not useful for the identification of peaks. Compared to retention time, retention factor presents an advantage due to the inclusion of the unretained peak time, contouring changes caused by linear velocity discrepancies and column length differences. On the other hand, relative retention depends also on the phase ratio, so that the results are comparable if an identical reference peak is chosen, and the same column temperature is applied. However, the accuracy of this information can be degraded for peaks eluting far from the reference peak.

To overcome this limit É. Kováts [12] introduced a retention index (I) system in which a homologous series of paraffins arranged in straight chains (normal paraffins) were applied as reference peaks. As well-known, this homologous series elutes, when isothermal GC conditions are applied, with retention times increasing exponentially. Under such conditions a semilogarithmic relationship exists between the adjusted retention times (t'_{Ri}) of the *n*-paraffins and their carbon numbers (c_n); a, and b are constants [see *Eq. (1.12)*].

$$logt'_{Ri} = a \times c_n \times b$$

Eq. (1.12)

This system was based on the fact that each analyte is referenced in terms of its position between the two *n*-paraffins that bracket its retention time. Furthermore, the index calculation is based on a linear interpolation of the carbon chain length of the two bracketing paraffins. In the original definition, the retention index of a particular substance was calculated using only *n*-paraffins with even carbon atoms as references; [as represented in *Eq. (1.13)*]:

$$I_x = 100_n + \frac{100(logt'_x - logt'_n)}{(logt'_{n+1} - logt'_n)}$$

Eq. (1.13)

where I_x is the isothermal retention index at temperature T, x is the compound of interest, n is the carbon number; n and n+1 are *n*-alkanes with n and n+1 carbon numbers, respectively. By definition, the retention index of the *n*-paraffins equals to 100 times their carbon number for any stationary phase and at any column temperature, e.g., *n*-C_6 has an index of 600.

The retention indices, as firstly proposed, are attained under isothermal elution conditions; on the contrary, by applying a column temperature program the series of *n*-paraffins elutes in a linear mode. To each successive peak, a constant increment is added to the retention time of its predecessor, instead of a non-linear increment, as could be observed under isothermal conditions. A similar relationship was observed between the programmed-temperature retention times ($t^T{}_R$) of the *n*-paraffins and their carbon numbers (c_n); a' and b' represent proportionality constants, can be expressed as in *Eq. (1.15)*.

$$logt^T{}_R = a' \times c_n \times b'$$

Eq. (1.14)

The programmed-temperature retention index calculation is based on the following equation proposed by H. van den Dool and D. J. Kratz [13], which does not use the logarithmic form.

$$I_x = 100_n + \frac{100(t'_x - t'_n)}{(t'_{n+1} - t'_n)}$$

Eq. (1.15)

As previously cited, when the latter equation is applied for the calculation of indices, these are commonly denominated as linear retention indices (*LRI*).

It must be pointed out that the retention indices calculated for isothermal and temperature-programmed conditions depend on the applied temperature rate and the initial temperature. Besides, since the reproducibility of temperature-programmed retention indices is dependent on working variables, such as carrier gas flow rate, stationary phase film thickness, and linear temperature programming rate, those parameters should be standardized. Basically, retention index systems are based on the incremental structure-retention relationship, so that any regular increment in a series of chemical structures should provide a regular increment in corresponding retention times. This means that the retention index concept is not restricted to the use of *n*-alkanes as standards. In practice any homologous series presenting a linear relationship between the logarithm of the adjusted retention time and the carbon number may be used. In the characterization of volatiles, the most applied reference series is *n*-alkanes. However, commonly *n*-alkanes present fluctuant behavior on polar stationary phases. In consideration of the fact that retention index values are correlated to retention mechanisms, alternative standard series of intermediate polarity were introduced, such as 2-alkanones, alkyl ethers, alkyl halides, alkyl acetates, alkanoic acid methyl esters [1].

1.2 Multidimensional Gas Chromatography.

The development of GC was substantially fast, as demonstrated by the fact that, in around ten years from its introduction, this innovative separation method became one of the most employed analytical techniques for the separation of volatile compounds. Probably, the spread of advanced methods followed the demand of high-throughput separations, robustness, and reasonable analysis time.

The need for multidimensional separations arises from a general lack of resolving power in single column methods. A considerable mismatch occurs between the capabilities of even very long GC columns and the requirements for the analysis of complex mixtures, commonly met in petroleum, natural product, flavours and fragrances.

The peak capacity, n, of a single-column chromatographic system generating N theoretical plates is given by *Eq. (1.16)* for a retention window from time t_1 to t_2.

$$n = \frac{\sqrt{N}}{4\,R_S}\, ln\left(\frac{t_2}{t_1}\right) + 1$$

Eq. (1.16)

The limitations of one-dimensional chromatography are clear when considering real mixtures; for example, to resolve over 80 % of 100 components would be necessary a column generating 2.4 million plates, approximately 500 m long for a conventional internal diameter of 250 μm [14]. A considerable increase in peak capacity is achieved if the mixture to be analyzed is subjected to two independent displacement processes with axes z and y orientated at right angles, and along which the peak capacities are, respectively, n_z and n_y. For the orthogonality criterion to be satisfied, the coupled separations must be based on different separation mechanisms; the maximum peak capacity is then $n_z \times n_y$, with a considerable improvement in resolving power [15]. Thus, a peak capacity of 200 in the first-dimension and one of 50 in the second, as is quite possible in comprehensive two-dimensional (2D) GC, yields a total peak capacity of 10^4. The latter, considering one dimensional GC, would correspond to a plate number of approximately 4×10^8 plates in a 250 m i.d. column of 80 km in length [14]. Nevertheless, the peak capacity of 10^4 of the two-dimensional system would permit resolution of 98 of the 100 components in the mixture discussed above.

Basically, multidimensional separation techniques are a result of combining two or more independent or nearly independent separative steps. The coupling of chromatographic dimensions is clearly attractive for the analysis of complex mixtures, and numerous combinations have been proposed and developed.

Nowadays, both heart-cut (GC-GC) and comprehensive (GC×GC) approaches can be considered as valuable techniques for high-end applications dealing with challenging samples. Basically, MDGC systems are equipped with two (or more) capillary GC columns coupled in series via a "transfer device". In classical two-dimensional GC, the second-dimension (2D) column has similar dimensions (length, i.d, peak capacity) as the first-dimension (1D) column but differs in stationary phase (or phase ratio). This is different from GC×GC, whereby the entire sample is transferred to the second-dimension in very small fractions, typically using transfer windows smaller than the 1D peak width. The second-dimension column is very short and has a limited peak capacity, because the second-dimension separation needs to be completed in the time frame of the transfer window (modulation time).

Regarding potential peak capacity, it is clear that heart-cut 2D-GC where the theoretical peak capacity of the 2D-GC separation equals the sum of the peak capacities of both dimensions, is largely overpowered by comprehensive 2D-GC whereby the peak capacity equals the multiplication of the peak capacities of both dimensions. Although the peak capacity of the short column operated at very high speed in the second-dimension is limited, comprehensive 2D-GC has the potential to provide an order of magnitude higher peak capacity than 1D-GC or heart-cut 2D-GC. However, the comparison between GC-GC and GC×GC exclusively based on potential peak capacity is however not fair. Classical two-dimensional heart-cut GC offers some very interesting advantages for practical applications. In general, GC×GC is more often exploited for sample "fingerprinting", while GC-GC is extremely useful for target compound analysis, focusing on selected (trace) compounds in a complex matrix [16].

1.2.1 Heart-cut MDGC.

The transfer of one or more selected groups of compounds eluted from a gas chromatographic column into a second column is usually referred to as "Heart cutting" or "Cutting". More commonly, a fraction, based on chemical type, molecular weight, or volatility, is 'heart-cut' from the eluent of the primary column and introduced into a secondary column for carrying out a further separation [17].

Within the field of analytical chemistry, the generic term "two-dimensional gas chromatography" is often used to denote what will be called heart-cutting 2D GC. Basically, such an approach allows to separate target fractions of the primary column effluent, which are directed to the secondary column by an interface. The latter is normally in a bypass state where the primary column effluent is directed to an exhaust flow restrictor; while it is switched from the bypass state to an inject state immediately before an analyte elutes from the primary column. In the inject state, the primary effluent is directed to the head of the secondary column. As soon as the analyte has been loaded onto the secondary column, the interface is switched back to the bypass state. In this way, heartcutting removes the sample matrix components that would potentially recombine with the analytes in the secondary column (see Figure 1.2.1). Thus, the target analytes result fully isolated in the chromatogram acquired at the exit of the secondary column [18].

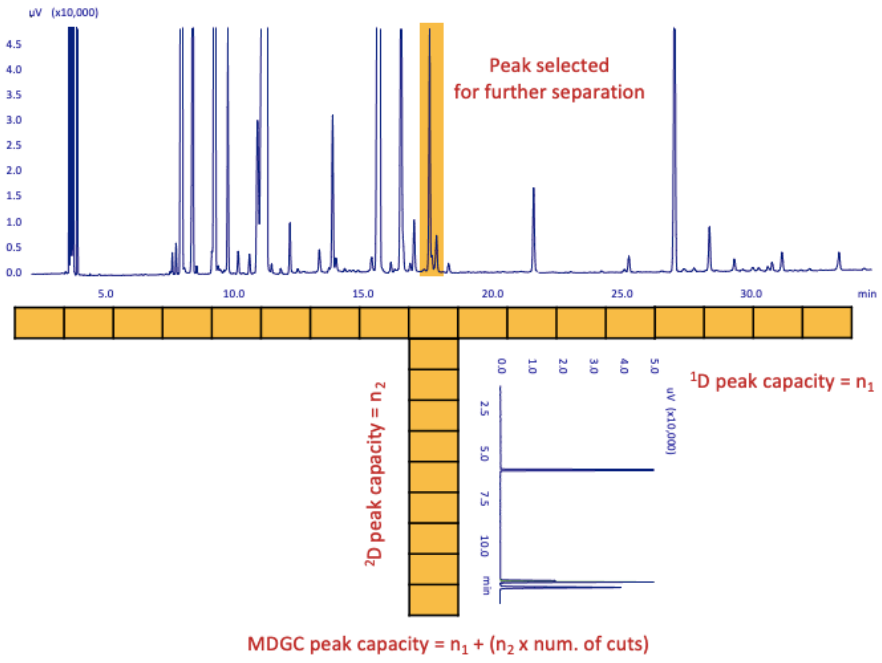

Figure 1.2.1. **Heart-cutting MDGC provides orthogonal two-column separation, with target fractions transfer from the first column (^{1}D) to the second column (^{2}D).**

There are numerous interfaces which can be used to execute heart-cuts. Up today the transfer systems developed can be classified in three groups: in-line valve, out-line valve and valveless systems. In the first group, a valve interfaces the two columns in a direct manner; out-line valves are employed to regulate the direction of gas flow towards the column interface, while valveless systems form a third minor MDGC group. When an MDGC instrument (in- or outline

valve) is in the stand-by mode, a one-dimensional analysis can be carried out; when the configuration is switched to the cutting mode, the primary-column effluent is directed towards the second column. The greater the number of transfers achieved, the higher the possibility of a mix-up of previously separated compounds. Although such an occurrence goes against a golden rule of multidimensional chromatography, namely that all compounds resolved in the first-dimension, must remain so in the second, the event is acceptable if all target analytes remain separated.

Multiport valves have been used extensively in the past, but many current methods employ a Deans switch. The Deans switch is a fluidic device [17] which uses an auxiliary flow to control the direction of the primary column effluent. A Deans switch is constructed from a two-way, three-port solenoid valve and an assembly of tee junctions. A schematic of a simple Deans switch is shown in Figure 1.2.2.

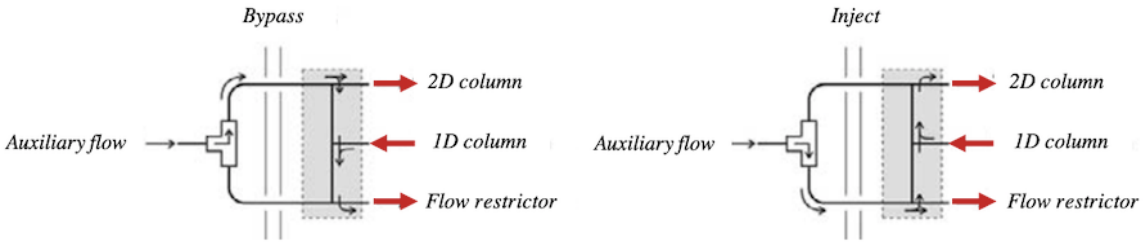

Figure 1.2.2. **Scheme of a Deans switch device.**

The exit of the primary column is connected to the central tee junction, while the secondary column and an exhaust flow restrictor are connected to the peripheral tee junctions. The auxiliary flow passes through the solenoid valve and then to one of the two peripheral tee junctions. The bypass state is generated by having the solenoid valve introduce the auxiliary flow to the tee junction connected to the secondary column (see the left part of Figure 1.2.2). The vast majority of the auxiliary flow goes to the secondary column while a smaller portion moves toward the center tee junction where it directs the incoming primary column effluent to the exhaust flow restrictor. The inject state is generated by having the solenoid valve introduce the auxiliary flow to the tee junction connected to the exhaust restrictor (see the right part of Figure 1.2.2). A small portion of the auxiliary flow goes to the center tee junction where it directs the primary column effluent to the secondary column. Deans switches show several advantages over multiport valves. The only moving part of the Deans switch, the solenoid valve, is not in the sample path; thus, it can be placed outside of the oven. The portion of the

device which contacts the sample, the tee junction assembly, is a static device that can be assembled from inert materials that can operate over a broad range of temperatures. Tee junction assemblies can be constructed by combining three individual tee unions, but now several manufacturers make assemblies which integrate all the necessary flow paths and connections into a single device [19]. This reduces dead volume within the device and decreases the likelihood of leaks. Transitioning a Deans switch between the bypass and inject state does not significantly disturb the flow in the primary or secondary columns. Thus, heart-cuts can be performed without affecting the primary retention times of later eluting analytes. This allows multiple heart-cuts to be made with high precision. In contrast, multiport valves require mechanical activation and cause brief but significant disturbances to the primary and secondary flows.

The current generation of heartcutting 2D GC instruments can make numerous, precisely timed heart-cuts. It is important to note that if multiple heart-cuts are performed, care must be taken to ensure that the peaks from the adjacent fractions do not remix on the secondary column. This can be prevented by keeping the range of secondary retention times within each fraction less than the time between heart-cuts. This measure ensures that a slow-moving component from a prior heart-cut does not recombine with a fast-moving component from a subsequent heart-cut. Thus, multiple heartcutting 2D GC requires that additional attention be paid to the chromatographic conditions including the column dimensions, carrier gas flow rates, and the column temperatures. Fortunately, GC instrumentation is constantly improving and new technologies are giving analysts unprecedented control.

An ultimate generation of multidimensional systems became available after the introduction of a series of capillary column coupling devices by Agilent Technologies [20]. The Agilent Technologies Deans switch CFT (capillary flow technology) consists of a three-way valve (external) controlled by the GC mainboard (and software), and a CFT device fixed inside the oven. In addition, the three-way valve is connected to an auxiliary pressure control (AUX EPC) or pneumatic control module (PCM), controlling midpoint pressure and/or makeup flow. The first-dimension column is connected to the middle port of the CFT device. The second-dimension column and a restrictor capillary to the monitor detector are connected to the other ports. The dimensions of the restrictor capillary are determined based on column flows in both columns, and this restrictor capillary should give a flow resistance similar to the flow resistance of the second-dimension column. This results in a constant 1D flow during the heart-cutting mode compared to the standby mode. The 2D-GC system is typically operated in constant flow mode, whereby the flow in the second column is about 1 mL min^{-1} higher than in the first-

dimension column. Switching events (ON/OFF external valve) are controlled by the software. An additional calculation software is available for correct setup of the parameters and selection of restrictor dimensions.

A further effective Deans-switch MDGC system has been developed and introduced by Shimadzu Corporation [21]. The first- and second-dimension capillaries are linked by using a low dead-volume, thermally stable and chemically inert stainless-steel interface. The latter is housed in the first oven, and it is characterized by very small dimensions (ca. 3 cm long), is connected to an auxiliary pressure source (2 ports) and to a stand-by detector (DET). Furthermore, a fused-silica restrictor (R_3) is fixed inside and crosses the interface. Figure 1.2.3 reports two schemes of the entire Shimadzu transfer system in the stand-by (Figure 1.2.3.a) and cut positions (Figure 1.2.3.b).

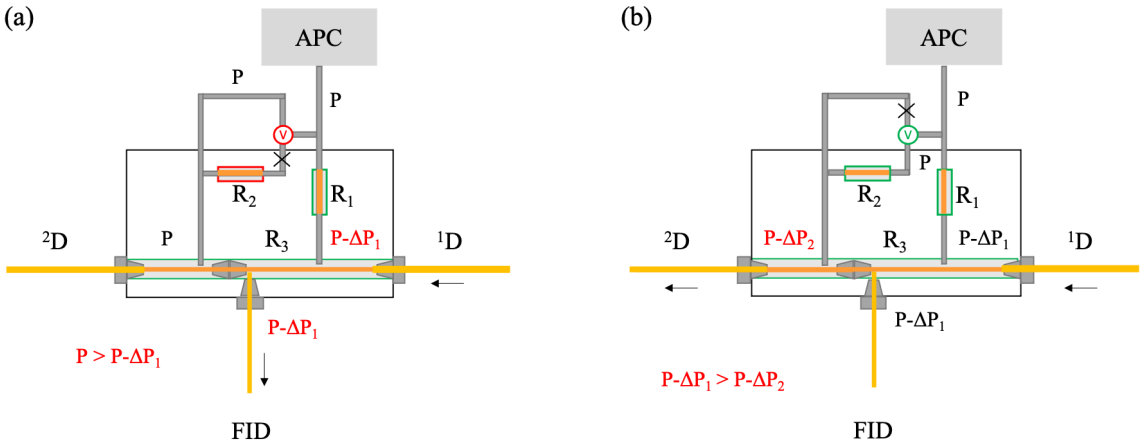

***Figure 1.2.3*. Scheme of the Shimadzu Deans switch in the stand-by (a) and cut (b) configurations.**

Though the five-port metallic interface is located in the first GC, defined as ^{1}D (Figure 1.2.2.a), it is obvious that a web of external connections is necessary to create the required MDGC conditions. In both operational modes, an advanced pressure control unit (APC) supplies a gas flow at constant pressure (P) to an external (with respect to the GC oven) fused-silica restrictor (R_1) and to a two-way solenoid valve (V). The latter is connected to two metal branches, one with another fused-silica restrictor (R_2) and one without: R_1 produces a pressure drop, slightly higher than that generated by R_2. In the stand-by mode (Figure 1.2.3.a), the APC pressure is reduced on the side of the first-dimension, while it reaches the second-dimension branch, passing through the solenoid valve, unaltered. It is clear that through such a configuration, analytes eluting from the first (apolar) column are directed to DET. Once the solenoid valve is activated, the transfer device passes to the cutting mode (Figure 1.2.3.b): the pressure on the

first-dimension side of the interface remains unaltered, while the pressure on the second-dimension side becomes lower ($P\text{-}\Delta P_1 > P\text{-}\Delta P_2$). It is clear that, under such conditions, the primary-column eluate is free to reach the second (polar) capillary. The instrument is automatically controlled by using a dedicated software that also enables the calculation of fundamental GC parameters, such as gas flows, linear velocities, and analyte recovery.
Using state-of-the-art commercially available multidimensional systems based on a Deans switch, method setup is relatively straightforward. Firstly, although capillary columns with various dimensions can be combined, the coupling of two (or more) columns with similar dimensions is easier and correct pressure balancing is faster. Mostly, the combination of two 30 m × 0.25 mm i.d. columns give a good compromise between analysis time, resolution, and solute capacity (loadability). Regarding stationary phase choice, all combinations are used, including chiral columns and ionic liquids. Obviously, the maximum operating temperature of the columns should be considered and therefore independent column heating offers higher flexibility. Most commercial systems also offer pressure/flow calculators that can be used to verify and set carrier gas flows on both dimensions and calculate optimum restrictor lengths and internal diameters between Deans switch devices and detectors. The possibility of using multiple cuts from a first-dimension separation depends on the complexity of the sample and the number and nature of solutes of interest. Normally the heart-cut windows are determined from the signal observed at the monitor detector after the first-dimension separation. Start and stop times are programmed in the GC control software. Alternatively, retention indices and n-alkane reference standards can be used to “lock” heart-cut windows.

During the past decades, many practical examples have illustrated the potential and advantages of classical 2D-GC [16]. These advantages can be summarised as follows:

- Increased resolution of critical sample fractions: increased separation of the solutes of interest is of course the first and most important goal for two-dimensional GC. Many samples contain “critical fractions”, while other fractions are of little or no interest. On the first-dimension column, the fractions (peaks) of interest are isolated from the bulk of the sample and transferred (with or without intermediate trapping) to a high resolution second-dimension column with different selectivity or phase ratio. Efficiency and selectivity of the second-dimension column can be fully exploited for detailed separation of the heart-cut fraction(s). Moreover, if the second-dimension

column temperature can be programmed independently from the first-dimension column, full flexibility is obtained to optimize the separation.

- Avoiding introduction of solvent or matrix onto the analytical column: since in most heart-cut applications, only the fraction(s) of interest is (are) transferred, the second-dimension column and the detector are not exposed to solvent, bulk compounds and/or high molecular weight, late eluting compounds that are of no interest. In such a respect, heart-cut GC-GC is often combined with backflush of the first-dimension column after the transfer of all fractions of interest is completed. Two-dimensional GC can therefore be considered as an excellent "clean-up" method, reducing the need for maintenance on an MS detector.
- Optimized detection: heart-cut 2D-GC also offers interesting possibilities for hyphenation with mass spectrometry and other spectroscopic detectors. In general, the isolation of single peaks by 2D-GC is the best option to obtain high-quality mass spectra for unknowns. Also, MDGC has proved to be extremely useful prior isotope ratio mass spectrometry detection [22].
- Hyphenation with preparative GC: multidimensional GC whereby a single compound can be fully separated from a complex matrix is also an excellent tool for hyphenation with fraction collection. Especially in fragrance analysis, it has been demonstrated that heart-cut GC techniques can efficiently be used for micro preparative sampling of fractions for subsequent nuclear magnetic resonance and other spectroscopic analysis [23, 24, 25, 26, 27, 28, 29].

1.3 Gas Chromatography-Mass Spectrometry.

Although chromatography represents an indispensable tool for the analysis of most samples, the employment of such technique must be inserted in a wider context in which the coupling of diverse analytical techniques or separation dimensions may be indispensable to provide a comprehensive characterization of a complex matrix. In this context, the hyphenation of chromatography to mass spectrometry (MS) represents the most convenient and widely used coupling, since this approach combines the high separation power of the first technique and the enormous potential in structural elucidation and components identification of the latter. In fact, MS deals with the study of analytes through the formation of gas-phase ions, with or without fragmentation, which are detected and characterized based on their mass-to-charge ratios (m/z) and their relative abundance. Hyphenated analytical techniques are based on the coupling of two or more different techniques, in which the first generally deals with the separation of the mixture, while the subsequent/s are designated for identification and/or quantitation of the analytes. The term hyphenated analytical techniques was introduced by Thomas Hirschfeld in 1980 [30], who highlighted the importance of the "hyphen" as a symbol of their common principle, that is the "marriage" of separated analytical techniques by means of proper interfaces. Such definition has been therefore used to refer to the online combination of a separation technique and one or more spectroscopic detection techniques. The need of coupling diverse analytical techniques not only derives from the simple interest in analyzing real-world samples, but also from the attempt to characterize "all possible compounds" present in a highly complex matrix.

Gas chromatography coupled with mass spectrometric detection (GC–MS) is one of the most widely utilized analytical techniques. The explosion of applications stems from the excellent qualitative information obtained the high sensitivity inherent with mass spectrometric detection. The great majority of GC–MS applications utilize capillary GC with quadrupole MS detection and electron ionization (EI). Nevertheless, there are substantial numbers of applications utilising different types of mass spectrometers and ionisation techniques coupled with multidimensional high-speed and pyrolysis–gas chromatographic methods [31].

The most common configuration for a GC-MS experiment is a single capillary GC column directly coupled to an EI quadrupole mass spectrometer. The growth of this type of system results from its relatively low cost, low maintenance, high sensitivity, high information content, and the ready availability of reliable commercial instruments. The potential of combined gas chromatography-mass spectrometry (GC-MS) for determining volatile compounds, contained

in very complex flavour and fragrance samples, is well-known. The subsequent introduction of powerful data acquisition and processing systems, including automated library search techniques, ensured that the information content of the large quantities of data generated by GC-MS instruments was fully exploited. These early successes were the foundation of an increasingly diverse range of applications, exploiting many different mass spectrometric techniques.

Basically, mass spectrometry (MS) may be defined as the study of systems causing the formation of gaseous ions, with or without fragmentation, which are then characterised by their mass to charge ratios (*m*/*z*) and relative abundances. The analyte may be ionised thermally, by electric field or by impacting energetic electrons, ions, or photons.

It is expected that a mass spectrometer can form, separate, and detect ions; to fulfill these requirements three fundamental units are required; an ion source, a mass analyzer and a detector [32]. The components of the mass spectrometer are contained in a housing usually kept at moderately high vacuum (10^{-3} to 10^{-6} torr) which ensures that once the ions formed in the ion source begin to move towards the detector, they will not collide with other molecules. The collision of ions would result in further fragmentation or deflection from their desired path. Furthermore, the vacuum also protects metal and oxide surfaces of the ion source, analyser, and detector from corrosion by air and water vapour, which could compromise the spectrometer's ability to form, separate and detect ions. Concisely, the sample must be introduced into the ionization source of the instrument; volatile compounds are most commonly ionized by electron ionization (EI) sources. In an electron impact source, a high energy beam of electrons is used to displace an electron from the organic molecule forming a radical cation ($M^{+}\bullet$), the molecular ion. This form of ionization normally imparts considerable energy to this first formed ion, so that it is almost immediately fragmented. The product ions formed may themselves fragment to produce a characteristic fragmentation pattern, creating a cascade of ion forming reactions before leaving the ion source [33]. The collection of ions is then focused into a beam and accelerated into the magnetic field and deflected along circular paths according to the masses of the ions. By adjusting the magnetic field, the ions can be focused on the detector. The individual ion current intensities at each mass are sequentially recorded, generating a mass spectrum. The latter is a histogram of the relative abundance of the ions generated by ionization of the sample and their subsequent separation, based on their *m/z*. The mass spectrum is a fingerprint of the molecule conveying information about its molecular

weight, and in case fragmentation occurs during ionization or collision induced dissociation, structurally useful fragment ions characteristic of the bond order of the structure [34].

An MS generates an enormous amount of data, especially when allied to separation techniques such as GC. The raw data is stored in the form of a three-dimensional array with time, *m/z*, and intensity as independent axes [1], while as aforementioned, the mass spectrum itself is a two-dimensional representation of signal intensity versus *m/z* [31]. The raw data is generated by repetitively scanning the mass analyzer over a particular mass range during the separation procedure and storing the intensity data for each scan separately. Alternatively, the mass analyzer is set to switch between a few selected ions, and only these ion intensities are stored during the chromatographic separation in selected ion monitoring [1,33].

In general mass spectrometers are classified based on their mass analyser; the quadrupole mass spectrometer (qMS) and the isotope ratio mass spectrometer (IRMS) will be briefly presented in the following sections.

1.3.1 Quadrupole Mass Spectrometry (qMS).

A type of mass analyzer commonly used in the flavour and fragrance research field is the quadrupole mass spectrometer (or quadrupole mass filter). This analyser, besides being more compact, inexpensive, and easy to operate, can transmit only the ion of choice by filtering sample ions according to their *m/z*.

The mass analyzer comprises four parallel hyperbolic or cylindrical metal rods arranged in a square array (see Figure 1.3.1); each pair of opposing rods is held at the same potential which is composed of a direct current (DC) and an alternating current (AC) component. If the applied voltage is composed of a DC voltage (U) on which an oscillating radio-frequency (RF) voltage, $Vcos(\omega t)$, is applied between one pair of rods, and the other, the field within the analyzer is created. A direct current voltage is then superimposed on the RF voltage (V) and the ions introduced into the quadrupole field undergo complex trajectories. Only ions of a certain *m/z* will be transmitted to the detector for a given ratio of voltages, while all other ions will oscillate with greater amplitudes, causing them to become unstable and neutralized through collision with one of the rods. This allows selection of a particular ion, or scanning by varying the voltages [33].

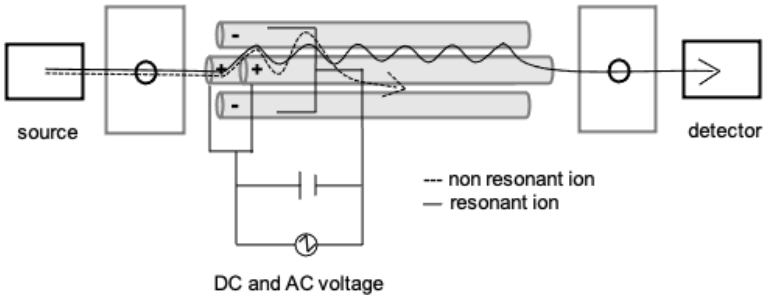

Figure 1.3.1. **Scheme of a quadrupole mass analyser.**

The mass range is scanned by varying the DC and RF fields whilst keeping the voltage ratio and oscillator frequency constant. This produces a low-resolution spectrum. In general, when the amplitude of *U* equals zero a wide band of *m/z* values will be transmitted, and as the value of *U*/*V* increases, resolution is enhanced so that at the stability limit only a single value of *m/z* corresponds to the trajectory, resulting in the transmission and collection of a single ion [35]. In this manner qMS acts as a mass filter and can be referred hereafter as a quadrupole mass filter. Standard quadrupole analyzers have rods of 15 to 25 cm length and 10 to 20 mm in diameter. The RF is in the order of 1 to 4 MHz, and the DC and RF voltages are in the range of 10^2 to 10^3 V; ions of about 10 eV kinetic energy undergo approximately 100 oscillations during their passage [32]. A mass spectrum may be generated by scanning values of *U* and *V* with a fixed *U*/*V* ratio and constant drive frequency, or by scanning the frequency and holding *U* and *V* constant [31]. The transmitted ions of certain *m/z* are then linearly dependent on the voltage applied to the quadrupoles, producing an *m/z* scale that is linear with time. The voltages applied to the rods are usually chosen to give equal peak widths over the entire mass range and unit resolution throughout the mass spectrum. The latter is then evaluated to determine the original structure of the analytes and compared with reference libraries for positive identification, providing an unparalleled qualitative ability.

1.3.2 Isotope Ratio Mass Spectrometry (IRMS).

According to the basic principles of chemistry, a chemical element's atomic number is the number of protons in the nucleus of each of its atoms. This number characterizes a given element, being invariant for all atoms of that element. Thus, if some atoms of an element have a different atomic weight from others, the difference must lie in the number of neutrons. By definition, atoms of the same atomic number but different atomic weights are called isotopes.

Most elements of biological interest, including C, H, O, N, and S, have two or more stable isotopes, with the lightest of these present in much greater abundance than the others. Pure gases, as CO_2, H_2, N_2, O_2, and SO_2, are employed in the measurement of each element. Among stable isotopes the most investigated are the heavy isotope of carbon ^{13}C with a natural abundance of ~1% or less [36], and the light isotope ^{12}C.

Isotope ratio mass spectrometry (IRMS) is nowadays considered as a standard tool in disciplines as diverse as biomedicine, geochemistry, archaeology, forensic science, and food authentication. The origin of IRMS is traceable to the first mass spectrograph developed by F. W. Aston in 1919, who demonstrated definitively that the *m/z* 22 observed by J. J. Thomson, in 1912, was indeed a minor isotope of neon [37] and the latter was a mixture of three isotopes (^{22}Ne, ^{20}Ne, and ^{21}Ne). Improving mass spectrometers, Aston, discovered 212 of the 287 naturally occurring isotopes, and measured their masses with 0.1% of precision, determining their abundances and calculating the atomic weights of elements [38].

High-precision IRMS may be defined as the technique which deals with the measurement of deviations of isotope abundance ratios from an agreed standard by only a few parts per thousand for C, H, N, O, and S. Each element must be converted from its current chemical state into the required gaseous species and purified prior to its introduction into the ion source [36]. In contrast to organic mass spectrometers that yield structural information by scanning a mass range over several hundred Dalton for characteristic fragment ions, IRMS instruments achieve highly accurate and precise measurement of isotopic abundance at the expense of the flexibility of scanning MS [39].

In general, IRMS for gases may be differentiated into three modes: absolute IRMS, dual-inlet IRMS, and continuous-flow IRMS. Absolute IRMS, with the aid of small correction factors, measures absolute abundance ratios, albeit with limited precision. Dual-inlet IRMS measures the isotopic difference between two gases with high precision. The third mode, continuous flow IRMS, requires much less sample, and time, than dual-inlet IRMS, but is less precise. Continuous-flow IRMS involves on-line chemical separation techniques, such as gas chromatography-combustion (GC-C-IRMS) or elemental analysis (EA-IRMS).

The value of an isotope ratio (R) in a sample is expressed by a dimensionless quantity, the delta scale, relative to a stated reference. The major problem of "differential" or "delta-measurements" is however, to ensure the comparability of results obtained in different laboratories over different moments in time. To nevertheless ensure comparability of results, a common reference was established to which all measurements should be linked, and which

would, by definition, anchor the delta-scale. Variations of isotopic abundances are so usually presented as δ values [see *Eq. (1.17)*]:

$$\delta\,{}^{y}X_{SPL}(‰) = [(R_{SPL} - R_{STD})/\,R_{STD}] \times 1000$$

Eq. (1.17)

where SPL and STD correspond to sample and standard, respectively; and y designates the minor isotope or isotopomers in the ratio considered. Since a delta value is normally a highly precise value between -0.1 and $+0.1$, it is commonly multiplied by 1000 and denoted by per mille (‰). Moreover, the sensitivity of a GC-C-IRMS is such that trace ratios down to 10^{-5} can be reliably detected [40].

For standardization purposes the principal light elements of interest are measured against four widely accepted standard materials, all assigned a value of zero on their respective $\delta\,{}^{y}$X scales; for hydrogen and oxygen measurements the Vienna Standard Mean Ocean Water (VSMOW) is used and for carbon and oxygen determinations the Vienna Pee Dee Belemnite (VPDB), moreover, for measurements of nitrogen atmospheric air is most commonly applied, since the N in air is a constant 0.3660%. For Sulphur Vienna Canyon Diablo Troilite (VCDT) is the standard material of choice and was selected and expected to be representative for the mean cosmic abundance of Sulphur isotopes.

Taking in consideration that exclusively carbon measurements were carried out in the present research, only the standards related to this application will be highlighted.

Historically, the PeeDee Belemnite (PDB), also known as Chicago PDB Marine Carbonate Standard, was agreed to be used as the common reference to define the zero-point of the carbon isotope "delta"-scale (R_{PDB} = 0.0112372 ± 0.0000009). This material, a carbonate sample of organic origin obtained from a Cretaceous marine fossil, *Belemnitella americana*, from the natural abundance of PeeDee formation in South Carolina, U.S.A., relatively rich in ^{13}C, has a higher $^{13}C/^{12}C$ ratio than nearly all other natural carbon-based substances. Indeed, for convenience it was assigned a $\delta^{13}C$ value of zero. Almost all other naturally occurring samples present negative delta values. However, PDB is virtually exhausted and no longer available, being replaced by secondary standards prepared by the National Institute of Standards and Technology (NIST) and the International Atomic Energy Agency (IAEA). However, "real" PDB and SMOW do not exist and never existed, both were concepts. A "virtual" material, Vienna Pee Dee Belemnite (VPDB) was introduced as the new common reference and linked

to the formerly used scale. To establish the relation between the historical PDB-scale and the currently applied VPDB-scale, a consensus value of $\delta^{13}C_{VPDB}$ = 1.95‰ was assigned to the limestone material NBS19 (NIST) [41]. Thus, today the comparability of carbon isotope ratio measurements depends on the quality, homogeneity, stability, and availability of NBS19.

The reference material terminology commonly adopted in the IRMS research field will be briefly described [42].

- *Primary reference material (or international standard)*: a natural, synthetic, or virtual material versus which, by general agreement, the relative variations of stable isotope ratios in natural compounds are expressed. It is used to define a conventional scale for reporting variations of stable isotope ratios (*e.g.,* VPDB).
- *Calibration material (or primary standard)*: a natural or synthetic compound which has been calibrated versus the primary reference material, and which calibration values have been internationally agreed and adopted. It is used in case the primary reference material is not existing or available to calibrate measurements and instruments (*e.g.,* NBS19).
- *Reference material (RM)*: a natural or synthetic compound which has been calibrated versus the primary reference material and which property values are sufficiently homogeneous, well established and associated with well determined uncertainties. It is used to calibrate laboratory equipment and measurement methods for analysis of materials of a composition different from that of the primary reference material. The available reference materials cover a broad spectrum of chemical compositions and a wide range of stable isotope ratios (*e.g.,* isotopically calibrated *n*-hydrocarbons).
- *Working standard (or transfer standard)*: This term describes a gas used as a reference for analysis of isotope ratios of samples. All measurements of prepared samples and reference materials are made versus this working standard; a more suitable term would be "laboratory reference gas" (*e.g.*, CO_2).
- *Internal standard (or reference standard)*: These materials, of similar composition as the investigated samples, are routinely used as a standard to calibrate or check measurements, as also the instrument.

Moreover, it is worth to point out that the attainment of results with higher accuracy and precision by GC/IRMS, on-line isotopic calibration is essential. The standard practice consists

of the introduction of reference gas pulses of an isotopically standardized gas (working standard), such as CO_2 for $^{13}C/^{12}C$ analysis, at any chosen position in the chromatogram [39]. Generally, the system is composed of a GC hyphenated to an IRMS by means of a combustion furnace; see scheme in *Figure 1.3.2*. In the combustion furnace the compounds eluting from the analytical column are oxidized to CO_2 in a capillary reactor at 940 - 980°C. The oxidation reactor consists of a capillary ceramic tube loaded with twisted Ni and Cu wires, and Pt as catalyst (NiO-CuO catalyst). At that temperature, CuO exists in equilibrium with Cu and O_2, and compounds eluting into the furnace are combusted. The products of this combustion, CO2 and H_2O are directed to the water separator constituted of a nafion™ capillary; only water diffuses through nafion™ membrane which effects the removal of water while retaining CO_2 and maintaining chromatographic resolution. The oxidation reactor shall be oxidized periodically, according to the sample's nature, by flushing oxygen through the oven. A backflush system is also comprised, which can eliminate all solvents in front of the oxidation furnace by reversing the flow through the oxidation reactor towards an exit directly after the GC column. The instrument is also equipped with a reduction reactor (presenting a capillary design identical to the oxidation reactor) commonly operated at 600 – 640 °C, which removes any O_2 bleed from the oxidation reactor.

For high precision isotope ratio determination, the ion source pressure must be kept absolutely constant. For this reason, each continuous flow system must be interfaced to the IRMS via an open split. Most frequently this movable, valve-free open split is computer-controlled, able to couple and decouple to the IRMS without changing the ion source pressure while being compatible to the strict requirements of GC capillary technology. So, after having moved through the water separator, the dried CO_2 passes through the open split, then through the admittance valve into the ion source of the mass spectrometer. When the open split is in decoupled mode no transfer of sample gas is made into the IRMS.

Furthermore, as previously mentioned, measurements of isotope ratio through IRMS requires that sample gases be measured relative to a reference gas of known isotope ratio to achieve the required high precision. For sample-standard referencing, a cylinder of calibrated reference gas (here CO_2) is used for extended periods of time. An inert fused silica capillary supplies the reference gas in the μL min^{-1} range into a miniaturized mixing chamber, also denominated as reference gas injection port, where the reference gas, after having been mixed with helium, flows into the IRMS via a second gas line. This generates a rectangular, flat top gas peak without changing any pressures or gas flows. The system is equipped with a magnetic analyser, an electron ionization ion source, the flight tube, a collector assembly, and a turbomolecular

pump. The electron impact ion source is self-aligning and plugs into the front flange of the analyzer block. The system's ion optics accepts an extremely wide angular ion distribution, leading to extremely high ion transmission from the source to the collectors, which directly translates into sensitivity. Mass-filtered ions are focused onto dedicated open-ended metal cups, the Faraday cup (FC) detectors, positioned specifically for the masses of interest, *e.g.,* in the measurement of CO_2 three FCs are used to determine *m/z* 44, 45, and 46, positioned in a way that the ion beam of each mass falls simultaneously on the appropriate cup. The ion beam is allowed to collide with the interior walls of a FC, and all secondary electron emission is suppressed. FCs are the detectors of choice for IRMS, due to two major considerations. Firstly, the absolute precision required for IRMS determinations is at least 10^{-4}, which is attainable based on counting statistics with at least 10^8 particles detected. Ion currents that achieve these levels are well within the range detectable by FCs. Secondly, FCs are highly stable and rugged, rarely needing replacement, compared to electron multipliers (EM), whose sensitivity degrades with the use.

1.4 Preparative gas chromatography: basic principles.

Preparative gas chromatography (Prep-GC) represents a chromatographic technique which smartly includes a sample preparative step as an integral part of the analysis, allowing the volatile component of interest to be isolated from complex matrices, and then to be collected after GC analysis.

The history of Preparative chromatography goes together with the development of analytical chromatography. While analytical chromatography is used to assess the purity of a sample by separating all the components and quantifying them, preparative chromatography is used to remove impurities from a target component of a mixture. The two objectives are quite different but rely on the same principle, and the optimisation of a preparative separation requires the understanding of multiple factors such as selectivity, efficiency, and resolution.

Prep-GC applications range from the use of GC as a bulk isolation method for compounds in mixtures that are well known, but simply cannot be otherwise separated from mixture components in large-scale amounts, to applications where much smaller quantities of compounds that require more substantial structure elucidation than available with classical GC detectors [43]. A preparative approach may play an important role, when compounds either need to be enhanced in abundance (enriched) or need to be isolated due to inadequate elucidation of structure with available on-line detection methods.

Considering the analytical-scale process, prep-GC has been utilised for a wide range of applications, which can be categorized into the following situations: isolation of target analytes in complex samples; separation of isomers and enantiomers; collection of impurities which require precise structural characterization; collection of trace-level compounds requiring further concentration or enrichment to meet the needs of the detection limits for quantitative and qualitative analysis. Basically, the goal of Preparative chromatography is to achieve the target purity at the lowest possible cost. The throughput quantities injected are usually significantly larger than typical analytical injections, and this also influences the peak shape and the retention times of the different species depending on their concentration. However, many applications usually need a higher-resolution separation method; in these cases, a smaller phase ratio will reduce the effect of peak broadening due to overloading effects if larger amounts of analyte are injected. The loading quantity is one of the key factors that affect the separation efficiency for prep-GC. Hence, special attention should be paid to sample overloading, because this can result in poor separation of the compounds or broader peaks that decrease the resolution [44]. Also, the stationary phases used should be physically and

thermally stable, and chemically inert, to avoid taking part in chemical reaction during the preparative process. The collection of the fractions eluted from prep-GC is as important as the separating process [45], and the success of the prep-GC method is strictly related to the efficiency of the trapping system. The efficiency of a trap used to collect the target effluent may simply be expected to be as high as possible. However, affected by various factors, recovery values of the selected eluates may be low and fluctuating. Poor trapping efficiency is sometimes caused by the formation of aerosol especially for those components with poor volatility. It has been demonstrated that the recovery values were proportional to the volatility of target compounds, and the temperature of the collecting device also intensely affected the efficiency [46]. It is mandatory that the temperature of the connecting channel between the collecting device and the GC system be maintained above the boiling point of the constituents to prevent undesired condensation [47].

Conventionally, a prep-GC system is equipped with a wide or a narrower capillary column; additionally, a suitable collection or trapping device allows to operate at sub-ambient or cold temperature by using a cooling system. Moreover, a detector and a switching system are also incorporated. The switching device, which is directed to the detector in normal operation, allows selection of the component(s) to be transferred to the trapping system by switching the flow to the trapping channel; also, optional cooling system, could increase the recovery efficiency of the semi-volatile or volatile target components [43]. Sample collection includes preparative fraction collectors (PFC) into vials, trapping onto capillary columns or using sorbent materials attached to the end of the column.

A commercially available fraction collector for GC (Gerstel PFC) is an automated device, equipped with six sample traps and one waste trap, which is capable to collect both individual compounds and specific classes of compounds after GC separation. Trap tubes are offered in 1 mL or 100 mL volumes. To increase recovery efficiency, PFC can be equipped with optional N_2 (liq) or cryostatic trap cooling systems. Microprocessor control allows the trap switching times to be selected to within 0.01 min, which permits reliable collection of individual compounds which result closely resolved. The reliability and reproducibility of the system make it possible to trap compounds over the course of hundreds of injections. This allows further analyses of the fractions by techniques requiring larger sample mass such as NMR or IR. Although the PFC has been used in several studies [48, 49, 50] the technical limitation to only six collectable fractions using one PFC still hinders its applications.

Prep-GC is widely used in various fields, either to obtain an individual compound for structural identification or to produce a certain amount of pure compound for application in industrial large-scale preparation.

The aim of preparative Prep-GC can be briefly defined as the isolation and purification of components present in mixtures, which could be further analysed; on the contrary, analytical chromatography would separate and identify the components of a mixture. In addition to various pattern recognition studies and quantitative determinations of known components, the structural elucidation of unknown ultra-trace constituents is of key importance for fields such as food flavour, fragrance, pheromones, and environmental chemistry. When dealing with complex natural products it is frequently necessary to obtain complementary chemical and/or spectroscopic data, which necessitates the isolation of the individual components. In general, the structural elucidation practice may be a demanding analytical task and requires extensive clean-up and fractionation of the starting materials. After the collection step, structure elucidation is usually the following in preparative gas chromatography, and different analytical techniques as mass spectrometry (MS), Fourier Transform Infrared Spectroscopy (FTIR), and Nuclear Magnetic Resonance (NMR), are used for this purpose.

1.5 Gas chromatography hyphenated to olfactometry.

The human nose perception of volatile compounds, released from foods and fragrances, depends on the extension of the release from the matrix and the odor properties of the compounds. It is known that only a small portion of the large number of volatiles occurring in a fragrant matrix contributes to its overall perceived odor [51, 52]. Further, these molecules do not contribute equally to the overall flavour profile of a sample, hence, a large GC peak area, generated by a chemical detector does not necessarily correspond to high odor intensities, due to differences in intensity/concentration relationships. Consequently, the general interest of researchers was directed to the determination of the contribution of single constituents to the overall flavour of a sample. In general, the sensory importance of an odour-active compound depends on its concentration in the matrix, and on its human nose limit of detection. Moreover, the unpredictable extent of interaction of flavour molecules with each other, and with other constituents must also be considered. Gas chromatography hyphenated to olfactometry (GC-O) is the most appropriate analytical solution to such issues, as it enables the assessment of odor-active components in complex mixtures, through the specific correlation of an olfactive sensation with a chromatographic peak; this is possible because the eluted substances are perceived simultaneously by two detectors, one of them being the human olfactory system. Consequently, GC-O provides not only an instrumental, but also a sensorial analysis. The latter is defined as a science responsible for the quantification of the human responses to the stimuli perceived by the senses of sight, smell, taste, touch, and audition [53]. When coupled to analytical techniques, such as in GC-O, it becomes a precise, descriptive approach to characterise stimuli, evaluating and measuring impressions, as also an important process which enables the comprehension and quantification of sensorial characteristics. The introduction and diffusion of GC-O, proved to be vital for the development in the research field of odour-active compounds, providing valuable information on the chromatogram locations on which to focus attention and resources. GC-O is a unique analytical technique which associates the resolution power of capillary GC with the selectivity and sensitivity of the human nose. The discriminatory capacity of mammalian olfactory system is such that thousands of volatile chemicals are perceived as having distinct odours. Due to the great efforts over the last decade using various experimental approaches [54, 55], the complex pathways of this intriguing system are emerging, including the mechanisms through which the brain decodes and discriminates odorants. In vertebrates, the detection of odors starts in the olfactory sensory neurons (OSNs) located in the olfactory epithelium, also named *regio olfactoria*, situated in

the roof of the nasal cavities of the nose. These OSNs extend a single dendrite terminating in a ciliated knob at the surface of the epithelium. Each OSN has 8 to 20 cilia that are whip-like extensions of 30-200 microns in length. The cilia are considered as the first active site of the olfactory pathway and contain the odorant receptor (OR) proteins, also defined as odorant binding proteins (OBPs). Chemicals dispersed in the air may interact with the OBPs according to their concentration and properties.

Since sensory analysis involves human subjects as a measuring tool, this presents an immediate problem due to the innate variability between individuals, not only because of their previous experiences and expectations, but also their sensibility [56]. To contour this drawback, odor panels consist of individuals that are selected and screened for specific anosmia. One modality for screening the evaluators for that physiological dysfunction is by using the standard solution set proposed by Friedrich *et al.* [57]. In the case no insensitivities are found, the panelists are introduced to two sensorial properties, quality, and intensity. Odor quality shall be described according to the odor families that compose the aromatic wheel, or according to Kraft *et al.* [58], the olfactive spectrum. An odor family may be described as a class of odors which due to the presence of certain features are related to each other. The families may also present sub-classifications, enabling a more detailed description of an olfactive impression. With regards to intensity, a sensation triggered by an odor shall be measured through its rating on an intensity interval scale. Basically, the odour activity depends on the volatility of the molecule, and the odor note is strictly related to the chemical structure.

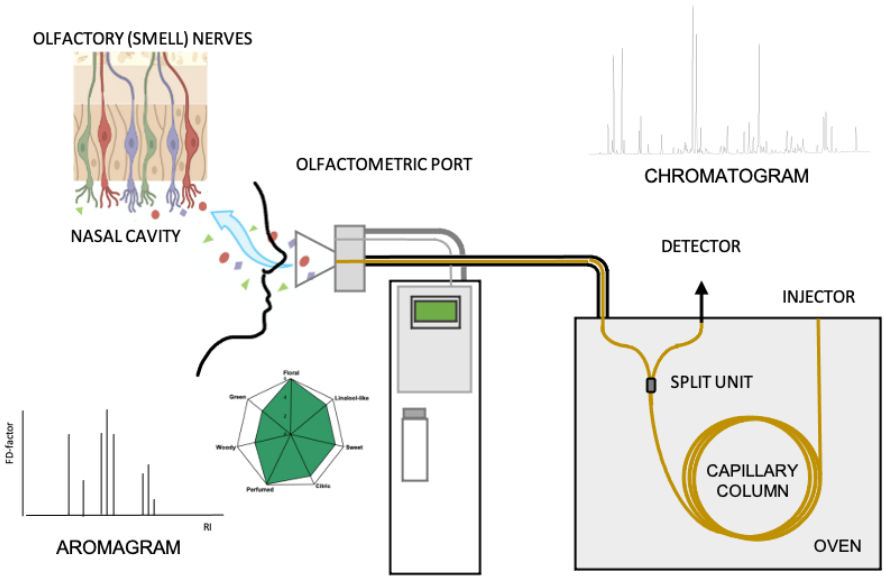

Figure 1.5.1. **Scheme of a GC-O system and analysis workflow: both sensorial and instrumental steps are reported.**

- ***GC-O system***

In general, GC-O is carried out on a standard GC that has been equipped with a sniffing port (*Figure 1.5.1*) in substitution of, or in addition to, the conventional detector. When a flame ionization detector (FID) or a mass spectrometer is also used to record, the analytical column's effluent is split and transferred to the conventional detector and to the human nose. The splitting of the column effluent is enabled through the installation of a splitting unit in the column's outlet. Among the most common splitter types are the T-union and the four-port splitter. In case a T-union is used, one port is connected to the analytical column outlet and the two remaining ports to the conventional detector and to the transfer line; in the four-port splitter the fourth port is connected to an auxiliary gas outlet. The flow division occurs according to the splitting unit and the dimensions of the retention gaps (length and internal diameter).

The sniffing port is effectively a nose-cone, ergonomically designed, to which the eluting volatiles are directed via a connecting transfer line. The nose-cone is typically positioned with a short distance, about 30 to 60 cm, from the instrument. Moreover, since the transfer line extends from the oven, it must be heated to avoid that late eluting compounds with high boiling points condensate [59]. The position of the nose-cone must be such that the assessor feels comfortable; standing or sitting position during analysis is subjective, and may also depend on the length, flexibility and adjustability of the transfer line.

A further important aspect, early realized in GC-O analysis was the fact that the carrier gas eluting from a GC is typically hot and dry, effectively drying out the nose, and causing considerable discomfort for the assessors, and as such, affecting sensitivity. This issue was addressed by using humidified air as a make-up carrier gas to deliver the odorants to the human assessors [60] preventing nasal mucosa dry-out. Nowadays, volatiles are typically carried to the nose in a stream of heated and humidified air; about 50 % to 75 % relative humidity.

With regards to detectors, splitting column flow between the olfactory port and a mass spectral detector provides simultaneous identification of odor-active compounds [8, 9].

- ***Sample preparation procedures***

Additionally, some considerations must be made on a rather laborious, but significant step of flavour and fragrance analysis by means of GC, namely sample preparation. The odor profile of a matrix is closely related to the isolation procedure, which should yield a product which is representative of the sample; therefore, the choice of an appropriate sample preparation method becomes crucial. According to the properties of the matrix the preparation may include mincing, homogenization, centrifugation, steam distillation (SD), solvent extraction (SE),

fractionation of solvent extracts, simultaneous distillation-extraction (SDE), supercritical fluid extraction (SFE), pressurized-fluid extraction, Soxhlet extraction, solvent assisted flavour evaporation (SAFE), microwave-assisted hydrodistillation (MAHD), direct thermal desorption (DTD), headspace techniques (HS), cryofocusing, solid-phase microextraction (SPME), matrix solid-phase dispersion (MSPD) and/ or methylation, among others.

The analyst must deal with decomposition of labile compounds, loss of highly volatile compounds and heat-induced artifact formation.

In general, the extracts obtained by SE can be very complex, so that many co-elutions may occur in GC-O, making the identification of individual odour-active compounds difficult. The fractionation of these extracts is a time-consuming, but reasonable, mode to overcome this problem. A further very popular method is SAFE, which may be applied after SE techniques or be used as an individual extraction method for solvent extracts or food matrices. Moreover, HS techniques are a valuable tool for GC-O analysis combining simplicity, solvent-free procedures, requirement of small sample amounts, and no artifact formation. However, the relative concentration of volatile components in the headspace does not correspond to the concentration in the sample due to the differences in volatility of flavour compounds.

A further technique, worthy of note is SPME, a widely applied solvent-free method which exploits the high adsorption power of a fused silica fiber coated with a specific extraction phase, which is selected according to the type of matrix [61, 62]. However, the use of SPME as isolation method prior to GC-O analysis, presents some limits due to the possible non-representative nature of the extracts. The chemical profile of the collected volatiles depends upon the type, thickness, and length of the fiber, as well as on the sampling time and temperature. Although a series of volatile isolation methods are known, the most appropriate way to attain an optimum recovery of the odorant chemicals is the employment of more than one extraction technique.

- ***Data measurements methods***

Over the last decades, GC-O has been largely used in combination with sophisticated olfactometric methods which were developed to collect and process GC-O data, and hence, to estimate the sensory contribution of a single odour-active compound. These methods are commonly classified in four categories: dilution, time-intensity, detection frequency, and posterior intensity methods [63, 64, 65, 66]. Dilution analysis, the most applied method, is based on successive dilutions of an aroma extract until no odor is perceived by the panelists. This procedure, usually performed by a reduced number of assessors, is mainly represented by

CHARM (combined hedonic aroma response method) [67], developed by Acree and co-workers, and AEDA (aroma extraction dilution analysis), first presented by Ullrich and Grosch [68]. In AEDA samples are evaluated by the panelists in increasing dilution order and the impact of an odour-active compound is given by its dilution factor (FD) value. The latter is calculated by dividing the largest volume analyzed by the lowest volume in which the respective odour-active compound was still detectable. The overall results are reported in an aromagram presenting the FD value, or its logarithm, against the retention index, or simply by listing the FD values. On the other hand, in CHARM analysis the dilutions are presented to the panelists in a randomized order, avoiding bias introduced by the knowledge of the dilution being analysed. The panelists record the start and end of each detected odour; the detection duration for each individual is then compiled, and an aromagram is generated by plotting the duration of the odour sensation against the dilution value. CHARM values can be calculated according to *Eq. (1.18)*, where *n* is the number of coincident responses between panelists and *d* is the dilution value. The latter is analogous to the FD value in AEDA.

$$c = d^{n-1}$$

Eq. (1.18)

AEDA presents limitations, such as controversial statistical data manipulation, the non-consideration of odorant losses during the isolation procedure and of synergistic or suppressive effects of distinct compounds in a flavour mixture. With regards to CHARM, limitations can be observed in quantification analyses, which require the replication of the experiment by at least three different trained assessors.

The choice of the GC-O method is of extreme importance for the correct characterization of a matrix, since the application of different methods to an identical real sample can distinctly select and rank the odour-active compounds according to their odour potency and/or intensity. Commonly, detection frequency and posterior intensity methods result in similar odor intensity/concentration relationships, while dilution analysis investigate and attribute odour potencies.

As well-known odours can be quantified by distinct parameters; one of the terms used is threshold concentration, which can be further described at three levels, namely detection, recognition, and difference thresholds. Detection threshold is defined as the lowest concentration or intensity that is perceived by the panelist, while recognition threshold is the lowest concentration or intensity at which a substance or an olfactive quality attribute can be

identified and described. On the other hand, difference threshold is the magnitude of a stimulus above which there is no increase in the perceived intensity of the appropriate quality for that stimulus [56]. The thresholds of volatile compounds may differ by many orders of magnitude (parts per trillion at the low extreme to odorless compounds). Therefore, in a sample composed of many different volatile compounds, some flavour and fragrance chemicals may present an increased intensity in odour-activity according to a proportional increment of their concentration, while with others the change in intensity may be the opposite or just less marked. The dependence of intensity upon concentration regards a constant which quantifies odors and is denominated as slope. The idea of slope as a constant, which is characteristic of a substance, assumes the validity of the Stevens's power law [69]. This law states that equal changes in stimulus magnitude (Φ) produce the corresponding change in perceived intensity (Ψ); k is a constant and n is the Steven's exponent, as presented in *Eq. (1.19)*.

$$\Psi = k\Phi^{n}$$

Eq. (1.19)

It must be noted that the slope depends upon the method by which it was determined. Generally, a relatively high value for the slope indicates a strong dependence of intensity upon concentration, while a low-slope odorant is typically not very powerful when assessed in the undiluted form.

1.6 References.

1. C. F. Poole, The Essence of Chromatography, Elsevier Science B.V., Amsterdam (2003).
2. M. Tswett. *Ber. Deut. Botan. Ges.* 24 (1906) 316-384.
3. A. J. P. Martin, R. L. M. Synge. *Biochem. J.* 35 (1941) 1358.
4. A. T. James, A. J. P. Martin. *Biochem. J.* 50 (1952) 679.
5. M. J. E. Golay. In Gas Chromatography (1957 Lansing Symposium), V. J. Coates, H. J. Noebels, I. S. Fagerson (eds.), Academic Press, New York (1958).
6. M. L. Lee, B. W. Wright. *J. Chromatogr.* 184 (1980) 234.
7. M. Novotny. *Anal. Chem.* 50 (1978) 16A.
8. L. S. Ettre, J. V. Hinshaw, Basic relationships of Gas Chromatography, Advanstar Data, Cleveland (1993).
9. H. M. McNair, J. M. Miller. Basic Gas Chromatography. Wiley & Sons, New York (1998).
10. M. Novotny, Gas Chromatography in: Encyclopedia of Physical Science and Technology (Third Edition), R. A. Meyers (Editor), Academic Press, San Diego (2001) pp. 455-472.
11. M. J. E. Golay, in: Gas Chromatography, V. J. Coates, H. J. Noebels, I. S. Fagerson (Editors), Academic Press, New York, USA (1958).
12. E. S. Z. Kováts. *Helv. Chim. Acta* 41 (1958) 1915.
13. H. van den Dool, P. D. Kratz. *J. Chromatogr.* 11 (1963) 463.
14. W. Bertsch, in Multidimensional Chromatography Techniques and Applications, H. J. Cortes (Ed.), Marcel Dekker, New York, pp. 75–110 (1990).
15. L. Mondello, A. C. Lewis, K.D. Bartle (Editors), Multidimensional chromatography, Wiley & Sons, Chichester, England (2002).
16. F. David, in Hyphenations of Capillary Chromatography with Mass Spectrometry, Elsevier, pp. 135-182 (2020).
17. D. R. Deans, *Chromatographia* 1 (1968) 18.
18. J. V. Seeley, in Gas Chromatography, Elsevier, pp. 161-183 (2012).
19. D. Quimby, J.D. McCurry, W.M. Norman, *LCGC Eur.* (2007) 7-15.
20. Agilent Technologies Inc.http://www.agilent.com/en/products/gas-chromatography/gc-gc-ms-technologies/capillary-flow-technology.
21. Shimadzu Corp. http://www.shimadzu.com/an/gc/multidimgc/multidimmdgc.html.
22. D. Sciarrone, A. Schepis, M. Zoccali, P. Donato, F. Vita, D. Creti, A. Alpi, and L. Mondello, *Anal. Chem.* 90 (2018) 6610-6617.
23. G. T. Eyres, S. Urban, P.D. Morrison, J.-P. Dufour, P.J. Marriott, *Anal. Chem.* 80 (2008) 6293-6299.
24. G. T. Eyres, S. Urban, P.D. Morrison, P.J. Marriott, *J. Chromatogr. A* 1215 (2008) 168-176.

25. C. P. G. Ruehle, J. Niere, P.D. Morrison, R.C. Jones, T. Caradoc Davies, A.J. Canty, M.G. Gardiner, V.-A. Tolhurst, P.J. Marriott, *Anal. Chem.* 82 (2010) 4501-4509.
26. D. Sciarrone, S. Pantò, C. Ragonese, P.Q. Tranchida, P. Dugo, L. Mondello, *Anal.Chem.* 84 (2012) 7092-7098.
27. D. Sciarrone, S. Pantò, P.Q. Tranchida, P. Dugo, L. Mondello, *Anal. Chem*. 86 (2014) 4295-4301.
28. S. Pantò, D. Sciarrone, M. Maimone, C. Ragonese, S. Giofrè, P. Donato, S. Farnetti, L. Mondello, *J. Chromatogr. A* 1417 (2015) 96-103.
29. D. Sciarrone, S. Pantò, P. Donato, L. Mondello, *J. Chromatogr. A* 1475 (2016) 80-85.
30. T. Hirschfeld, *Anal. Chem.* 52 (1980)2, 297A–312A.
31. N. Ragunathan, K. A. Krock, C. Klawun, T. A. Sasaki, C. L. Wilkins, *J. Chromatogr. A* 856 (1999) 349–397.
32. J. Gross, Mass Spectrometry: A Textbook, Second Edition (2010).
33. F. W. McLafferty, F. Tureček. Interpretation of Mass Spectra. University Science Books, Mill Valley (1993).
34. R. E. March, R. J. Hughes. Quadrupole Storage Mass Spectrometry. Wiley & Sons, New York, 1989.
35. R. M. Silverstein, T. C. Morrill, Spectrometric Identification of Organic Compounds. Wiley & Sons, New York (1991).
36. J.T. Brenna. *Acc. Chem. Res*. 27 (1994) 340.
37. F.W. Aston. Mass Spectra and Isotopes. Longmans, Green and Co., New York (1942).
38. I.T. Platzner. Modern Isotope Ratio Mass Spectrometry. Wiley, West Sussex (1997).
39. W. Meier-Augenstein. *Anal. Chem. Acta* 465 (2002) 63.
40. J. T. Brenna, T. N. Corso, H. J. Tobias, R. J. Caimi. *Mass Spectrom. Rev*. 16 (1997) 227.
41. M. Gröning, K. Frohlich, P. De Regge, P. R. Danesi. In Intended use of the IAEA reference materials. Part II: Examples on reference materials certified for stable isotope composition.www.iaea.org.
42. K. Russe, S. Valkiers, P.D.P. Taylor. *Int. J. Mass. Spec*. 235 (2004) 255.
43. L. Kim, P. J. Marriott., in Gas Chromatography, Elsevier, pp. 161-183 (2012).
44. H.-L. Zuo, F.-Q. Yang, W.-H. Huang and Z.-N. Xia, *J. Chromatogr. Sci.* 51 (2013) 704-715.
45. K.P. Hupe, U. Busch, W. Kuhn, *J. Chromatogr. Sci.*, 3 (1965) 92-97.
46. M. Verzele; *J. Chromatogr. A* 13 (1964) 377-381.
47. G.R. Fitch, *J. Soc. Cosmet. Chem.* 17 (1966) 657–667.
48. C. Meinert, E. Schymanski, E. Kuster, R. Kuhne, G. Schuurmann, W. Brack; *Environ. Sci. Pollut. Res*. 17 (2010) 885-897
49. H. Sugie, M. Teshiba, Y. Narai, T. Tsutsumi, N. Sawamura, J. Tabata, *Appl. Entomol. Zool.* 43 (2008) 369-375.

50. M. Mandalakis, H. Holmstrand, P. Andersson, O. Gustafsson, *Chemosphere* 71 (2008) 299-305.
51. S. M. van Ruth, *Biomolec. Eng.*, 17 (2001) 121-128.
52. W. Grosch, "Review Determination of Potent Odorants in Foods by Aroma Extract Dilution Analysis (AEDA) and Calculation of Odor Activity Values (OAVs)" (1994).
53. M. Meilgaard, G. V. Civille, and B. T. Carr, Sensory evaluation techniques. CRC Press (1999).
54. S. Bieri, K. Monastyrskaia, and B. Schilling, *Chem Senses*, 29, 6, pp. 483–487 (2004).
55. S. L. Sullivan and L. Dryer. *J. Neurobiol.* 30, 1, pp. 20-36 (1996).
56. A. Richardson. In The Chemistry of Fragrances, D. H. Pybus, C. S. Sell (eds.). Royal Society of Chemistry, Cambridge (1999).
57. J. E. Friedrich, T. E. Acree, E. H. Lavin. In Gas Chromatography-Olfactometry: The State of the Art., J. V. Leland, P. Schieberle, A. Buettner, T. E. Acree (eds.). American Chemical Society, Washington, D.C. (2001).
58. P. Kraft, J. A. Bajgrowicz, C. Denis, G. Fráter. *Angew. Chem. Int. Ed.* 39 (2000) 2980.
59. N. Abbott, P. X. Étiévant, S. Issanchou, D. Langlois. *J. Agric. Food Chem.* 41 (1993) 1698.
60. A. Dravnieks, A. O' Donnell. *J. Agric. Food Chem*. 19 (1971) 1049.
61. H. Kataoka, H. L. Lord, J. Pawliszyn. *J. Chromatogr. A* 880 (2000) 35.
62. W. Wardencki, M. Michulec, J. Curylo. *Int. J. Food Sci. Technol.* 39 (2004) 703.
63. S. M. van Ruth. *Biomolec. Eng.* 17 (2001) 121.
64. V. Ferreira, J. Pet'ka, M. Aznar. *J. Agric. Food Chem.* 50 (2002) 1508.
65. S. Le Guen, C. Prost, M.J. Demaimay. *J. Agric. Food Chem.* 48 (2000) 1307.
66. C. M. Delahunty, G. Eyres, J. P. Dufour. *J. Sep. Sci.* 29 (2006) 2107.
67. T.E. Acree, J. Barnard, D. Cunningham. *Food Chem.* 14 (1984) 273.
68. F. Ullrich, W. Grosch., *Z. Lebensm. Unters. Forsch* 184 (1987) 277.
69. S.S. Stevens. *Psychol. Rev.* 64 (1957) 153.

Chapter 2: Overcoming the lack of reliability associated to monodimensional gas chromatography coupled to isotopic ratio mass spectrometry data by heart-cut two-dimensional gas chromatography.

2.1 Introduction.

Since the earliest stages of its development, GC coupled to combustion isotopic ratio MS (GC-C-IRMS) has proven to be much suitable to assess the authenticity of natural samples, based on the isotope ratio measurement of different elements of key volatile compounds. To this regard, GC-C-IRMS has been the workhorse in different fields, including environmental, geochemistry, drugs, food and beverage, and flavour and fragrance [1]. The investigation of key elements, mainly carbon ($^{13}C/^{12}C$), hydrogen ($^{2}H/^{1}H$), and nitrogen ($^{15}N/^{14}N$), allowed in many cases to highlight fraudulent practices across a wide range of food, beverages and natural ingredients [2]. Among the latter, essential oils have been extensively studied as key components of high economic value in cosmetics and in the food and beverage industry, whose composition and market price may vary greatly, depending on the geographical origin. The increasing demand for "premium quality" products has led to fraudulent practices, aiming to imitate the composition of natural essential oils, mainly in terms of their major volatile constituents. Different techniques have been applied to ascertain the genuineness of essential oils successfully, by the thorough investigation of both the volatile and non-volatile fractions [3,4], however nowadays more sophisticated adulteration approaches are hardly detected, by these means. GC-MS and GC-FID have been employed successfully to detect the presence of foreign compounds in essential oils, revealing adulterations based on the addition of cheaper oils. Likewise, the presence of synthetic compounds remained undetectable, until investigation of the enantiomeric distribution became feasible [5]. Soon after the introduction of capillary GC columns equipped with chiral selectors, enantio-selective (Es) GC [6] has been exploited to unveil fraudulent additions, through the evaluation of the enantiomeric excess of specific key compounds; later on, multidimensional Es-GC was also implemented by Schomburg et al. [7]. Chiral components in vegetable oils from different sources are characterized by distinctive enantiomeric ratios, as related to the biosynthetic pathway and plant metabolism, thus their addition can be easily revealed down to certain percentages, provided that reference data are available for the genuine samples. Chiral approaches have allowed to easily detect the addition of synthetic compounds such as limonene, linalool and linalyl acetate as racemic mixtures, resulting in final enantiomeric ratios different from those of the original oil [8]. In this context,

extensive work has been carried out by Dugo's research group, who reported the use of different approaches, including GC-FID, GC-MS, Es-GC [8-12] and GC coupled to combustion-isotope ratio MS [9-11], for the analysis of oil volatile fraction. Aiming to conceal the fraudulent addition of chiral compounds from different origins, these components are often selected from natural sources with enantiomeric distribution identical or similar to that of the genuine oil. Several chiral compounds extracted from natural sources are available on the market, such as linalool from ho wood oil, coriander oil or lavandin oil, and linalyl acetate from Lavandula [4]. In these cases, more sophisticated analytical tools are required to give evidence of the characteristic parameters related to the plant origin. The measurement of the $\delta^{13}C$ isotopic value of the volatile fraction by means of GC-C-IRMS is a valid method to assess sample genuineness, delivering highly precise measurements of the major sample components ($\pm$ 0.01‰ – 0.2‰) [1].

However, a number of specific problems strictly linked to the operational mode of this technique have severely limited its spreading. Even if data related to GC-C-IRMS are available in literature since the late 70's, the feasibility of this approach has been seriously hindered by an insufficient separation of the analytes. The latter is often originated by the system dead volumes associated to the combustion step and may preclude the production of CO_2 from pure single compounds, which is mandatory requirement. This has in turn resulted in low reliability of the GC-C-IRMS data obtained from unresolved peaks. Unlike other MS approaches where neighboring compounds, although coeluted, can be still identified by exploiting deconvolution, extracted-ion or tandem-MS approaches, in IRMS detection a partial peak integration would compromise the reliability of the measurement, for the well-known chromatographic isotope effect [1,13]. A complete separation is thus mandatory since, differently from the cited MS techniques, the $\delta^{13}C$ measurement is thereby achieved after conversion of all organic components to CO_2. To this purpose, the coupling of two (or more) stationary phases, characterized by different selectivity, provides increased separation capabilities for unresolved peaks. In heart-cut two-dimensional GC (HC-MDGC), selected fractions are transferred from a first to a second full-length column by means of a Deans switch device, whereas in the comprehensive mode only a short column segment is used [14]. After the first report by Nitz *et al*. on the coupling of multidimensional chromatography to IRMS [15], over 250 papers have been published in the field of gas chromatography coupled to IRMS only considering the last two decades. It is noteworthy that, to the best of our knowledge, less than 10% of these papers have reported the use of MDGC separation [16-29]. This gives evidence that most research is

still being conducted using one-dimensional chromatography. Moreover, some of these works reported the use of MDGC techniques as a mean to accelerate the sample purification procedure and increase the automation of the IRMS processes [24, 26, 28], while among the others, little insight was made into the causes of wrong $^{13}C/^{12}C$ ratio measurements resulting from peak coelution. The importance of applying a multidimensional separation to enhance the accuracy and precision of isotopic measurements has been highlighted in a limited number of studies [15, 21, 27, 29].

This work aims to urge IRMS practitioners to carefully evaluate the reliability of $\delta^{13}C$ data obtained by means of monodimensional GC-C-IRMS, given the likelihood for a number of critical issues. In spite of the fact that the detrimental influence of peak co-elutions is well known, this problem appears to have been often underestimated, so far. Hereby, a set of essential oils were selected as model samples, to provide a critical comparison of the reliability of $\delta^{13}C$ data obtained by means of monodimensional GC-C-IRMS, *vs*. MDGC-C-IRMS. In the latter, a Deans switch system already reported in applications by our group [30, 31] was employed, for the coupling to a secondary separation column, consisting of polyethylene glycol. Finally, a medium-polarity ionic liquid phase was exploited as secondary column in the MDGC system, with the aim to investigate the influence of the column bleeding on the $\delta^{13}C$ data for late eluted components.

2.2 Materials and methods.

- ***Samples and sample preparation***

Cold-pressed bergamot essential oil was kindly provided by Capua 1880 S.r.l. (Italy), while helichrysum, myrtus and rose essential oil samples were purchased in a local store (Messina, Italy). All the samples were diluted in hexane (1:10, *v/v*) prior to injection into the GC system. C_7 -C_{30} *n*-alkane and C_4 -C_{24} fatty acid methyl ester mix, used for the calculation of linear retention index (LRI) values were kindly provided by Merck Life Science (Darmstadt, Germany). In order to calibrate the measured $\delta^{13}C$ values to the VPDB scale, the CO_2 reference gas was calibrated using four reference compounds, namely iodomethane ($\delta^{13}C$ -54.59) and three from the Indiana mix A7, hexadecane ($\delta^{13}C$ -26.15), octadecane ($\delta^{13}C$ -32.70) and eicosane ($\delta^{13}C$ -40.91) (Indiana University, Bloomington, IN).

- ***Monodimensional GC-C-IRMS/qMS***

The GC-C-IRMS/MS system consisted of an AOC-20i autosampler, a GC2010 Plus gas chromatographer (Shimadzu Europa, Duisburg, Germany), directly connected via a zero dead-volume tee-union to a QP2010 Ultra quadrupole mass spectrometer (Shimadzu Europa, Duisburg, Germany) and to a VisION IRMS system by means of a GC V furnace system (Elementar Analysensysteme GmbH, Langenselbold, Germany) maintained at 850°C. A split/splitless injector was kept at 280°C, with a split ratio of 50:1. A capillary SLB-5ms column, 30 m × 0.25 mm i.d. × 0.25 μm d_f (Merck Life Science, Darmstadt, Germany) was operated at a constant flow rate of carrier gas (helium) of 1 mL min^{-1}. The GC oven temperature was ramped as follows: 50°C to 300°C at 3°C min^{-1}. The gas stream from the GC column outlet was split through a zero dead-volume tee-union (Valco) to the combustion chamber and afterwards to the IRMS and to the qMS system in the ratio 10:1, via a 0.85 m × 0.25 mm i.d. and a 1.5 m × 0.1 mm i.d. uncoated column, respectively. The qMS ion source and interface temperature were maintained at 200°C and 250°C, respectively, and a mass range of 40-400 *m/z* was monitored at 10 Hz of an acquisition speed. GCMS data were acquired by the GCMS solution software ver. 4 (Shimadzu Europa, Duisburg, Germany). The separated compounds were identified by searching their qMS spectra against the FFNSC 4.0 mass spectral library database (Shimadzu Europa, Duisburg, Germany), using a double filter based on the spectral similarity results and Linear Retention Index (LRI) values. The VisION IRMS (Elementar Analysensysteme GmbH, Langenselbold, Germany) was a bench top 5 kV system equipped with an integrated gas delivery monitoring system. The combustion chamber was equipped

with a high performing silicon carbide tube furnace for the quantitative, fractionation-free conversion of the delivered compounds to pure gases (CO_2 and H_2O). The CO_2 produced by combustion of each component was transferred to the IRMS, while the water produced was removed through a nafion membrane. The following settings were applied to the VisION system: acceleration voltage, 3789.907 V; trap current, 600.000 µA; magnet current, 3700.000 mA. IRMS data were handled by the IonOS stable isotope data processing software ver. 4.4.3.9348 (Elementar Analysensysteme GmbH, Langenselbold, Germany).

- ***Multidimensional GC-C-IRMS/qMS***

The MDGC-C-IRMS/qMS prototype configuration was previously developed [29] (see Figure 2.1). Two GC-2010 Plus gas chromatographs (defined as GC1 and GC2) were connected by means of a heated transfer line (Shimadzu Europa, Duisburg, Germany). GC1 was equipped with a Deans-switch (DS) transfer device, connected to an auxiliary pressure controller (APC) unit, which supplied the same carrier gas (He) (Shimadzu Europa, Duisburg, Germany) allowing to divert the first column eluent to the FID or to the second column in GC2.

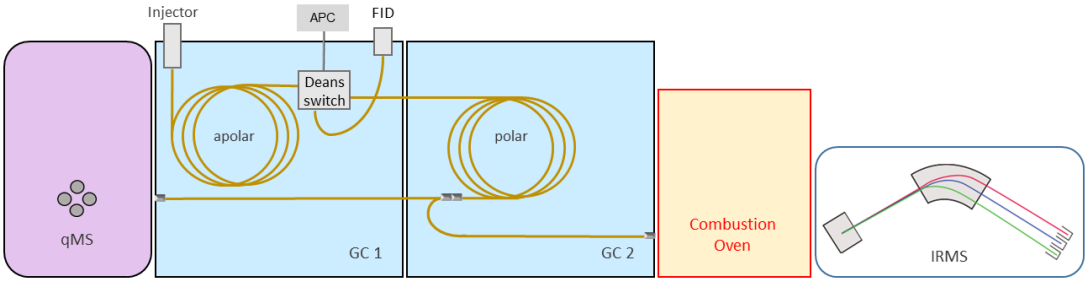

Figure 2.1. **Scheme of the MDGC-C-IRMS/qMS prototype [29].**

The split/splitless injector was maintained at 280°C, with a split ratio of 10:1. A capillary SLB-5ms column, 30 m × 0.25 mm i.d. × 0.25 µm d_f (Merck Life Science, Darmstadt, Germany) was operated at a constant flow rate of carrier gas (helium) at ≈1.0 mL min^{-1}. GC1 oven temperature was ramped as follows: 50°C to 300°C at 3°C min^{-1}. The FID (330°C; H_2 flow, 40.0 mL min^{-1}; air flow rate, 400 mL min^{-1}; sampling rate, 80 ms equal to 12.5 Hz) was connected to the DS device *via* a 0.25 m × 0.18 mm i.d. stainless steel uncoated column and used to monitor the first column eluent. GC2 was equipped alternatively with a SUPELCOWAX 10 column, 30 m × 0.25 mm i.d. × 0.25 µm d_f or a SLB-IL60i column, 30 m × 0.25 mm i.d. × 0.20 µm d_f (Merck Life Science, Darmstadt, Germany), operated under the following temperature program: 50°C (hold for 10 min) to 250°C at 3°C min^{-1}. GC2 was

connected on one side to the DS device while on the other side a T-union was used to split the effluent to the qMS and C-IRMS systems (as in the monodimensional applications). A pressure program was applied to the APC unit in order to maintain the carrier gas flow rate constant also in the second column (≈1 mL min^{-1}) in order to avoid loss of sensitivity [32]. The qMS and C-IRMS conditions were the same as in the monodimensional configuration. Apart for the IRMS, all data were acquired by the MDGC solution control software package (Shimadzu Europa, Duisburg, Germany) allowing for setting up the DS device parameters and to monitor both the GC1 (FID) and GC2 (qMS), simultaneously.

2.3 Results and discussions.

The reliability of the GC-C-IRMS data obtained in the presence of coeluted components was evaluated, for different samples, and the extent to which such co-elutions affected the measured $\delta^{13}C$ values was assessed. Apart from the insufficient separation resulting from the sample complexity, a number of specific problems were taken into account, severely hampering the usefulness of this technique. Although the coupling of IRMS to GC by means of a combustion furnace was readily recognized as a powerful approach toward the assessment of sample genuineness, yet this technique has traditionally suffered from a number of limitations/drawbacks inherent to the characteristics of the single techniques employed. Possible sources of potential errors may be envisaged in natural isotopic abundances, chromatographic effects, and issues related to analytes conversion to CO_2 prior to IRMS measurement.

- ***Natural isotopic abundances***

Attention must be paid in GC-C-IRMS applications, especially when dealing with natural samples, which are often characterized by a medium to high complexity and, moreover, by the presence of compounds in a wide concentration range. The sample amount to be injected should be carefully chosen trying to compromise between the desired sensitivity and the column capacity, i.e., trying to attain good sensitivity for the trace components, while at the same time avoiding overloading the chromatographic column with respect to the most abundant sample constituents. In this concern, it is furthermore crucial to introduce sufficient quantities of the analytes, in view of the reduced sensitivity of the technique. In fact, much higher detection limits than those observed with other MS techniques are encountered in IRMS, due to an approximately 100 times lower natural relative abundance of ^{13}C compared to that of ^{12}C and to the open split incorporated in the GC-C-IRMS interface [32]. In comparison with other detection approaches, the sensitivity of IRMS techniques is affected to even a higher extent by the low chromatographic efficiency caused by dead volumes in the system and the lowered signal-to-noise ratio. Significant dead volumes may be introduced by the combustion furnace, which is characterized by a wider internal diameter with respect to the capillary column.

- ***Chromatographic effects***

As a result of the different Van der Waals dispersion forces during the solute/stationary interaction, those species which are richest in the heavier isotope have a slightly lower retention and thus tend to elute in the first part (front) of a peak, while the peak tail contains molecules

with higher amounts of the lighter isotope due to a slightly higher retention [33]. Furthermore, the background ion current can influence the determination of the correct isotope ratio values significantly, especially for low concentrated components (low signal-to-noise ratio). Under ideal conditions, acceptable standard deviation values of ± 0.1‰ for signals of sufficient intensity are typical, increasing to about ± 0.5‰ for signals close to 0.5-1 nA intensity [34]. It is therefore evident that, especially in the presence of analytes at small amounts, the precision of the measurements can be much affected by fluctuations above the accepted value of ± 0.5‰. As a consequence, it may be difficult to discriminate between the same analytes of different origin, often characterized by small differences in the isotope ratio values measured.

- ***Analytes conversion to CO_2***

Being impossible to assess the origin of CO_2 produced in the combustion step, the incomplete separation of two or more compounds by the chromatography will result in the incorrect evaluation of the isotope ratio. Specifically, three cases may occur: if the coelution affects the front of the peak, the ^{12}C rich tail of the peak eluting first will overlap with the ^{13}C rich front of the following peak resulting in a more negative $\delta^{13}C$ value of the following peak being measured than observed. Conversely, for the peak eluting first a somewhat more positive $\delta^{13}C$ value than otherwise observed will be measured due to the overlap with the ^{13}C rich front of the following peak. A third case can arise if the peak of interest is completely coeluted: such an occurrence will be not evidenced, unless CO_2 ratio differentiation is used, making it impossible to rectify the isotope ratio value. As a consequence of the foregoing, a complete separation of the peak before its conversion to CO_2 and its complete integration, from base-to-base level, is mandatory requirement to avoid errors arising from chromatographic isotope fractionation [1, 13, 34].

- ***Column bleed***

While apolar stationary phases are characterized by high thermal stability and low bleed, more polar stationary phases suffer from lower thermal stability, and this often leads to a pronounced bleeding effect. In this situation, the additional CO_2 produced by the combustion of the stationary phase will affect the $\delta^{13}C$ data measured, especially for low-concentrated components. Nowadays, low-bleed stationary phases based on room temperature ionic liquids (RTILs) are available, characterized by polarity comparable to that of polyethylene glycol (SLB-IL60i) phases, but with a different selectivity. These columns thus represent a viable separation alternative, in cases where additional resolution is required [35-36].

- ***Monodimensional vs MDGC-C-IRMS analysis***

Essential oil samples of bergamot (*Citrus bergamia* Risso & Poiteau), helichrysum (*Helichrysum italicum* (Roth) G. Don), myrtus (*Myrtus communis* L.) and rose oil (*Rosa damascena* Mill.) were analysed by monodimensional and multidimensional GC. Given the lack of identification capability of IRMS detection, due to the conversion of the organic molecules to CO_2, the GC effluent was splitted between the IRMS and a qMS detector. In monodimensional applications, identification was achieved using a commercial MS database and applying a double filter, consisting of minimum spectral similarity and a LRI tolerance window. The GCMS software automatically calculated LRIs for the compounds of interest referring to C_7-C_{30} alkanes homologous series analysed under the same chromatographic conditions.

In multidimensional separations, since MS detection was available only after the second dimension, LRI values were calculated according to the 1D stand-by analysis (FID) retention times after the injection of a homologous alkane series. Heart-cuts windows corresponding to +/- 5 LRI units were then selected for each component of interest, because the high repeatability to be expected on the apolar stationary phase employed as 1D [35]. According to the different peak widths, the LRI units (cut windows) were enlarged to fit the wider chromatographic bands. After the 2D separation, the qMS spectra acquired were first filtered according to a minimum spectral similarity of 90% within the MS database, and afterwards selected on the basis of the LRI values, according to the 1D separation.

In a first step, all the samples were subjected to conventional GC-C-IRMS analyses. The need to use a combustion furnace introduces dead volumes into the system, affecting the chromatographic separation negatively; to this concern particular precautions were taken, to minimize these phenomena. Specifically, the use of a high-performance silicon carbide tubular furnace with a small internal diameter allowed to limit the loss of efficiency as well as to preserve the chromatographic resolution. The high efficiency separation of a bergamot essential oil sample showed no significant peak broadening in the resulting GC-C-IRMS chromatogram. In this case, despite the sample complexity, the almost homogenous component distribution along the chromatographic space allowed for a satisfactory separation to be achieved by a monodimensional approach. The absence of significant chromatographic co-elutions, which in turn would affect the accurate estimation of the $\delta^{13}C$ values of the sample components, is reflected in the data listed in Table 2.1.

Table 2.1. **Comparison of the $\delta^{13}C$ data obtained for the main terpene constituents of a bergamot essential oil sample, analysed by conventional GC-C-IRMS and by MDGC-C-IRMS (average of three replicates and standard deviations).**

ID	*Target compound*	*GC-C-IRMS*		*MDGC-C-IRMS*	
		$\delta^{13}C$	Std. dev	$\delta^{13}C$	Std. dev
1	β-Pinene	-29.21	0.21	-29.14	0.20
2	Limonene	-29.00	0.20	-28.94	0.13
3	γ-Terpinene	-30.60	0.12	-31.12	0.11
4	Linalool	-28.70	0.10	-28.97	0.10
5	Linalyl acetate	-29.26	0.24	-29.02	0.12

The $\delta^{13}C$ values measured after monodimensional GC separation and those obtained after multidimensional separation of the bergamot oil components were in good agreement, ranging from 0.10‰ to 0.24‰. While the effectiveness of a conventional GC separation is evident in such situations, on the other hand, unpredictable sources of variations in the chromatographic profile make the employment of multidimensional GC separation highly recommendable. Variations of peak relative amounts may be observed in samples obtained in different harvesting periods, and this could generate unexpected coelutions. Similarly, the formation of oxidation products may occur, leading to additional peak components in the samples, depending on the different storage conditions and sample ageing. The latter would ultimately affect reliability of the $\delta^{13}C$ values measured for the sample components. In other critical separations chosen as case studies, different elution regions of the monodimensional chromatograms were selected for a deeper study under multidimensional conditions. For a summary of the results from data comparison later on discussed, see Table 2.2.

Table 2.2. **Comparison of the $\delta^{13}C$ data obtained for selected constituents of *Myrtus communis* L., *Helichrysum italicum* (Roth) G. Don and *Rosa damascena* Mill. essential oil samples, analysed by conventional GC-C-IRMS and by MDGC-C-IRMS. Linear retention indices are reported, relative to an apolar (5%) stationary phase for the monodimensional application, and to a polar (wax) stationary phase, used as secondary column in the multidimensional applications (n.d.: not detected).**

Sample	*ID*	*Target compound*	*GC-C-IRMS*		*MDGC-C-IRMS*	
			^{1}D LRI	$\delta^{13}C$	^{2}D LRI	$\delta^{13}C$
***Myrtus communis* L.** (Figure 2.2)	1	α-Terpineol	1195	-27.22	1099	-31.24
	2	Myrtenol	1202	-43.52	1191	-30.21

***Helichrysum italicum* (Roth) G. Don** (Figure 2.3)	1	Limonene	1030	-32.29	608	-32.36
	2	α-Copaene	1375	-30.20	898	-31.30
	3	Geranyl acetate	1380	-37.33	1159	-33.34
	4	β-Caryophyllene	1424	-31.08	996	-30.81
	5	*trans*-α-Bergamotene	1432	-11.07	985	-33.23
	6	Trimethyl-dec-en-dione	1434	-41.92	1289	-29.89
	7	Selina-4,11-diene	1476	-27.39	1076	-30.22
	8	γ-Curcumene	1480	-29.75	1090	-30.04
	9	α-Curcumene	1482	-37.92	1173	-33.20
***Rosa damascena* Mill.** (Figure 2.4)	1	Limonene	1030	-27.72	608	-28.55
	2	Eucalyptol	1032	-32.78	614	-29.60
	3	Nerol	1229	n.d.	1189	-26.28
	4	Citronellol	1232	-27.02	1166	-27.24
	5	Geraniol	1255	-24.83	1232	-25.15

The first critical case investigated was myrtus essential oil (Figure 2.2). As in the case of bergamot essential oil, a high number of components were present, but in this sample, the resolution capability of monodimensional GC was insufficient, e.g., in the case of α-terpineol (peak 1) and myrtenol (peak 2), as can be clearly seen in Figure 2.2.a.

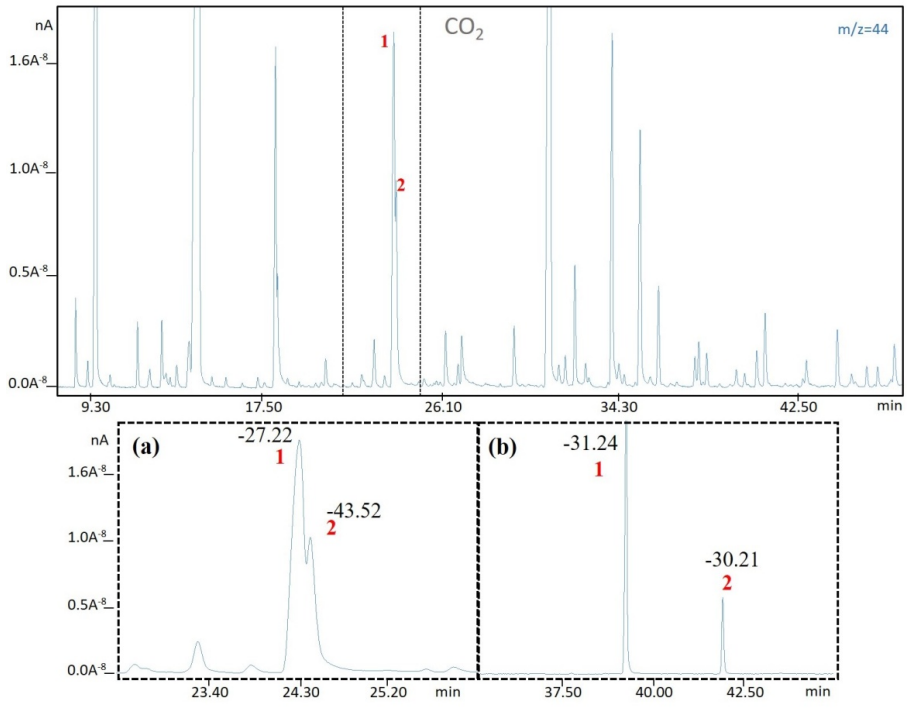

***Figure 2.2. Myrtus communis* L. essential oil GC-C-IRMS chromatogram (upper trace) with zoomed regions showing monodimensional (a) and multidimensional GC separation (b) of two compounds. Peak IDs: (1) α-terpineol, (2) myrtenol.**

These two compounds were characterized by slight differences in LRIs on the 1D (apolar) column (1195 vs 1202), resulting in an insufficient chromatographic resolution. Comparing the

$\delta^{13}C$ values measured after a conventional GC approach with those obtained after multidimensional GC separation (Figure 2.2.b) (see Table 2.2), a significant shift of the isotope values measured was observed for both peaks, due to the incomplete separation achieved in the monodimensional GC separation. In the MDGC approach, the use of a more polar stationary phase in 2D afforded additional selectivity, as it was predictable from the LRI values known for polar phases. As for the latter, LRI values are generally calculated against a fatty acid methyl ester homologue series (FAMEs), in place of the *n*-alkane mixture used for apolar stationary phases. The higher difference in LRI_{FAMEs} on the secondary column (viz, 1099 vs 1191) finally led to the baseline resolution of the two compounds. As a consequence, the ^{13}C value measured for α-terpineol changed from -27.22‰ in monodimensional GC to -31.24‰ in multidimensional GC, while for myrtenol the same values were -43.52‰ and -30.21‰, respectively. A second critical case investigated was helichrysum essential oil. The overall sample composition was mainly represented by oxygenated monoterpenes (≈ 50%) and sesquiterpenes (≈ 15%), eluting in a limited chromatographic space. As showed in Figure 2.3, different critical couples showed up after the monodimensional GC-C-IRMS separation.

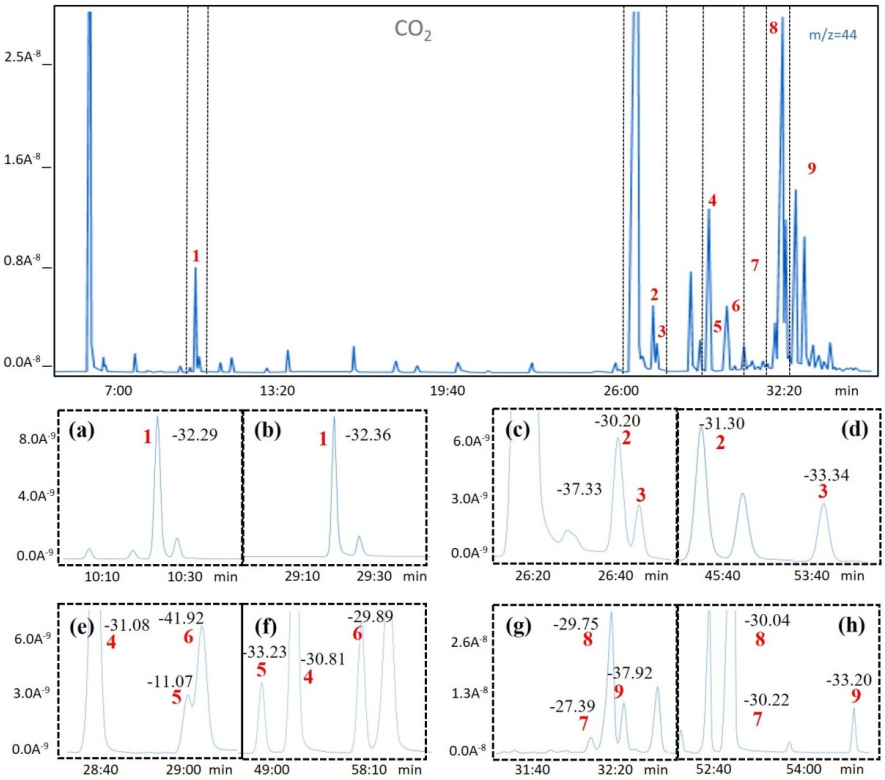

***Figure 2.3. Helichrysum italicum* (Roth) G. Don essential oil GC-C-IRMS chromatogram (centre trace) with zoomed regions showing monodimensional separation (a, c, e, g) and the same zone separated by multidimensional GC (b, d, f, h). Peak IDs: (1) limonene (2) α-copaene, (3) geranyl**

acetate, (4) β-caryophyllene, (5) *trans*-α-bergamotene, (6) trimethyl-dec-en-dione, (7) selinadiene, (8) γ-curcumene, (9) α-curcumene.

As for limonene (peak 1: Figure 2.3.a), since it eluted in the early part of the chromatogram where few terpenes were present, it was sufficiently separated in the monodimensional approach, and its $\delta^{13}C$ value (-32.29‰) was practically the same as the one measured in multidimensional conditions (Figure 2.3.b), where a $\delta^{13}C$ value of -32.36‰ was obtained. On the contrary, moving further in the chromatogram to the busiest zone, it is clear that different coelutions arose.

As predictable, for all the compounds investigated in this crowded part of the chromatogram, a multidimensional approach was highly beneficial in terms of separation, affording much higher resolution compared to the monodimensional analysis. Although the separation between α-copaene (peak 2) and geranyl acetate (peak 3) obtained by monodimensional GC (Figure 2.3.c) apparently was not affected by a significant coelution, yet the comparison of their $\delta^{13}C$ values with those achieved by multidimensional GC (Figure 2.3.d) showed shifted values, according to the mechanisms discussed earlier. In fact, the $\delta^{13}C$ value for α-copaene was slightly more positive (-30.20‰ vs -31.30‰) as a consequence of the coelution occurring at the right end of the peak. However, the variation was rather small, probably due to the lower amount of the compound eluted as the next peak. The situation was exactly the opposite for geranyl acetate, for which an important $\delta^{13}C$ value shift was measured, when comparing the monodimensional and multidimensional approaches, *viz*. -37.33‰ *vs* -33.34‰. In this case, a significantly more negative $\delta^{13}C$ value was obtained in monodimensional GC, since the left-end of the peak was affected by coelution with a higher amount of compound from the previous peak. A comparison of the $\delta^{13}C$ values obtained for β-caryophyllene (peak 4), eluted as a pure peak in both approaches (Figure 2.3.e and f), showed very similar values (-31.08‰ vs -30.81‰). Likewise, an important coelution occurred in the monodimensional GC separation between trans-α-bergamotene (peak 5, LRI 1432) and trimethyl-dec-en-dione (peak 6, LRI 1434), with strong variations attained for $\delta^{13}C$ values of the coeluted peaks, accordingly. An undoubtedly highly positive $\delta^{13}C$ value of -11.07‰ was measured for trans-α-bergamotene, with respect to a $\delta^{13}C$ value of -33.23‰ after baseline separation by MDGC (Figure 2.3.e and f). The same coelution generated an opposite result for trimethyl-dec-en-dione, whose $\delta^{13}C$ values changed from -41.92‰ when partially co-eluted, to -29.89‰ when completely separated by MDGC, as a result of the different selectivity of the polar column (LRI_{FAMEs} differing by around 300 units, *viz*. 985 *vs* 1289). A further example illustrated for this sample

regards selinadiene (peak 7), γ-curcumene (peak 8) and α-curcumene (peak 9). Also in these cases, the $\delta^{13}C$ values measured after monodimensional GC (Figure 2.3.g) were different from those obtained by MDGC measurements (Figure 2.3.h), as a result of the isotopic effect discussed earlier. In fact, only few LRI units spaced the three components on the apolar column, namely 4 LRI units between selinadiene and γ-curcumene (1476 *vs* 1480), and 2 LRI units between γ-curcumene and α-curcumene (1480 *vs* 1482). The coupling of a polar secondary column in MDGC resulted in improved separation and increased LRI_{FAMEs} differential, namely 14 LRI units between selina-4, 11- diene and γ-curcumene (1076 *vs* 1090), and 83 LRI_{FAMEs} units be- tween γ-curcumene and α-curcumene (1090 *vs* 1173). The respective $\delta^{13}C$ values in monodimensional and MDGC were as follows: -27.39‰ *vs* -30.22‰ for selina-4, 11-diene, -29.75‰ *vs* -30.04‰ for γ-curcumene (the highest abundant component, and thus the less affected by other interferences), and -37.92‰ *vs* -33.20‰ for α-curcumene.
Another sample investigated was rose essential oil, illustrated in Figure 2.4.

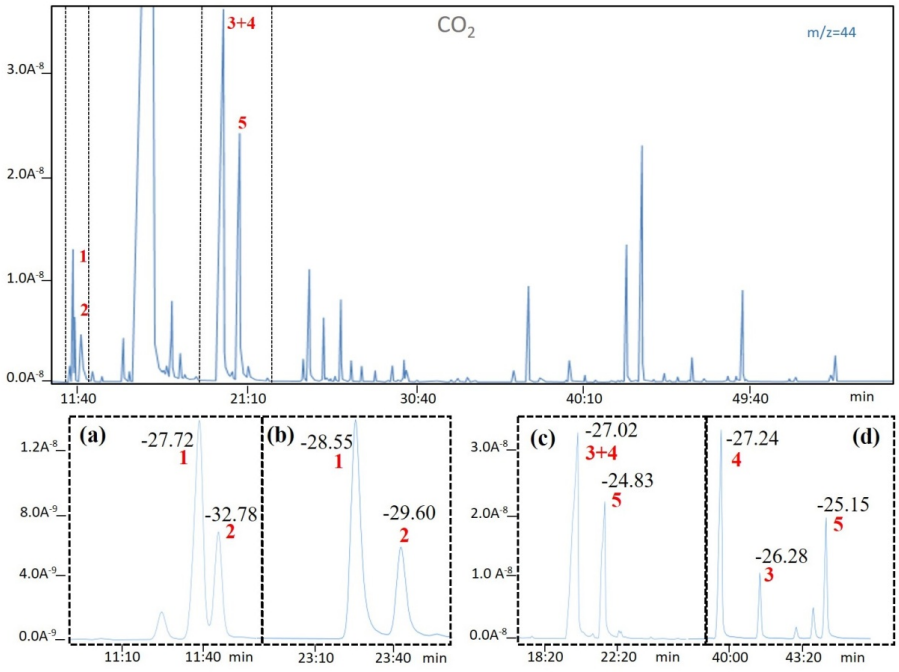

Figure 2.4. Rosa damascena* Mill. *essential oil GC-C-IRMS chromatogram (centre trace) with zoomed regions showing mono (a, c) and relative separation after multidimensional GC (b, d). Peak IDs: (1) limonene, (2) eucalyptol, (3) nerol, (4) citronellol, (5) geraniol.

The first critical pair was represented by limonene and eucalyptol, which on the apolar column were closely eluted peaks as reflected in their similar LRIs, *viz*. 1030 and 1032. Depending on the relative amount of each component in a given sample, these two terpenes may be coeluted;

such evidence usually occurs in Citrus essential oils [9]. In the Rose oil, even if only a tiny coelution was observed for these two components, shifted values were again observed when comparing the $\delta^{13}C$ measurements: limonene (peak 1, Figure 2.4.a) $\delta^{13}C$ value was slightly more positive in monodimensional GC (-27.72‰) with respect to MDGC (Figure 2.4.b) (-28.55‰). Likewise, an important variation was observed for eucalyptol (peak 2), with a more negative value in monodimensional GC, due to the coelution of the left-end of the peak with a higher concentrated component (-32.78‰ *vs* -29.60‰). The most important case to be highlighted is related to nerol (peak 3) and citronellol (peak 4), a similar situation to the limonene-eucalyptol case, with an LRI difference of only three units on an apolar phase (1229 *vs* 1232).

Differently from the previous case where low concentrated components were investigated, citronellol represents one of the major sample components (≈ 10%), and this resulted in the complete coelution with the close-eluted nerol peak; a $\delta^{13}C$ value of -27.02‰ was obtained (Figure 2.4.c). Such a value would be regarded as a correct estimation, being compatible with C_3 plants $\delta^{13}C$ values, since the shape of the peak did not suggest the presence of a coelution, and moreover no qualitative information was available, due to the oxidation of all the components to CO_2. Thus, this can be regarded as the worst situation to be faced when dealing with a GC-C-IRMS investigation, in which the analyst is prone to a wrong estimation of the $\delta^{13}C$ values, caused by the limitations of the monodimensional GC approach.

The potential and usefulness of a multidimensional GC-C-IRMS approach is more evident in such situations. As showed in Figure 2.4.d, nerol and citronellol were baseline separated by MDGC with an inverted elution order with respect to the 1D apolar phase, with LRI_{FAMEs} of 1189 and 1166 on the polar secondary column, respectively. As for their $\delta^{13}C$ value measurements, a value of -27.24‰ was obtained for citronellol, the major sample component, much similar to the value of -27.02‰ attained in monodimensional GC.

Likewise, a value of -26.28‰ was obtained for nerol, being purified only after separation on the 2D column. Also, for the next eluted peak geraniol (peak 5), the MDGC approach allowed for more accurate measurement of the $\delta^{13}C$ value, namely -25.15‰ *vs* -24.83‰ (MDGC *vs* monodimensional GC). A last case involved the investigation of a higher boiling point analyte, namely nootkatone. Due to the higher eluting temperature, when a medium polarity stationary phase is employed as secondary column in a multidimensional column set, the $\delta^{13}C$ measurement would be affected by the stationary phase release, an effect commonly known as column bleed, causing an increased baseline noise. The consequent production of CO_2 in the

combustion step then generates a possible source of error for the evaluation of components eluting in this retention zone. Room temperature ionic liquids (RTILs) have been recently introduced as GC stationary phases, characterized by higher thermal stability compared to stationary phases with similar polarity degree [35,36]. Aiming to evaluate the influence of column bleed, an ionic liquid-based SLB-IL60i with similar polarity was exploited as an alternative to the polyethylene glycol secondary column. A remarkable bleeding effect was observed for the polyethylene glycol column, while with the SLB-IL60i an almost flat baseline was obtained. Concerning the $\delta^{13}C$ measurement, a more negative value was obtained when using the polyethylene glycol column, with respect to that achieved on the ionic liquid stationary phase (-33.64‰ *vs* -32.80‰). Such a result suggests an influence of the different noise level present during the combustion of nootkatone before IRMS detection. In the light of this evidences, the use of a low-bleed column is advisable for compounds that are eluted at high temperatures from a medium-polarity stationary phase.

2.4 Conclusions.

The present research highlighted the common limitations to be faced when dealing with the isotopic ratio evaluation of volatile components separated by gas chromatography. The sample complexity plays a fundamental role in GC-C-IRMS, but unlike what is common in other techniques, where the concept of complexity is commonly associated to a high number of components in a sample, in this technique complexity is more linked to the presence of highly crowded areas of the chromatogram, rather than to the number of components. In general, any type of coelution should be avoided, as deconvolution of overlapping peaks by software algorithms is not straightforward. Insufficient selectivity rather than column overloading effects can lead to incomplete separation, with consequent incorrect measurement of the isotope ratio of the analytes. In addition to cases in which clear coelutions are known, for which the advantage of using the multidimensional technique is foreseeable, also unpredictable coelutions may occur, occasionally generated by oxidative compounds or by compounds added for fraudulent practices. In this context, multidimensional chromatography appears to be of fundamental importance to prevent the aforementioned problems and finally aiming to guarantee accurate results. As with other techniques for which an MDGC approach has made it possible to overcome separation problems (such as GC-FID or enantio-GC), or to simplify the work required of a mass spectrometer, also in GC-C-IRMS it is evident that multidimensional separations play a pivotal and essential role. While in the past this technique could have appeared complex and at the exclusive use of highly specialized personnel, nowadays, thanks to software automation of the heart-cut devices and their wide diffusion in research and quality control laboratories, there is no reason for any IRMS analysis to be left exposed to any of the risks described, when coupled to monodimensional GC separation.

2.5 References.

1. W. Meier-Augenstein, *J. Chromatogr. A* 842 (1999).
2. F. Camin, L. Bontempo, M. Perini, E. Piasentier, *Rev. Food Sci. Food Saf.* 15 (5) (2016).
3. F. Cacciola, P. Donato, D. Sciarrone, P. Dugo, L. Mondello, *Anal. Chem.* 89 (2017) 429.
4. T.K.T. Do, F. Hadji-Minaglou, S. Antoniotti, X. Fernandez, *Trends Anal. Chem.* 66 (2015) 146-157.
5. E. Schimdt, J. Wanner, in: Handbook of Essential Oils, CRC Press, Taylor & Francis Group (2016), pp. 727-728.
6. E. Gil-Av, R.Z. Korman, S. Weinstein, *Biochim. Biophys. Acta* 211 (1970) 101.
7. G. Schomburg, H. Husmanm, E. Hubinger, W.A. Konig, *J. High Resolut. Chromatogr.* 7 (1984) 404-410.
8. I. Bonaccorsi, D. Sciarrone, A. Cotroneo, L. Mondello, P. Dugo, G. Dugo, in Citrus essential oils, RBF 21 (:5) (2011) 841-849.
9. G. Dugo, I. Bonaccorsi, D. Sciarrone, L. Schipilliti, M. Russo, A. Cotroneo, P. Dugo, L. Mondello, V. Raymo *J. Essent. Oil Res.* (24:2) (2012) 93-117.
10. I. Bonaccorsi, D. Sciarrone, L. Schipilliti, P. Dugo, L. Mondello, G. Dugo, *J. Chromatogr. A* 1226 (2012) 87-95.
11. L. Schipilliti, I. Bonaccorsi, D. Sciarrone, L. Dugo, L. Mondello, G. Dugo, *Anal. Bioanal. Chem.* 405 (2-3) (2012) 679-690.
12. P. Dugo, C. Ragonese, M. Russo, D. Sciarrone, L. Santi, A. Cotroneo, L. Mondello, *J. Sep. Sci.* 33 (2010) 3374-3385.
13. J.T. Brenna, T.N. Corso, H.J. Tobias, R.J. Caimi, *Mass Spectrom. Rev.* 16 (1997) 227-258.
14. P.Q. Tranchida, D. Sciarrone, P. Dugo, L. Mondello, *Anal. Chim. Acta* 716 (2012) 66-75.
15. S. Nitz, B. Weinreich, F. Drawert, *J. High Resolut. Chromatog.* 15 (6) (1992) 387-391.
16. H.J. Tobias, G.L. Sacks, Y. Zhang, J.T. Brenna, *Anal. Chem.* 80 (2008) 8613-8621.
17. H.J. Tobias, Y. Zhang, R.J. Auchus, J. T. Brenna, *Anal. Chem.* 83 (2011) 7158-7165.
18. S. Reichert, D. Fischer, S. Asche, A. Mosandl, *Flavour Fragr. J.* 15 (2000) 303-308.
19. Y. Horii, G. Petrick, T. Gamo, J. Falandysz, N. Yamashita, K. Kannan, *Environ. Sci. Technol.* 39 (2005) 4206-4212.
20. S. Sewenig, D. Bullinger, U. Hener, A.J. Mosandl, *Agric. Food Chem.* 53 (2005) 838-844.
21. H. Nara, F. Nakagawa, N. Yoshida, *Rapid Commun. Mass Spectrom.* 20 (2006) 241-247.
22. M. Greule, A. Mosandl, Eur. Food Res. Technol. 226 (2008) 1001-1006.
23. X.F. Sang, I. Gensch, W. Laumer, B. Kammer, C.Y. Chan, G. Engling, A. Wahner, H. Wissel, A. Kiendler-Schar, *Environ. Sci. Technol.* 46 (2012) 3312-3318.
24. A.D. Brailsford, I. Gavrilovìc, R.J. Ansell, D.A. Cowan, A.T. Kicman, *Drug Test. Anal.* 4 (12) (2012).

25. E. Dumont, B. Tienpont, N. Higashi, K. Mitsui, N. Ochiai, H. Kanda, F. David, P. Sandra, *J. Chromatogr. A* 1317 (2013) 230-238.
26. A. Casilli, T. Piper, F. Azamor de Oliveira, M. Costa Padilha, H.M. Pereira, M. Thevis, F.R. de Aquino Neto, *Drug Test. Anal.* 8 (2016).
27. V. Ponsin, E.T. Buscheck, D.J. Hunkeler, *J. Chromatogr. A* 1492 (2017) 117-128.
28. M. Putz, T. Piper, A. Casilli, F. Radler de Aquino Neto, F. Pigozzo, M., *Anal. Chim. Acta* 1030 (2018) 105-114.
29. D. Sciarrone, A. Schepis, M. Zoccali, P. Donato, F. Vita, D. Creti, A. Alpi, L. Mondello, *Anal. Chem.* 90 (2018) 6610-6617.
30. L. Mondello, A. Casilli, P.Q. Tranchida, D. Sciarrone, P. Dugo, G. Dugo, LC-GC Europe 21 (3) (2008) 130-137.
31. S. Pantò, D. Sciarrone, M. Maimone, C. Ragonese, S. Giofrè, P. Donato, S. Farnetti, L. Mondello, *J. Chromatogr. A* 1417 (2015) 96-103.
32. A.L. Sessions, Isotope-ratio detection for gas chromatography, J. Sep. Sci. 29 (2006) 1946-1961.
33. M. Matucha, W. Jockisch, P. Verner, G. Anders, *J. Chromatogr. A* 588 (1-2) (1991) 251-258.
34. M.P. Ricci, D.A. Merritt, K.H. Freeman, J.M. Hayes, *Org. Geochem.* 21 (1994) 561-571.
35. C. Ragonese, D. Sciarrone, P. Dugo, G. Dugo, L. Mondello, *Anal. Chem.* 83 (2011) 7947-7954.
36. J. L. Anderson, D.W. Armstrong, *Anal. Chem.* 77 (2005) 6453-6462.

Chapter 3: Expanding the knowledge related to flavours and fragrances by means of three-dimensional preparative gas chromatography and molecular spectroscopy.

3.1 Introduction.

Myrtus communis L., commonly known as myrtle, is an aromatic perennial shrub belonging to the Myrtaceae family. This plant grows in damp and sunny places and is typical of all the low Mediterranean scrub, from Northern Africa to Southern Europe [1]. Myrtle leaves are evergreen, ovate, or lanceolate, while the flowers are lonely and axillary, white or rosy, and manifest abundantly from late spring to summer. The fruits consist of spherical berries, dark red to violet or white in color depending on the specific variety, which ripen in late fall and persist for long on the plant [2]. Since ancient Greek and Egyptian times, the beneficial properties of *Myrtus communis* L. have been recognized and valued by perfumery and traditional medicine. Myrtle is attributed to several pharmacological effects, and its antimicrobial, anticancer, antidiabetic, antiulcer, antidiarrheal, and anti-inflammatory activities were mentioned in early ethnopharmacological studies [3]. The leaves and berries are sources of essential oil (EO), which is predominantly composed of monoterpenes and oxygenated monoterpenes; the latter is most abundant in extracts obtained from the leaves [4]. However, significant differences have been reported in the volatile fraction, whose chemical composition may differ depending on the geographical origin of the plant [5–7], the organ selected, and the extraction method [8–10]. Moreover, different varieties/cultivars/genotypes of the plants bring about variations in the volatile organic compounds (VOCs) composition [11, 12]. Still, achieving detailed knowledge of EO composition is mandatory to correlate its activities with the presence of specific volatile organic compounds (VOCs). All plant properties are ascribed to the presence of certain components or may result from the synergistic association of some of them. Common approaches to the structural elucidation of unknown VOCs usually involve a chromatographic step for compound isolation, consisting of preparative-GC (prep-GC). The collection of target analytes of suitable purity and in appropriate amounts may be an arduous task when dealing with natural matrices since most of them show medium-to-high complexity. In particular, the analysis of EOs may be cumbersome, as they typically include a multitude of volatile compounds from different chemical classes and in a wide concentration range. Reliable compound identification and quantification for these samples may not be achieved after a single dimension separation, demonstrating the likelihood for (odour/flavour-active) stereoisomers,

which may lead to ambiguous MS library matches [13]. Multidimensional GC (MDGC) performed in the heart-cut mode focuses on selected components in complex matrices and offers interesting advantages for the analysis of target compounds [14]. The potential of multiple heart-cut MDGC has been extensively exploited in flavour and fragrance analysis, and such an approach has been proven effective for removing matrix interferences [15]. Implementing a prep-GC approach requires high-resolution separations, as well as viability for large volume injections of neat samples. To this concern, column selection plays a pivotal role in delivering adequate sample capacity for preparative applications, and mega-bore columns often represent the most suitable choice [16–18]. Nonetheless, the low efficiency of such columns represents a clear disadvantage compared to their narrower-bore counterparts. To overcome this limitation, multiple stationary phases with different selectivity may be combined whenever high resolution is required, and such an approach has been extensively used in prep-GC applications [19–23]. In this study, the essential oil and hydrosol extract of *Myrtus communis* L. leaves obtained from plants collected in the region of Boujmil, Morocco, were analyzed by GC-MS. A total of 75 components were identified, accounting for 98.6% and 93.8% of the oil and the hydrosol extract, respectively. For this purpose, the experimental MS data were matched against MS library databases, with the additional support of the Linear Retention Index (LRI) as a filter. However, identification was not possible for one of the sample constituents, accounting for around 0.78% of the oil and 7.29% of the hydrosol extract since no significant match was obtained by commercial MS libraries. To allow for the structural elucidation of the target compound, a 3D prep-MDGC system was exploited, combining the well-known resolution capability of the heart-cut mode [24,25] with the high sample capacity of wide-bore capillary columns. By these means, the collection of target fractions from a complex sample was attained, with a higher purity degree with respect to that afforded by conventional approaches. Noticeably, the overall analysis time was also conveniently reduced. Afterwards, the target compound was subjected to structural elucidation studies, consisting of MS, NMR, and FTIR spectroscopy.

3.2 Materials and methods.

- ***Plant material and sample preparation***

Myrtus communis L. leaves were randomly collected in January 2020 from wild plants growing in the surroundings of Boujmil (northern Morocco, at 35°45′27″ N altitude and 5°26′25″ W longitude). The myrtle leaves (≈ 500 g) were subjected to conventional hydrodistillation (5–6 h), and the extracted essential oil was treated with anhydrous sodium sulfate and stored at + 4 °C, shielded from the light. The remaining water (700 mL) was poured into a separating funnel, and liquid–liquid extraction of the volatile constituents from the hydrosol was achieved by adding GC-grade ethyl acetate (300 mL) from Merck (Merck Life Science, Darmstadt, Germany). After manual agitation and decantation, the organic phase was separated from the aqueous layer and evaporated to dryness. Finally, the obtained hydrosol extract was stored at +4 °C, shielded from the light. The samples were diluted 1:20 (*v*/*v*) in GC grade n-hexane from Merck (Merck Life Science, Darmstadt, Germany) prior to analysis. A C_7-C_{30} saturated *n*-alkanes (ALKs) mixture and *n*-nonane were used for LRI measurements and internal standardization purposes, respectively, kindly provided by Merck (Merck Life Science, Darmstadt, Germany). Deuterated chloroform ($CDCl_3$ 99.8% atom D, Merck Life Science, Darmstadt, Germany) was used to dissolve the target analyte collected after the 3D-MDGC-prep step prior to NMR experiments.

- ***GC-FID and GC-MS***

GC analyses were performed on a Shimadzu GC-2010 Plus gas chromatograph equipped with an AOC-20i series auto injector and a GCMS-QP2010 Ultra system mass spectrometer (Shimadzu Europa, Duisburg, Germany) with an electron ionization (EI) source. The column was an SLB-5ms (silphenylene polymer, virtually equivalent to poly (5% diphenyl/95% methylsiloxane)), 30 m × 0.25 mm i.d. × 0.25 μm d_f, capillary stationary phase from Merck (Merck Life Science, Darmstadt, Germany). The separations were performed under the following conditions: oven temperature program, 50 °C to 300 °C, at 3 °C min^{-1}; split/splitless injector, 280 °C; injection mode, split (1:10 ratio); injection volume, 0.5 μL. For GC-FID analyses, helium was used as a carrier gas at a constant linear velocity of 30.0 cm s^{-1}, and the inlet pressure was set to 99.5 kPa. FID (310 °C) gases were H_2 at 40.0 mL min^{-1} and air at 400 mL min^{-1}; the sampling rate was 80 msec. Data were acquired by LabSolutions software ver. 5.92 (Shimadzu Europa, Duisburg, Germany). GC-MS analyses were carried out as follows: inlet pressure, 26.7 kPa; carrier gas, He at a constant linear velocity of 30 cm s^{-1}; source

temperature, 220 °C; interface temperature, 250 °C; mass scan range, 40–400 m/z; scan speed, 10 Hz. Data were acquired using GCMS solution software ver. 4.30 (Shimadzu Europa, Duisburg, Germany). Identification was achieved by searching the experimental data in the W11N17 (Wiley11-NIST17, Wiley, Hoboken, NJ, USA) and FFNSC ver. 4.0 (Shimadzu Europa, Duisburg, Germany) mass spectral databases for library matching with the additional support of an LRI filter.

- ***Preparative Multidimensional GC***

The prep-MDGC system employed, illustrated in Figure 3.1, consisted of three Shimadzu GC-2010 Plus gas chromatographs (GC1, GC2, GC3), each equipped with a Deans switch (DS) transfer device (Shimadzu Europa, Duisburg, Germany), and an advanced pressure control system (APC1, APC2, APC3) which supplied the carrier gas (He); for more details see Sciarrone et al. [26]. The first dimension (1D) column was an Equity-5 [poly (5% diphenyl/95% dimethylsiloxane)], 30 m × 0.53 mm i.d. × 5 μm d_f (Merck Life Science, Darmstadt, Germany), preceded by a 1 m segment of an uncoated column of the same i.d. FID1 (300 °C) connected to DS1 via a 1 m × 0.22 mm i.d. segment of the uncoated column. Carrier gas pressure was maintained constant at 124.7 kPa, while a constant pressure of 110 kPa was applied to APC1. The oven temperature program in 1D was: 40 °C to 230 °C at 10 °C min^{-1} and 230 °C to 280 °C at 3 °C min^{-1} (held for 40.00 min); the transfer line between GC1 and GC2 was maintained at 240 °C. The second dimension (2D) column was a Supelcowax-10 (100% polyethylene glycol, PEG), 30 m × 0.53 mm i.d. × 1.0 μm d_f (Merck Life Science, Darmstadt, Germany). FID2 (300 °C) was connected to DS2 via a 0.5 m × 0.25 mm i.d. segment of the uncoated column. The oven temperature program in 2D was: 50 °C (held for 32.50 min) to 200 °C at 10 °C min^{-1} and 200 °C to 240 °C at 5 °C min^{-1} (held for 20.00 min); the transfer line between GC2 and GC3 was maintained at 240 °C. APC2 pressure was maintained constant at 95 kPa. The third dimension (3D) column was an SLB-IL59 (custom-made ionic liquid) 30 m × 0.53 mm i.d. × 0.8 μm d_f (Merck Life Science, Darmstadt, Germany). FID3 (300 °C) was connected to DS3 via a 0.6 m × 0.18 mm i.d. segment of the uncoated column. The oven temperature program in 3D was: 100 °C (held for 54.10 min) to 240 °C at 5 °C min^{-1}. APC3 pressure was programmed as follows: 43.5 kPa (held for 54.10 min) to 60 kPa at 400 kPa min^{-1} (held for 28.00 min). Detector gases (for FID1, 2, and 3) were H_2 at 50.0 mL min^{-1} and air at 400 mL min^{-1}; the sampling rate was 40 msec. Data were collected by MDGCsolution software ver. 2.43.00 (Shimadzu Europa, Duisburg, Germany). A lab-made modified GC injector port was used as the collection device. The collection system (Figure 1) consisted of a heated (250

°C) aluminium block (3 cm length × 1.5 cm width × 11 cm height), with two liners in series located inside and held in position by means of two nuts: the bottom *liner* was fixed to drive the retention gap (0.3 m × 0.18 mm i.d.) into the upper one, which was removable and used to collect the condensed gas stream. After analyte isolation, the collection tube was removed and flushed in a 2 mL vial with 100 µL deuterated chloroform. The collected fraction containing the target compound was analysed by GC-MS and GC-FID for qualitative and quantitative purposes, respectively, prior to GC-FTIR and NMR analyses.

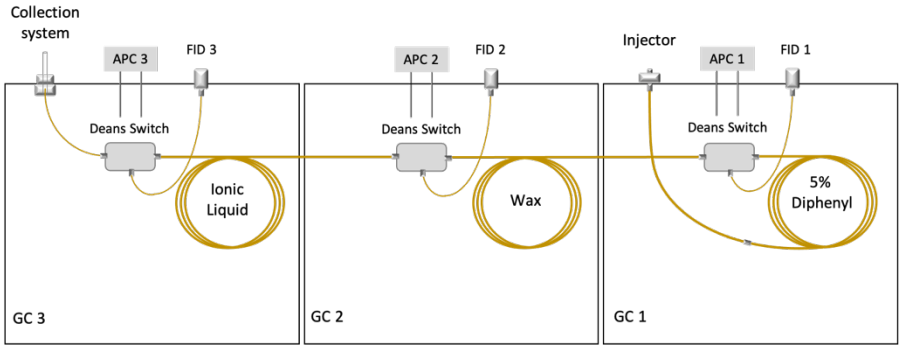

Figure 3.1. **Scheme of Prep-MDGC prototype.**

- ***Nuclear Magnetic Resonance***

^{1}H and $^{13}C\{1H\}$ NMR spectra were recorded on an Agilent Propulse 500 MHz spectrometer equipped with a OneNMR probe (Agilent Technologies, Inc., Santa Clara, CA, USA) operating at 499.74 (^{1}H) or 125.73 MHz ($^{13}C\{^{1}H\}$). After collection by prep-MDGC, the sample was dissolved in chloroform-d, poured into a 5 mm test tube, and analyzed after locking on the deuterium lock signal, searching for a good field homogeneity (shimming), and setting the frequency modulation (tuning). The ^{1}H saturation 90° pulse was calculated as 8 µs at 61 dB of power level, while the protonic spectrum was recorded under 2 s acquisition time, 2 s scan delay, and 16 scans. Complete and unambiguous assignment was achieved by processing homo nuclear 2D-Correlation Spectroscopy (2D-COSY), Total-Correlation Spectroscopy (TOCSY), and Rotating Frame Overhauser Effect Spectroscopy (ROESY) [27] experiments together with the heteronuclear ^{13}C $\{^{1}H\}$-Heteronuclear Single-Quantum Coherence (HSQC) and ^{13}C-Heteronuclear Multiple Bond Correlation (HMBC) experiments, as described elsewhere [28]. Calibration was attained using the residual proton signal of the solvent as the internal standard ($CDCl_3$ singlet at δ = 7.26 ppm and ^{13}C solvent triplet at δ = 79.0 ppm). Data were processed by Agilent VnmrJ software version 4.2 (Agilent Technologies, Inc., Santa Clara, CA, USA) and by the ACD/Spectrus Processor 2015 Pack 2 inside the ACD Lab software package

(Advanced Chemistry Development, Inc., Toronto, ON, CA, USA), which was also exploited for validation.

- ***Solid Phase GC-FTIR***

The GC-FTIR spectra were acquired by a DANI Master GC (Dani Instruments, Milan, Italy) coupled with a DiscovIR-GC (Spectra Analysis Instruments, Inc., Marlborough, MA, USA) detector. The same column as for the GC-MS experiment was used. GC parameters were as follows: injection volume, 1 μL at 280 °C in the split mode (1:10); carrier gas, He at constant linear velocity, 30 cm s^{-1}; temperature program, 50 °C to 280 °C, at 5 °C min^{-1} (held for 5 min). The transfer line and restrictor temperature were 280 °C. FTIR spectra were acquired from 4000 to 700 cm^{-1}, at a resolution of 4 cm^{-1}. The column eluent was directly deposited on a cryogenically cooled ZnSe sample disc, which was cooled down to -50 °C by means of liquid nitrogen and rotated at 3 mm min^{-1}. The FTIR instrument was equipped with a Mercury Cadmium Telluride (MCT) cryogenically cooled detector. GRAMS/AI Spectroscopy software version 9.3 (Thermo Fisher Scientific, Inc., Waltham, MA, USA) was used to perform the calculation of IR response *vs*. time.

3.3 Results and discussions.

- ***GC-MS and GC-FID analyses***

The composition of the EO and hydrosol volatile fractions of the *M. communis* L. leaves was investigated by GC-MS (Figure 3.2) and GC-FID analyses; 75 components were detected in both samples, accounting for 98.6% and 93.8% of the oil and extract, respectively. Peak identification was achieved by means of GC-MS exploiting the linear retention indices (LRIs) calculated against a C_7–C_{30} alkane homologous series. Two filters were applied as criteria for positive identification in the library search, namely a minimum MS similarity of 85% and a tolerance window of ±5 LRI units with respect to the experimental LRI. Only one component, accounting for about 0.78% of the oil and 7.29% of the hydrosol extract, was not identified due to the lack of any spectral and LRI data in the MS libraries.

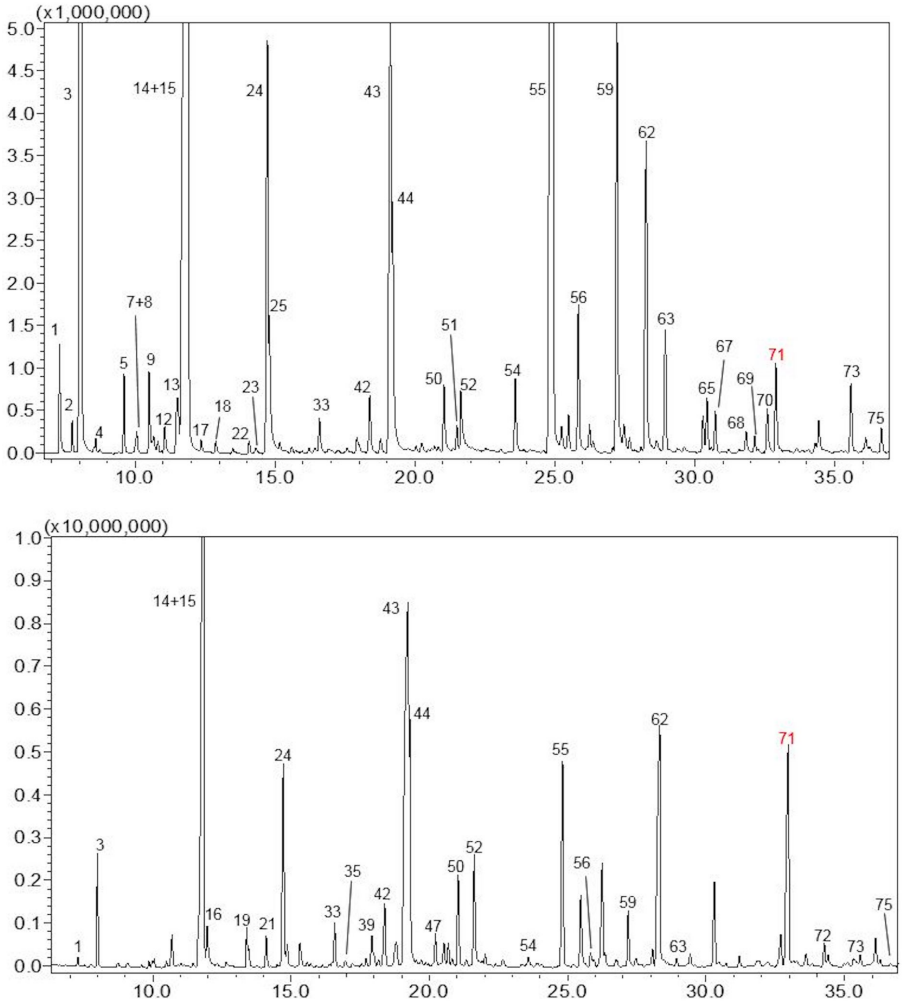

***Figure 3.2*. GC-MS chromatograms of *M. communis* L. essential oil (upper trace) and hydrosol extract (lower trace). For peak identification, refer to Table 1 (the unknown compound is labeled in red).**

Table 3.1. **VOCs quali-quantitative profile of *M. communis* L. leaves essential oil and hydrosol extracts.**

ID	Compounds	LRI_{theor}	LRI_{exp}	Essential Oil	LRI_{exp}	Hydrosol
1	Isobutyl isobutyrate	913	912	0.64	912	0.15
2	α-Thujene	927	925	0.19	-	-
3	α-Pinene	933	934	14.61	933	1.75
4	Camphene	953	948	0.08	-	-
5	β-Pinene	978	977	0.51	977	0.05
6	6-methyl-Hept-5-en-2-one	986	-	-	984	0.07
7	trans-5-Isopropenyl-2-methyl-2-vinyl-tetrahydrofuran	989	990	0.13	990	0.14
8	Myrcene	991	989	0.04	-	-
9	isobutyl 2-methyl Butyrate	1002	1002	0.57	1002	0.13
10	cis-dehydro-Linalool oxide	1006	1006	0.19	1006	0.12
11	δ-3-Carene	1009	1009	0.08	-	-
12	Isopentyl isobutyrate	1014	1015	0.23	1014	0.04
13	*p*-Cymene	1025	1026	0.68	1025	0.08
14	Limonene	1030	1029	3.54	1029	1.03
15	Eucalyptol	1032	1035	27.25	1033	22.46
16	Benzyl alcohol	1040	-	-	1036	0.91
17	trans-β-Ocimene	1046	1046	0.08	-	-
18	γ-Terpinene	1058	1058	0.09	-	-
19	cis-Linalool oxide	1069	-	-	1070	0.71
20	*m*-Cresol	1073	-	-	1078	0.04
21	trans-Linalool oxide	1086	-	-	1086	0.60
22	Terpinolene	1086	1086	0.11	-	-
23	*p*-Cymenene	1093	1092	0.07	-	-
24	Linalool	1101	1101	4.94	1101	4.81
25	3-methylbutyl-2-methyl-Butyrate	1104	1103	1.24	-	-
26	trans-*p*-Mentha-2,8-dien-1-ol	1122	-	-	1123	0.04
27	Fenchyl alcohol	1123	1120	0.05	1120	0.09
28	α-Campholenal	1125	-	-	1127	0.03
29	Limona ketone	1131	-	-	1132	0.04
30	cis-Limonene oxide	1134	1134	0.05	-	-
31	cis-p-Mentha-2,8-dien-1-ol	1138	-	-	1137	0.07
32	Nopinone	1139	-	-	1140	0.06
33	trans-Pinocarveol	1141	1142	0.34	1142	0.84
34	trans-Verbenol	1145	1148	0.09	-	-
35	cis-β-Terpineol	1149	-	-	1150	0.15
36	Camphene hydrate	1156	-	-	1156	0.08
37	Menthone	1158	1157	0.04	-	-
38	Pinocarvone	1164	1164	0.06	1163	0.04
39	δ-Terpineol	1170	1171	0.24	1171	0.98
40	Borneol	1173	1173	0.06	1173	0.15
41	trans-Linalool oxide (pyranoid)	1174	1176	-	1176	0.15

42	Terpinen-4-ol	1184	1181	0.58	1181	1.58
43	α-Terpineol	1195	1198	7.14	1200	22.74
44	Myrtenol	1202	1199	2.14	1201	3.85
45	Verbenone	1208	-	-	1210	0.13
46	Fenchyl acetate	1219	1218	0.04	-	-
47	trans-Carveol	1223	1222	0.10	1222	0.67
48	cis-*p*-Mentha-1(7),8-dien-2-ol	1230	1230	0.06	1232	0.43
49	cis-Carveol	1232	-	-	1235	0.11
50	Pulegone	1241	1240	0.63	1240	2.02
51	Linalyl acetate	1250	1250	0.20	-	-
52	Geraniol	1255	1253	0.68	1253	2.59
53	Geranial	1268	-	-	1269	0.05
54	trans-Pinocarvyl acetate	1296	1296	0.65	1296	0.18
55	Myrtenyl acetate	1324	1327	15.96	1327	5.16
56	α-Terpenyl acetate	1349	1348	1.39	1347	0.43
57	cis-Geranyl acetate	1361	1360	0.15	-	-
58	α-Copaene	1375	1376	0.10	-	-
59	trans-Geranyl acetate	1380	1379	4.22	1378	1.22
60	trans-Myrtanol acetate	1387	1385	0.32	-	-
61	β-Elemene	1390	1390	0.12	-	-
62	Methyl eugenol	1403	1403	3.33	1405	8.50
63	β-Caryophyllene	1424	1420	1.11	1419	0.17
64	Perillyl acetate	1435	1436	0.06	-	-
65	α-Humulene	1454	1456	0.47	-	-
66	β-Santalene	1459	1459	0.05	-	-
67	Myrtenyl isobutyrate	1463	1463	0.34	-	-
68	β-Selinene	1492	1489	0.24	-	-
69	α-Selinene	1501	1497	0.14	-	-
70	Geranyl isobutyrate	1507	1508	0.42	-	-
71	Unknown	-	1515	0.78	1515	7.29
72	Elemicin	1548	-	-	1550	0.53
73	Caryophyllene oxide	1587	1583	0.65	1583	0.26
74	Geranyl 2-methylbutyrate	1596	1597	0.19	-	-
75	Humulene epoxide II	1613	1612	0.24	1611	0.07
	TOT			98.60		93.79

LRI $_{exp}$, calculated on SLB-5ms column;

LRI $_{theor}$, reported in the commercial MS library FFNSC 4.0 (Shimadzu Europa)

The composition data obtained for the oil (see Table 3.1) were in good accordance with the literature data relative to Moroccan *M. communis* L. leaves, with eucalyptol, myrtenyl acetate, and α-pinene being the oil's major components [7, 11, 29]. The presence of an unknown compound as a trace constituent of myrtle oil was previously described by Weyerstahl *et al.*, but in that study, only the relative abundances of the lower-mass ions (fragments) of the molecule were reported [30]. In a first step, those data were used to build the MS spectrum of

the molecule, with the aim to add it to a test MS database and to carry out a similarity search for the target component in the myrtle samples. Very low spectral similarity (66%) was obtained for the target compound, probably due to the lack of many ion fragments from the MS spectrum, which make the identification of the compound based on the literature data unreliable. Thus, isolation of the compound of interest was necessary to attain confident identification. With oxygenated compounds being predominant in hydrosol extract [31], the latter was used as the starting material for the collection and purification of the target compound by means of the prep-MDGC.

- ***Preparative MDGC analysis***

A mandatory prerequisite for the structural elucidation of unknown compounds is the isolation and collection of sufficient amounts of the target molecule with a suitable degree of purity. Depending on the technique employed (e.g., NMR), up to mg levels may be required to carry out spectroscopic analyses successfully. Apart from the obvious constraints in terms of limited separation capacity, conventional prep-GC methods involve a long analysis time to achieve the collection of adequate quantities of pure compounds. Micro-bore capillary columns typically employed in prep-GC deliver high efficiency, but limited volumes of diluted samples need to be injected, per run, to prevent peak skewing and loss of resolution. On the other hand, the lower separation efficiency resulting from the use of a wide bore column would be problematic for most applications due to the low purity of the collected fractions containing co-eluted compounds. In this research, a prep-MDGC method was implemented, aiming to overcome the major limitations associated with the use of monodimensional GC approaches. For this purpose, 0.53 mm i.d. columns were selected for all the separation steps to obtain increased sample capacity. To ensure we were not trading resolution and efficiency for load capacity, a three-dimensional prep-GC system was implemented by the coupling of three stationary phases with different selectivity. Specifically, a silphenylene polymer, virtually equivalent in polarity to poly (5% diphenyl/95% methylsiloxane), was employed as ^{1}D, a 100% polyethylene glycol as ^{2}D, and a medium-polarity ionic liquid-based column as ^{3}D. This setup allowed for highly pure fractions to be obtained by means of heart-cut MDGC. Moreover, mg amounts of the target compound could be collected in a reasonable analysis time due to the injection of a higher volume of the oil sample. ^{1}D stand-by analysis was performed by the direct injection of 2 μL of the sample. As can be appreciated in the ^{1}D stand-by chromatogram (black trace in Figure 3.3), a clear overload effect resulted for the target fraction, and thus a different retention mechanism was necessary to achieve satisfactory separation.

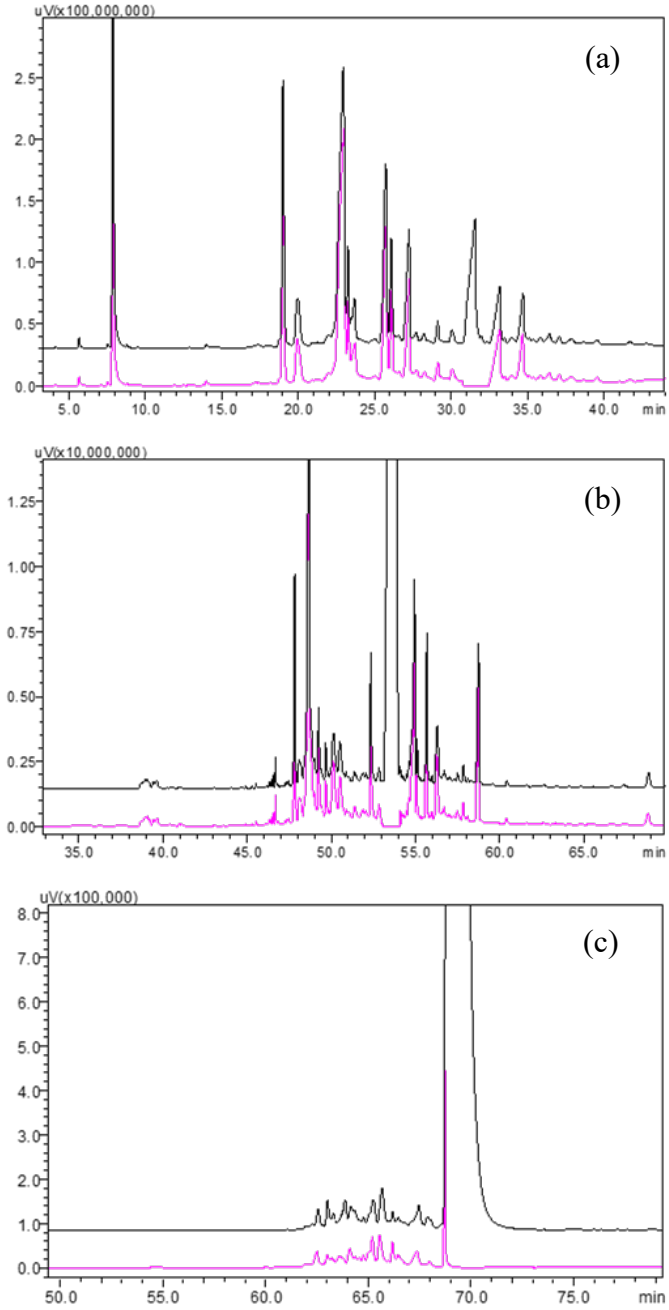

Figure 3.3. **Prep-MDGC stand-by (black trace) and cut (pink trace) chromatograms of *M. communis* L. hydrosol extract relative to the first, ^{1}D (a), second, ^{2}D (b), and third dimension, ^{3}D (c).**

A ^{1}D cut window from 30.70 to 32.50 min was selected, and the ^{2}D stand-by chromatogram was obtained on a PEG stationary phase. As can be noticed in Figure 3.3, the heart-cut fraction transferred from ^{1}D still resulted in being greatly impure due to the significant overload effect caused by the injection of a very high sample amount. In the stand-by analysis on the PEG column (^{2}D), the target peak indeed accounted for only 75% of the whole fraction transferred. In a conventional MDGC approach, consisting of two chromatographic steps, a final heart-cut

would have been applied for the collection of the target peak. Despite this, GC-MS analysis of the fraction collected after the ^{2}D separation still revealed the co-elution of many sample components with the target peak (data not shown). Hence, a second heart-cut step was performed by selecting a ^{2}D cut window from 53.00 to 54.10 min. As shown in the ^{3}D stand-by chromatogram in Figure 3, the target peak was further purified from the fraction transferred because of a third separation step on the ionic liquid stationary phase. The latter had similar polarity to the PEG column but different selectivity. A third heart-cut window, from 68.60 to 71.00 min, was performed to collect the purified compound through its diversion to the collector system located inside the modified ^{3}D injection port. Once the eluent was trapped, the collection tube was immediately removed and flushed in a 2 mL vial with 100 μL deuterated chloroform (to ensure compatibility with subsequent NMR analysis). To attain complete recovery of the fraction from the collection tube, the latter was washed again with the same solvent, and the solution obtained was injected into a GC-MS system: no peaks showed up, confirming the complete removal of the condensed fraction. A total of 12 prep-MDGC collections were performed to collect sufficient sample amounts for the NMR experiments. The solution obtained was spiked with *n*-nonane as the internal standard (10,000 ppm) and analyzed by means of GC-FID. Recovery was extrapolated from a calibration curve built using β-caryophyllene *vs* the internal standard. Around 2.0 mg were collected in a total of 16 h, with an average collection recovery of approximately 90% and a purity degree of 99%. GC-FID (Figure 3.4) and GC-MS analyses were carried out to check the degree of purity of the target compound, as well as for identification purposes.

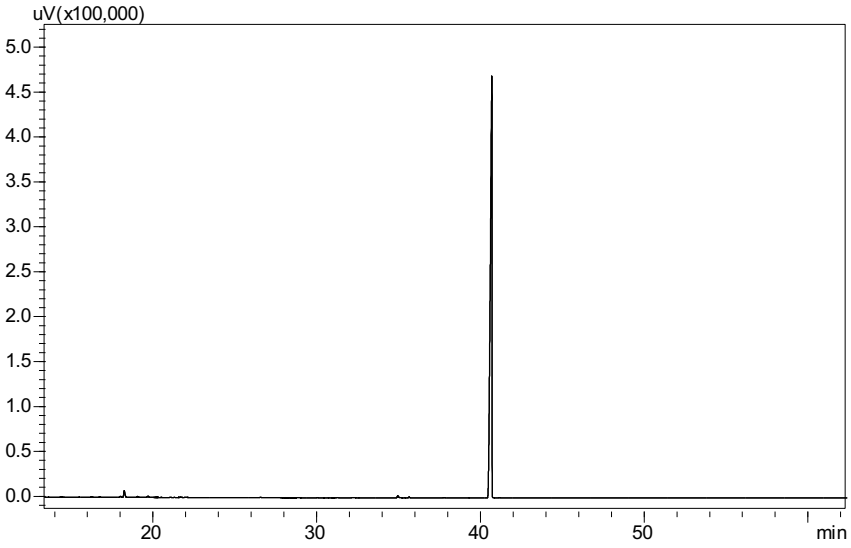

Figure 3.4. **GC-FID chromatogram of the target compound isolated from *M. communis* L. hydrosol extract.**

- ***Spectroscopic data and structural elucidation***

Once pure milligrams of the target molecule were collected by means of the prep-MDGC approach and spectroscopic analyses were carried out for structure elucidation, consisting of solid phase GC-FTIR and NMR. Although not widespread, hyphenated GC-FTIR provides a very useful identification tool through the combination of highly efficient separation and highly specific fingerprinting of functional groups in unknown substances. Furthermore, the information provided by FTIR detection is complementary to those afforded by MS and may assist in the discrimination between isobaric compounds and regioisomers. Noticeably, GC-FTIR techniques based on the use of solid deposition interfaces provide superior resolution and lower detection limits compared to gas phase devices [32,33]. In this study, FTIR analyses were performed by direct micro deposition of the column eluent after a GC separation on a cryogenically cooled ZnSe sample disc. Solid phase IR spectra of the eluted compounds were recorded in real-time from 10 μm × 10 μm spots in the 4000–700 cm^{-1} range, with a resolution of 4 cm^{-1}. Disc rotation speed plays a fundamental role in determining the overall performance of the GC-FTIR technique since it should allow for sufficient data points to be taken across the GC peak, to obtain a good quality IR spectrum [34]. Hereby, a disc speed of 3 mm min^{-1} provided the best results in terms of detection sensitivity whilst preserving the chromatographic resolution. A second parameter affecting the sensitivity of solid phase GC-FTIR is the amount of chilling provided to the ZnSe disc, which related to the volatility degree of the analytes to be deposited. In these experiments, the maximum analyte recovery in the solid state was obtained at a disc temperature of –50 °C. The reconstructed FTIR spectrum of the target compound obtained in the mid-IR is shown in Figure 5. In the high wavenumber region, absorptions due to C–H stretching were detected from 3000–2840 cm^{-1}, while the stretching vibrations of the C=C bonds gave rise to a band centered at 1637 cm^{-1}. Finally, a carbonyl stretching vibration band C=O showed up as a strong signal at 1715 cm^{-1}, typical of the saturated ketones.

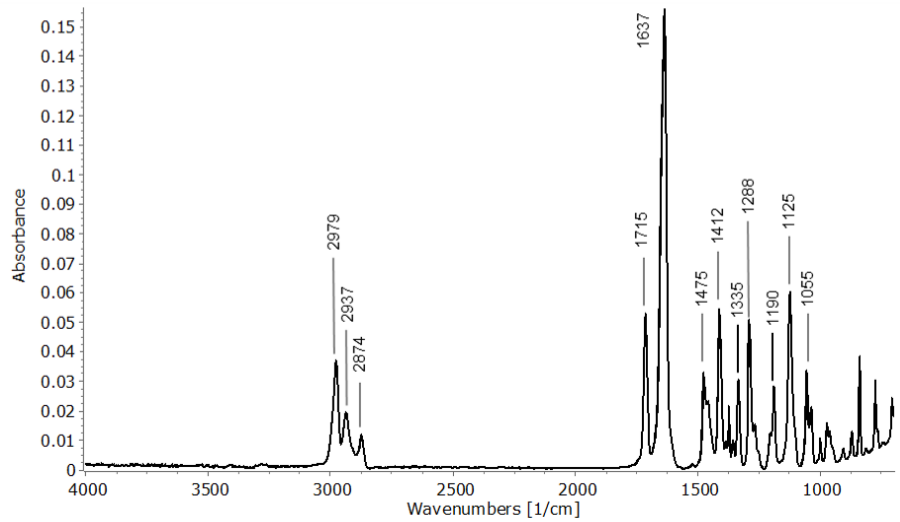

***Figure 3.5*. Solid phase GC-FTIR spectrum of the target compound.**

NMR spectra of the target molecule were acquired, exploiting both 1D and 2D NMR techniques to detect proton and ^{13}C resonances. Figure 6 show the monodimensional ^{1}H and two ^{1}H-^{13}C hetero-correlated experiments, namely HSQC and HMBC. The first two experiments define the unambiguous chemical shift (δ) assignment of the proton resonances and the relative ^{13}C parent resonances. The last HMBC spectrum, connecting ^{1}H and ^{13}C resonances through two or three bonds (^{2}J and ^{3}J), is shown in Figure 6c and allowed the assignment of the quaternary ^{13}C resonances opening the way to the definite structural elucidation.

(a)

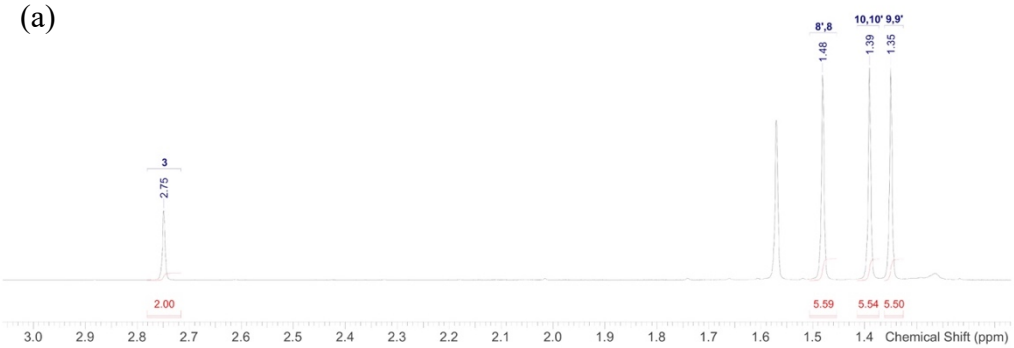

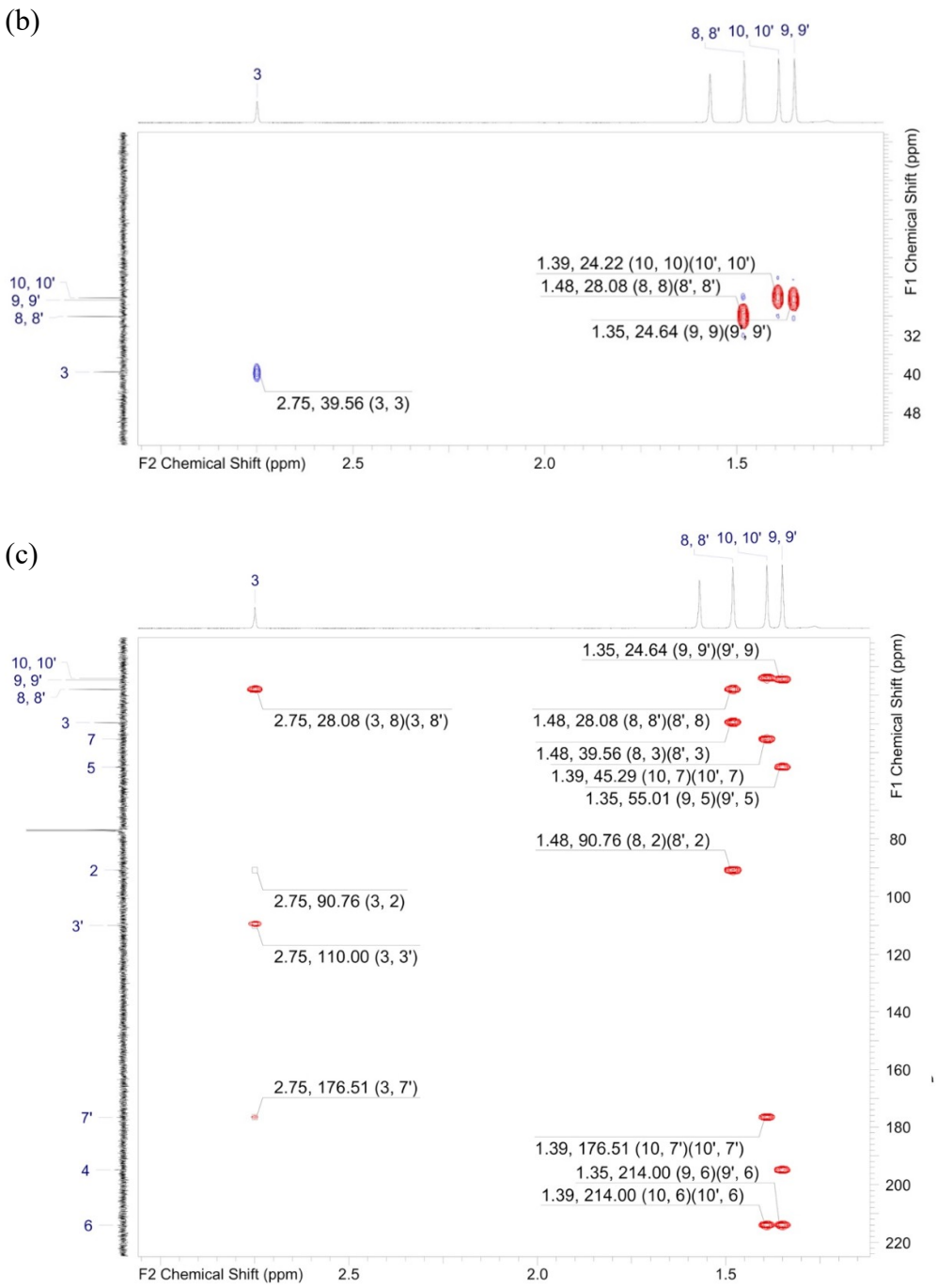

Figure 3.6. **(a) ^{1}H-NMR spectrum with the related assignment; (b) ^{1}H-^{13}C (HSQC) enlightening the presence of the hydrogen-connected carbon atoms; (c) ^{13}C{^{1}H}-HMBC spectrum detecting the carbon atoms and the related connectivity also represented in the molecular diagram.**

A molecular drawing with the number labelling scheme is represented in Figure 3.7, corresponding to the assignment in Table 3.2, also including the consistent connections.

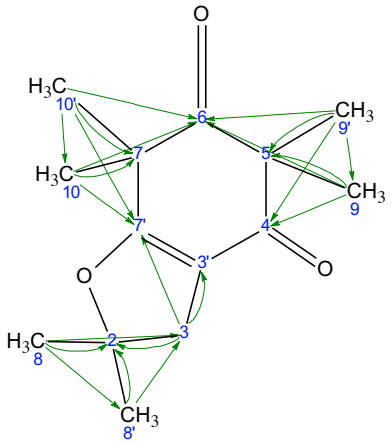

***Figure 3.7*. Molecular drawing with the atom-labelling scheme used for the assignment, according to the nomenclature rules.**

***Table 3.2*. Label, calculated, and assigned chemical shifts for any ^{1}H and ^{13}C of the molecule with the related heteronuclear connections.**

^{13}C Label	^{13}C Shift	Type	^{1}H Label	^{1}H Shift	^{13}C Calc Shift	^{1}H Calc Shift	^{13}C Count	^{1}H Count	^{1}H HMBC	^{13}C HMBC
C 2	90.8	C			87.93				8, 8', 3	
C 3	39.6	CH_2	H 3	2.749	37.73	2.706	1	2	8, 8'	8, 8', 2, 3', 7'
C 3'	110	C			112.96				3	
C 4	195	C			193.51				9', 9	
C 5	55	C			55.74				9', 9	
C 6	214	C			210.81				9', 9, 10', 10	
C 7	45.3	C			45.06				10', 10	
C 7'	177	C			171.22				10', 10, 3	
C 8	28.1	CH_3	H 8	1.482	28.39	1.411	2	6	3	3, 2
C 9	24.6	CH_3	H 9	1.351	21.25	1.335	2	6		5, 4, 6
C 10	24.2	CH_3	H 10	1.391	23.29	1.348	2	6		7, 7', 6

In detail, the protonic spectrum showed only four signals, with relative integrations 2:6:6:6. The related HSQC edited experiment highlighted the presence of six methyl groups distributed in three equivalent couples and one methylene group. Taking advantage of ^{2}D HMBC hetero-correlated spectroscopy, it was possible to detect seven quaternary carbon atoms. Among the latter ^{13}C signals, three were over 170 ppm. Considering that oxygen represented the only other atom type in the molecule, it was arguable that the three high-frequency ^{13}C were each connected to three different oxygen atoms. Such an observation was consistent with the

chemical formula $C_{14}H_{20}O_3$ and the molecular weight of 236 amu, obtained from the corresponding MS spectrum. The definite structure elucidation came from direct (COSY and HSQC) and long-range (TOCSY and HMBC) connections, eliciting the structure in Figure 7, corresponding to 2,2,5,5,7,7-hexamethyl-3,7-dihydro-1-benzofuran-4,6(2H,5H)-dione. Finally, an experimental LRI value of 1518 was calculated for the isolated compound on an SLB-5ms column against ALKs C_7-C_{30} homologous series. All the data collected were used to register the new compound in the FFNSC 5.0 MS database. This would allow future researchers to attain quick and reliable compound identification by database search. Despite being described as part of the volatile myrtle components [35], this compound was absent in commercial MS databases, and thus its identification could not be achieved by means of GC-MS. Additionally, recent studies described 2,2,5,5,7,7-hexamethyl-2,3-dihydrobenzofuran-4,6(5H,7H)-dione as a key biosynthetic precursor of the acylphloroglucinols myrtucommulone J and myrtucommuacetalone. A wide range of biological activities have also been demonstrated for these two compounds isolated from *M. communis* L. [36].

3.4. Conclusions.

A three-dimensional prep-MDGC setup was implemented, allowing for the collection of mg amounts of a target compound from the volatile myrtle fraction, with a high degree of purity and reduced time with respect to conventional approaches. Three consecutive heart cuts were performed on stationary phases of different selectivity prior to the structural elucidation of the target compound by means of GC-MS, GC-FTIR, and NMR spectroscopy. The complementary data gathered by different spectroscopic techniques allowed us to identify the target compound isolated as 2,2,5,5,7,7-hexamethyl-3,7-dihydro-1-benzofuran-4,6(2H,5H)-dione. This molecule was already registered with a CAS number 162885-71-4, but scarce information was available in the literature, and spectral data were absent in commercial MS libraries. It must be emphasized that if this target molecule was present in a sample different from Myrtus EO, no reference data would be found in the literature, and since no MS database contains information about this analyte, there would not be any chance to identify it. Hereby, after achieving detailed knowledge of the chemical structure and spectroscopic features of the purified compound, it was registered into the FFNSC 5.0 MS library, making it readily available for future research. Interestingly, this also lays the basis for further research aimed at the investigation of compound activities, which may be of interest to different concerns.

3.5. References.

1. A. Hennia, S. Nemmiche, S. Dandlen, M.G. Miguel, *J. Essent. Oil Res*. 31 (2019) 487–545.
2. J. Migliore, A. Baumel, M. Juin, F. Médail, *J. Biogeogr*. 39 (2012) 942–956.
3. M. Sisay, T. Gashaw, *Evid. Based Complement. Alternat. Med*. 22 (2017) 1035–1043.
4. M. Brada, N. Tabti, H. Boutoumi, J.P. Wathelet, G. Lognay, *J. Essent. Oil Res*. 24 (2012) 1–3.
5. A. Bouzabata, V. Castole, A. Bighelli, L. Abed, J. Casanova, F. Tomi, *Chem. Biodivers*. 10 (2013) 129–137.
6. M. Rahimmalek, M. Mirzakhani, A.G. Pirbalouti, *Ind. Crops Prod*. 51 (2013) 328–333.
7. O. Bazzali, F. Tomi, J. Casanova, A. Bighelli, *Flav. Fragr. J*. 27 (2012) 335–340.
8. A. Hennia, M.G. Miguel, M. Brada, S. Nemmiche, A.C. Figueiredo, *J. Essent. Oil Res*. 28 (2016) 146–156.
9. P. Pereira, M. Cebola, M.C. Oliveira, M.G. Bernardo-Gil, *J. Supercrit. Fluids* 113 (2016) 1–9.
10. B. Berka-Zougali, M.A. Ferhat, A. Hassani, F. Chemat, K.S. Allaf, *Int. J. Mol. Sci*. 13 (2012) 4673–4695.
11. M. Fadil, A. Farah, B. Ihssane, T. Haloui, S. Lebrazi, S., Rachiq, *J. Appl. Res. Med. Aromat. Plants* 7 (2017) 35–40
12. W.A. Wannes, B. Mhamdi, J. Sriti, B. Marzouk, *J. Essent. Oil Res*. 22 (2010) 13–18.
13. F. David, C. Devos, P. Sandra, *LCGC Eur*. (2006) 19, 602–616.
14. M.S.S. Amaral, P. J. Marriott, *Molecules* 24 (2019) 2080.
15. L. Mondello, A. Casilli, P.Q. Tranchida, D. Sciarrone, P. Dugo, G. Dugo, *LCGC Eur*. 21 (2008) 130–137.
16. G. Dong, X. Bai, A. Aimila, H. A. Aisa, M. Maiwulanjiang, *Molecules* 25 (2020) 3166.
17. Y. Li, G. Dong, X. Bai, A. Aimila, X. Bai, M. Maiwulanjiang, H. A. Aisa, *Nat. Prod. Res*. 35 (2020) 4202–4205.
18. R. Rahmani, F. Andersson, M.N. Andersson, J.K. Yuvaraj, O. Anderbrant, E. Hedenström, *Chemoecology* 29 (2019) 103–110.
19. G.T. Eyres, S. Urban, P.D. Morrison, P.J. Marriott, *J. Chromatogr. A* 1215 (2008) 168–176.
20. G.T. Eyres, S. Urban, P.D. Morrison, J.P. Dufour, P.J. Marriott, *Anal. Chem*. 80 (2008) 6293–6299.
21. D. Sciarrone, S. Pantò, A. Rotondo, L. Tedone, P.Q. Tranchida, P. Dugo, L. Mondello, *Anal. Chim. Acta* 785 (2013) 119–125.
22. D. Sciarrone, S. Pantò, P. Q. Tranchida, P. Dugo, L. Mondello, *Anal. Chem*. 86 (2014) 4295–4301.
23. D. Sciarrone, S. Pantò, P. Donato, L. Mondello, *J. Chromatogr. A* 1475 (2016) 80–85.
24. D. Sciarrone, D. Giuffrida, A. Rotondo, G. Micalizzi, M. Zoccali, S. Pantò, P. Donato, R.G. Rodrigues-das-Dores, L. Mondello, *J. Chromatogr. A* 1524 (2017) 246–253.
25. D. Sciarrone, A. Schepis, G. De Grazia, A. Rotondo, F. Alibrando, R.R. Cipriano, H. Bizzo, C. Deschamps, L.M. Sidisky, L. Mondello, *Faraday Discuss*. 218 (2019) 101–114.

26. D. Sciarrone, S. Pantò, C. Ragonese, P.Q. Tranchida, P. Dugo, L. Mondello, *Anal. Chem.* 84 (2012) 7092–7098.
27. A. Rotondo, R. Ettari, M. Zappalà, C. De Micheli, E. Rotondo, *J. Mol. Struct.* 1076 (2014) 337–343.

Chapter 4: Evaluation of the cryogenic effect for trapping highly volatile compounds by using a preparative multidimensional gas chromatographic system.

4.1 Introduction.

Gas chromatography for preparative purposes is by far a useful approach for the fractionation of mixtures and isolation of their components. The attainment of pure substances at relatively low costs and the possibility to reach high recovery efficiencies, make Prep-GC an advantageous approach over classical isolation techniques, such as distillation methods and synthetic procedures [1]. They are affected by several issues i.e., the significant time/solvent-consuming, and the yield of extraction or synthesis. On the contrary, Prep-GC methods are more environment-friendly and less time/solvent consuming strategies; also, the purity degree of the collected fraction is guaranteed by the gas chromatographic separation step. A mono-dimensional gas chromatographic (1D-GC) approach could be sufficient for analytes separation whenever the complexity of the matrices analysed does not exceed the peak capacity of a single capillary column. The collection of suitable amounts depends on the adequate volume injected and mega-bore columns are needed to satisfy the sample capacity looked-for preparative applications. However, their relatively low efficiency compared to the narrower-bore counterparts complicates the attainment of the desired purity degree, and pre-separation techniques are often required. Commonly, the complexity of real samples, make the isolation of pure fractions an arduous task, due to the coelution of interfering compounds which frequently arises. As previously demonstrated multidimensional GC methods could be effective for preparative purposes [2, 3]. Specifically, the *heart-cut* approach offers interesting advantages for target compounds analysis in complex matrices [4], and the attainment of highly pure fraction is guaranteed. The combined high resolution of a MDGC approach and the sample capacity given by mega bore columns, were suitably exploited for the development of a triple Deans switch preparative system [5]. The latter has proved to work effectively by using a collection device of low cost and simple construction. Different applications have been carried out exploiting both the efficient separation step which is mandatory for the collection of highly pure fractions, and the isolation of adequate analyte quantities [6, 7, 8, 9]. Nevertheless, such capabilities are strictly dependent on interconnected factors, including the analyte concentration, its physicochemical properties, and the collection conditions. Although some of them are compound linked, proper collection parameters could be modified for the achievement

of satisfactory recovery degrees. The present study focused on the evaluation of the isolation performance of target volatile organic compounds with a wide range of boiling points and different polarity. Specifically, the optimization of analyte condensation from the gas stream represented the crucial topic. Different techniques have been reported for the condensation of volatiles, after the chromatographic process, such as open tubular traps, commercially available preparative fraction collectors, and cooled glass tubes [10, 11, 12, 13]. In this study empty quartz liners were used and a proper collection device was developed; it was constructed providing a double configuration which worked both under room temperature and cryogenic conditions. Depending on the diverse physicochemical property of the substances, different temperature conditions were used in order to obtain the highest recovery degree for the target volatile compounds. Such an approach allowed to overcome the critical points of Prep-GC applications, minimizing both the effect of compound specific properties over the collection performance, and the conventional chromatographic limitations which typically influence the collected amount of the target compound, the purity degree obtained, and the analysis time.

4.2 Materials and methods.

- ***Samples and sample preparation***

n-Octane, α-angelicalactone, bis(methylthio)-methane, *n*-nonane, heptanal, 3-hexenoic acid methyl ester, α-pinene, myrcene, limonene, octanol, heptyl methyl ketone, linalool, citronellal, *n*-dodecane, thymol methyl ether, linalyl acetate, *n*-tetradecane, β-caryophyllene, caryophyllene oxide, nootkatone, acetone and *n*-hexane (GC grade) were kindly provided by Merck (Merck KGaA, Darmstadt, Germany). Five standard compounds mixtures, namely mix A, mix B, mix C, mix D, and mix E, were prepared at the 200,000 μg mL^{-1} level for prep-MDGC collection, and thus diluted in *n*-hexane at the 500 μg mL^{-1} level for quantifying through ISTD method by GC-FID analyses. Trapped standard compounds from the five mixtures A-E, were flushed using an Internal Standard (ISTD) solution at the 500 μg mL^{-1} level in *n*-hexane. *n*-Nonane, *n*-tetradecane, and β-caryophyllene were properly used as internal standards depending on the composition of the mixture injected. All the standard solutions and mixtures were stored at + 4 °C, and taken at room temperature before each analysis.

- ***GC-FID and GC-MS analysis***

GC analyses were carried out on a Shimadzu GC-2010 Plus gas chromatograph and a GCMS-QP2010 Ultra system mass spectrometer, both equipped with an AOC-20i series auto injector (Shimadzu Europa, Duisburg, Germany). The column was a SLB-5ms [silphenylene polymer, virtually equivalent to poly (5% diphenyl/95% methylsiloxane)], 30 m × 0.25 mm i.d. × 0.25 μm d_f from Merck (Merck Life Science, Darmstadt, Germany). Analyses were performed under the following conditions: oven temperature program from 50 °C to 230 °C, at 10 °C min^{-1}; then, from 230 °C to 300 °C, at 20 °C min^{-1}; split/splitless injector, 280 °C; injection mode, split (1:10 ratio); injection volume, 1.0 μL. For GC-FID analyses, helium was used as carrier gas, at a constant linear velocity of 30.0 cm s^{-1}, and the inlet pressure was set to 99.5 kPa. FID (310 °C) gases were H_2 at 40.0 mL min^{-1} and air at 400 mL min^{-1}; the sampling rate was 80 msec. Data were acquired by the LabSolutions software ver. 5.82 (Shimadzu Europa, Duisburg, Germany). GC-MS analyses were carried out as follows: inlet pressure, 26.7 kPa; carrier gas, He at constant linear velocity of 30 cm s^{-1}; source temperature, 220 °C; interface temperature, 250 °C; EI energy, 70 eV; mass scan range, 40-400 *m/z*; scan speed, 10 Hz. Data were acquired by the GCMSsolution software ver. 4 (Shimadzu Europa, Duisburg, Germany). Identification was achieved by searching the experimental data into the FFNSC 4.0 mass spectral library

database (Shimadzu Europa, Duisburg, Germany), exploiting a double filter approach based on spectral similarities and Linear Retention Index (LRI) values.

- ***Preparative Multidimensional GC***

The prep-MDGC system employed, illustrated in Figure 4.1, consisted of three Shimadzu GC-2010 Plus gas chromatographs (GC1, GC2, GC3) each equipped with a Deans switch transfer device (Shimadzu Europa, Duisburg, Germany), and an advanced pressure control system (APC1, APC2, APC3) which supplied the carrier gas (He); for more details see Sciarrone *et al.* [5].

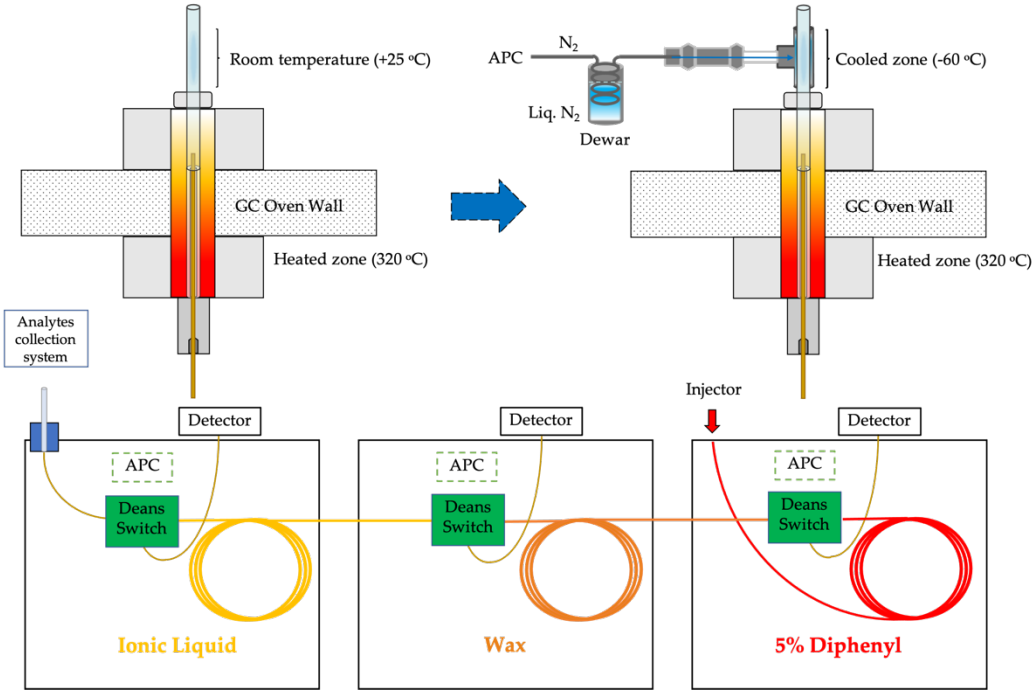

***Figure 4.1*. Triple Deans-switch Prep-MDGC system scheme: the double configuration of the collection device is illustrated.**

GC1 was equipped with a split/splitless injector (280 °C); the column (^{1}D) was an Equity-5 [poly (5% diphenyl/95% dimethylsiloxane)], 30 m × 0.53 mm i.d. × 5 µm d_f (Merck Life Science, Darmstadt, Germany), preceded by a 1 m segment of an uncoated column of the same I.D. FID1 (300 °C) was connected to Deans 1 *via* 1 m × 0.22 mm i.d. segment of uncoated column. Carrier gas pressure was maintained constant at 125 kPa, while a constant pressure of 110 kPa was applied to APC1. The oven temperature program in ^{1}D was: 50 °C to 260 °C, at 5 °C min^{-1} (held for 11.00 min); the transfer line between GC1 and GC2 was maintained at 200 °C. GC2 column (^{2}D) was a Supelcowax-10 (100% polyethylene glycol, PEG), 30 m × 0.53 mm i.d. × 1.0 µm d_f (Merck Life Science, Darmstadt, Germany). FID2 (300 °C) was connected

to Deans 2 *via* 0.5 m × 0.25 mm i.d. segment of uncoated column. The oven temperature program in ^{2}D was: 50 °C (held for 10.00 min) to 240 °C, at 5 °C min^{-1} (held for 5.00 min); the transfer line between GC2 and GC3 was maintained at 200 °C. APC2 pressure was maintained constant at 95 kPa. GC3 column (^{3}D) was an SLB-IL59 (custom-made ionic liquid) 30 m × 0.53 mm i.d. × 0.8 μm d_f (Merck Life Science, Darmstadt, Germany). FID3 (300 °C) was connected to Deans 3 *via* a 0.6 m × 0.18 mm i.d. segment of uncoated column. The oven temperature program in ^{3}D was: 50 °C (held for 15.00 min) to 240 °C, at 5 °C min^{-1}. APC3 pressure was 50 kPa. Detector gases (for FID1, 2, and 3) were H_2 at 40.0 mL min^{-1} and air at 400 mL min^{-1}; the sampling rate was 80 msec. Data were collected by the MDGCsolution software (Shimadzu Europa, Duisburg, Germany).

A lab-made modified GC injector port was used as the collection system. The device (Figure 2) consisted of a heated (300 °C) aluminium block (3 cm length × 1.5 cm width × 11 cm height), with two empty liners in series located inside and held in position by means of two nuts. The bottom liner is fixed in order to drive the retention gap (0.3 m × 0.18 mm I.D.) into the upper one, which is removable and it is used to collect the condensed analytes. As an option, a gaseous nitrogen stream (pressure at 8 bar maintained by a VICI DBS N_2-Wihisper-0) which flowed through a 1/8-inch tube (5 m length), could be controlled by an APC channel of GC3, and carried around the upper liner. Before reaching the collection system the final segment of the tube (2 m length) passed through a liquid nitrogen reservoir (1 L). When cryogenic conditions are needed, liquid nitrogen is poured into the reservoir and the gaseous nitrogen stream is switched on. Consequently, a rapid cooling process around the collection liner allowed to make the collection reliable for highly volatile components. The temperature at +25 °C, -30 °C, and -60 °C was measured by means of an external PT-100 sensor. In order to guarantee the purity degree of the isolated compounds, the collection liner was systematically flushed with acetone and hexane before each collection step, and then heated at 100 °C for 20 minutes; finally, it was kept at the desired collection temperature. After analyte isolation, the collection tube was removed immediately and flushed three times (in a 1.5 mL vial) with 100 μL of the internal standard solution (500 μg mL^{-1} level in *n*-hexane). The solutions containing both the internal standard and the collected standard compounds were then analysed by GC-MS and by GC-FID for qualitative and quantitative purposes, respectively.

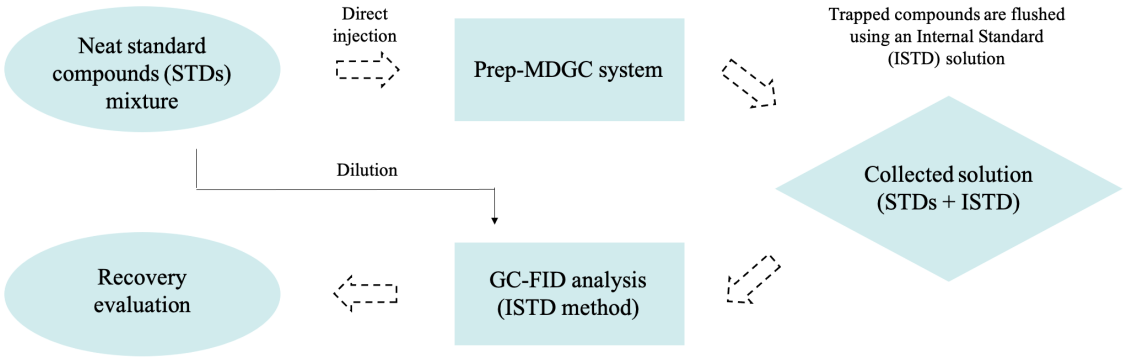

Figure 4.2. **Workflow.**

Table 4.1. **List of seventeen volatile compounds ordered by LRI[a] values.**

Compound	Chemical class	Formula	MW	b. p. (°C)	LRI[a]	LRI[p]
n-Octane	alkane	C_8H_{18}	114	126	800	-
Heptanal	alkyl aldehyde	$C_7H_{14}O$	114	146	906	598
bis(methylthio)-Methane	sulfide	$C_3H_8S_2$	108	147	893	692
α-Pinene	bicyclic monoterpene hydrocarbon	$C_{10}H_{16}$	136	156	933	427
Myrcene	acyclic monoterpene hydrocarbon	$C_{10}H_{16}$	136	167	991	567
α-Angelicalactone	butenolide	$C_5H_6O_2$	98	167	864	848
3-Hexenoic acid, methyl ester	fatty acid methyl ester	$C_7H_8O_3$	128	169	922	668
Limonene	monocyclic monoterpene hydrocarbon	$C_{10}H_{16}$	136	176	1030	608
1-Octanol	aliphatic alcohol	$C_{10}H_{18}O$	130	195	1076	959
Heptyl methyl ketone	ketone	$C_9H_{18}O$	142	195	1093	802
Linalool	acyclic monoterpene alcohol	$C_{10}H_{18}O$	154	198	1101	956
Citronellal	acyclic monoterpene aldehyde	$C_{10}H_{18}O$	154	208	1152	891
thymol methyl ether	monoterpenoid	$C_{11}H_{16}O$	164	214	1229	1000
Linalyl acetate	acyclic monoterpene ester	$C_{12}H_{20}O_2$	196	220	1250	964
n-Tetradecane	alkane	$C_{14}H_{30}$	198	254	1400	809
β-Caryophyllene oxide	cyclic sesquiterpene oxide	$C_{15}H_{24}O$	220	280	1587	1364
Nootkatone	cyclic sesquiterpene ketone	$C_{15}H_{22}O$	218	318	1806	1877

Linear retention indices are reported, relative to an apolar (5%) stationary phase, LRI[a], and to a polar (wax) stationary phase, LRI[p].

4.3. Results and discussion.

Seventeen standard compounds with diverse psychochemical properties were chosen for carrying out the study, evaluating their behaviour during the collection step (Table 4.1). Specifically, a quite large range of boiling points from 120 °C to 320 °C was considered for selecting a variety of volatile molecules among different chemical classes. Hydrocarbons and oxygenated compounds, both linear and cyclic ones were chosen. Specifically, saturated alkane, aliphatic alcohol, aldehyde, and ketone, sulfide, butenolide, fatty acid methyl ester, aromatic ether, acyclic, mono and bicyclic monoterpene hydrocarbons, acyclic monoterpene alcohol, aldehyde and ester, cyclic sesquiterpene ketone and oxide were considered. In addition to the chemical diversity within the compounds studied, three ranges of boiling points were considered; firstly, from 120 °C to 170 °C b.p. grouping the compounds as follows: *n*-octane, heptanal, bis(methylthio)-methane, α-pinene, myrcene, α-angelicalactone, 3-hexenoic acid methyl ester. Then, from 170 °C to 210 °C b.p., limonene, 1-octanol, heptyl methyl ketone, linalool, and citronellal were selected. Additionally, a third range was considered from 210 °C to 320 °C b.p., with thymol methyl ether, linalyl acetate, *n*-tetradecane, β-caryophyllene oxide, and nootkatone. Each compound was subjected to prep-MDGC analysis in order to evaluate the recovery efficiency both for specific ranges of boiling points and within different chemical classes. The study exploited the well-known capabilities of the prep-MDGC prototype developed by Sciarrone *et al*. [5], thus overcoming the lack of purity degree, the scarce amount collected and the time-consuming which typically affect preparative GC applications. Such an approach enabled to inject mixtures of standard compounds, neat and in splitless mode. Although the band broadening effect is observed, the injection of mixtures comprising a wide LRIs range (values referred to saturated *n*-alkanes on a 5% diphenyl stationary phase) did not affect the purity degree (≥ 95 %) of the collected compounds. Thanks to the *heart-cut* three-dimensional approach, the latter was maintained even in case of ± 30 LRI units between target compounds. Nevertheless, the seventeen standards were conveniently distributed in five mixtures making the collection step feasible. Also, the purity degree of the collected compounds was guaranteed by systematically flushing the collection liner before each analysis and then drying it as described in the previous section. Blank analyses were properly carried out overcoming the risk of contamination between each application. Each pure analyte was collected by using the affordable and lab-made collection device which was developed in order to work under room temperature and cryogenic conditions. Firstly, the evaluation of the collection performances was carried out at room temperature (+ 25 °C) in order to determine

the collection feasibility within the b.p. range considered. As shown in Figure 4.4, the room temperature was completely ineffective for the collection of VOCs with b.p. values under 170 °C and independently of the chemical class considered. Conversely, VOCs with b.p. values over 210 °C gave recovery degrees which were > 80 % for each representative compound of the chemical classes evaluated. Differently, variable percentages were obtained within the range from 170 °C to 210 °C. Such preliminary results suggested to test a "mild" cryogenic condition, reaching – 30 °C during the collection step. Aiming to obtain a constant temperature value, the exposure to the cryogenic agent was conveniently modulated for each application. Specifically, a pressure program was applied to the APC3 channel which supplied N_2, at constant pressure (20 kPa). A dewar with 1 L capacity was used and about 0.8 L of liquid nitrogen were poured into the proper reservoir before each analysis. The N_2 flow which passed through a 1/8-inch tube into the cryogenic bath was quickly cooled down and focused on the upper body of the collection liner. The temperature measurement was made by means of a PT-100 sensor for estimating the duration of the cooling process. Initially, the constant pressure at 20 kPa (hold time ≥ 10 min) allowed to maintain 0°C (T_0) across the collection liner zone; then, an increase up to 80 kPa, at 400 kPa min^{-1} kept the temperature at -30 °C; specifically, 10 min were needed before steadying the desired temperature. The latter was measured 1 min before and after the chromatographic band (peak width ≈ 1 min). Among the compounds included in the b.p. range 120 °C - 170 °C the average recovery degree was 80 % (± 12); however, a variation was observed within the group depending on the chemical class evaluated. The same happened within the 170 °C to 210 °C b.p. range, and the average recovery degree was 84 % (± 7). Nevertheless, as the b.p. increased, the values variability decreased, moving towards higher recovery efficiencies. Additionally, compounds with b.p. comprised into the range from 210 °C to 320 °C, showed 95 % (± 5) as average value. The results obtained were unsatisfactory at all, encouraging the use of harder cryogenic conditions and -60 °C was tested as further option. Thus, a constant pressure at 20 kPa (hold time ≥ 10 min) allowed to maintain 0°C (T_0) across the collection liner zone, again; then, an increase up to 120 kPa, at 400 kPa min^{-1} kept the temperature at -60 °C; specifically, 10 min were needed before reaching a plateau. Also, the temperature measurement was carried out 1 min before and after the chromatographic band (peak width ≈ 1 min). Such a condition, allowed to reach the highest average recovery degree in each b.p. range considered: 88 % (± 7), 90 % (± 5), 100 % (± 10) were the average values obtained for the b.p. ranges 120 °C - 170 °C, 170 °C - 210 °C and 210 °C - 320 °C respectively.

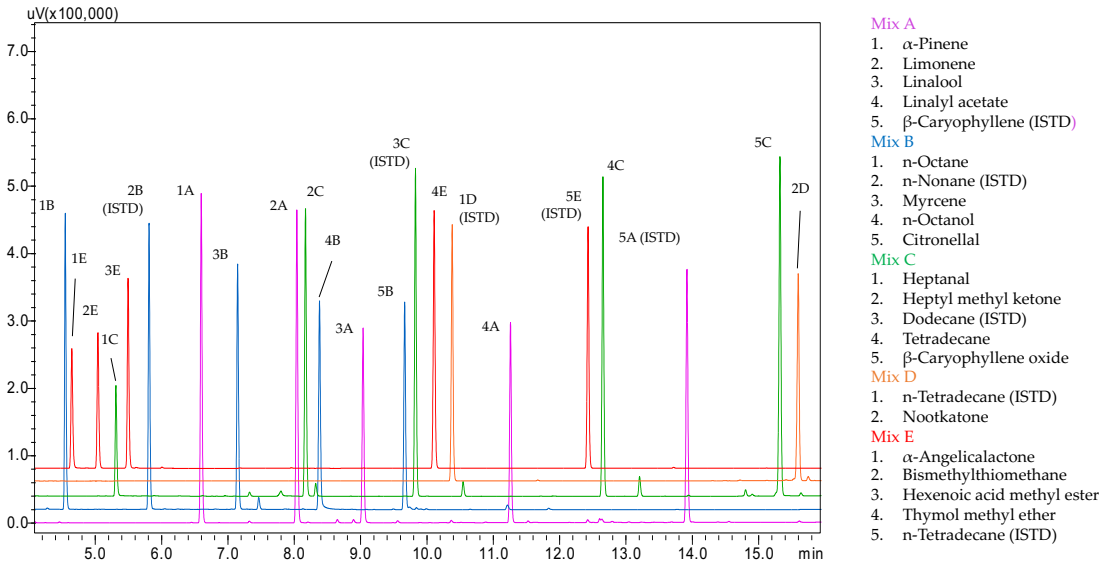

***Figure 4.3*. GC-FID chromatograms related to the VOCs mixtures A-E.**

The recovery measurements were carried out exploiting the ISTD method. Firstly, the mixtures A-E diluted at the 500 μg mL^{-1} level in *n*-hexane, each one containing an ISTD at the 500 μg/mL level, were subjected to GC-FID analysis; thus, the ratios ($R1$) between the average absolute area of each standard and the ISTD one, were calculated. Additionally, the target compounds collected by using an ISTD solution at the 500 μg mL^{-1} level were analysed by GC-FID following the VOCs combination in A-E mixtures. Then, the ratios ($R2$) between the average absolute area of each collected standard and the ISTD one, were calculated. Specifically, average values of peak areas obtained by three replicates were considered for each measurement. Finally, the recovery efficiency related to each collected VOC was calculated as follows *(Eq. 1.20)*:

$$Recovery\ \% = [(1 - (R1 - R2)] \times 100$$

Eq. (1.20)

The recovery of analytes calculated according to peak areas (GC-FID) after trapping on prep-GC systems have been reported in previous studies. However, for the best of our knowledge the ISTD method have never been applied for such a purpose, and the recovery measurements have been estimated by the ratio between the amount collected and the amount injected [14,15]. On the contrary, the introduction of the ISTD as equation formulated in this study allowed to obtain more accurate recovery values by using the ISTD.

Furthermore, the high sample capacity given by the wide bore columns-set allowed the injection of neat standards, in splitless mode. As a consequence, adequate quantities of each

analyte could be condensed from the gas stream during the collection step. Moreover, the purity degree of the isolated fractions was guaranteed by the heart-cut method. Specifically, three different stationary phases i.e., 5% diphenyl-polyethylene glycol-ionic liquid were orthogonally combined in order to provide different selectivity and high separation-power capability. Such an approach could be able to provide the highest recovery degree depending on the physicochemical properties of the target compound. Even if the chromatography was efficiently optimized for preparative purpose, as previously demonstrated by Sciarrone *et al.*, proper collection conditions could be conveniently modified for obtaining the highest recovery degree and depending on the specific volatile compound.

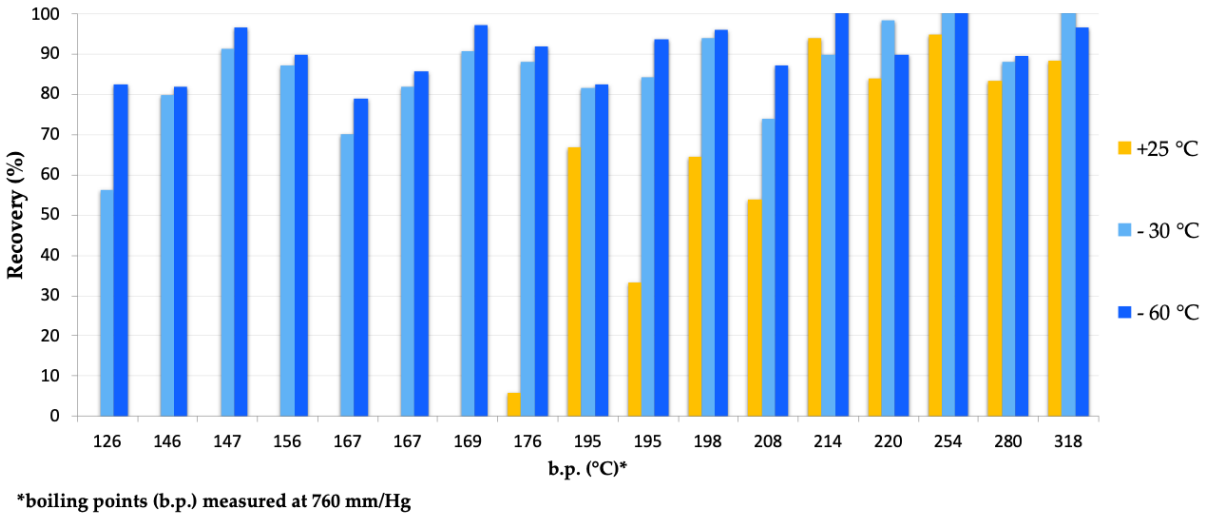

Figure 4.4. **Effects of Specific Collection Conditions (+25 °C, -30 °C, -60 °C) on Recovery Degrees of target VOCs with differing boiling points.**

4.4 Conclusions.

The recovery degrees obtained for the target VOCs resulted greatly influenced by the effectiveness of the injection, separation and collection conditions. The heart-cut approach combined with the mega bore columns allowed the collection of highly pure analytes in adequate quantities. Additionally, the collection device double configuration allowed to optimize the crucial condensation step in relation to the physicochemical properties of the analytes. Focusing on highly volatile compounds it was demonstrated the need of cryogenic conditions for recovering them efficiently.

4.5. References.

1. D. Sciarrone, S. Pantò, C. Ragonese, P. Dugo and L. Mondello, TrAC, Trends Anal. Chem. 71 (2015) 65-73.
2. G.T. Eyres, S. Urban, P. D. Morrison, P. J. Marriott, *J. Chromatogr. A* 1215 (2008) 168-176.
3. G. T. Eyres, S. Urban, P. D. Morrison, J.-P. Dufour, Philip J. Marriott, *Anal. Chem.* 80 (2008) 6293-6299.
4. P. Q. Tranchida, L. Mondello, Hyphenations of Capillary Chromatography with Mass Spectrometry, first ed., Elsevier, 2020, 135-182.
5. D. Sciarrone, S. Panto, C. Ragonese, P. Q. Tranchida, P. Dugo, L. Mondello, *Anal. Chem.* 84 (2012) 7092-7098.
6. D. Sciarrone, S. Pantò, A. Rotondo, L. Tedone, P. Q. Tranchida, P. Dugo, L. Mondello, *Anal. Chim. Acta*, 785 (2013) 119-125.
7. D. Sciarrone, S. Pantò, P. Donato, L. Mondello, *J. Chromatogr. A*, 1475 (2016) 80-85.
8. D. Sciarrone, D. Giuffrida, A. Rotondo, G. Micalizzi, M. Zoccali, S. Pantò, P. Donato, R. Goncalves Rodrigues-das-Dores, L. Mondello, *J. Chromatogr. A*, 1524 (2017) 246-253.
9. D. Sciarrone, A. Schepis, G. De Grazia, A. Rotondo, F. Alibrando, R. R. Cipriano, H. Bizzo, C. Deschamps, L. M. Sidisky, L. Mondello, *Faraday Discuss.* 218 (2019) 101-114.
10. S. Nojima, C.S. Apperson, C. Schal, *J. Chem. Ecol.* 34 (3) (2008) 418-428.
11. Codina, R.W. Ryan, R. Joyce, D.S. Richards, *Anal. Chem.* 82 (21) (2010) 9127-9133.
12. C. Meinert, M. Moeder, W. Brack, *Chemosphere* 70 (2) (2007) 215-223.
13. F. J. M. Novaes, P.J. Marriott, *J. Chromatogr. A*, 1644 (2021) 462135.
14. T. I. Eglinton, L. I. Aluwihare, *Anal. Chem.* 68 (1996) 904-912.
15. X. Zhang, L. Zhao, Y. Wang, Y. Xu, L. Zhou, *J. Sep. Sci.* 36 (2013) 2136-2144.

Chapter 5: Development of a three-dimensional gas chromatographic system coupled to olfactometry as a proof-of-concept model.

5.1 Introduction.

The analysis of aroma-impact compounds, particularly in complex samples, requires effective molecular separation approaches to identify trace or major analytes from the mixture of volatile components [1, 2, 3, 4]. The detection of trace odour active components from complex matrices represents a challenging purpose. Trained panellists need adequate analytical tools depending on the complexity of the matrix and target analyte threshold [5, 6]. In this study, a combined system having the capability to perform target heart-cut multidimensional GC (MDGC) using olfactometry (O), flame ionization (FID), and mass spectrometry (qMS) detection was developed. Specifically, three gas chromatographic dimensions coupled through Deans switch transfer devices and equipped with mega-bore capillary columns were exploited [7]. The use of mega-bore columns allowed the injection of neat samples in splitless mode, increasing the sample capacity necessary to enhance the odour perception. Moreover, the heart-cut approach enabled purifying target fractions prior to the olfactometry detection. Additionally, the simultaneous detection by qMS allows matching specific odours with target molecules. Finally, the TDGC-O-FID/MS system represented a proof-of-concept model by which odour perception of trace components from complex samples is sensibly enhanced compared to conventional GC-O approaches.

Conventionally, a splitting system diverts the column effluent into two parts, one of which is directed to a detector, whereas the other one is directed to a heated exit serving as “sniffing port”, where the “sniffer” performs the olfactory evaluation. Similarly, the system developed in this study exploited a Deans switch transfer device allowing to divert the third GC effluent to the MS detector (when in stand-by mode) or to the olfactometer (cut mode).

5.2 Materials and methods.

- ***Sample preparation***

A sulphur compound (p-mentha-8-thio-3-one) was used in each application. The standard compound (mixture of *cis* and *trans* isomers) and *n*-hexane (GC grade) were kindly provided by Merck (Merck KGaA, Darmstadt, Germany). Additionally, sweet orange essential oil, kindly provided by Capua 1880 S.r.l., was used as medium-complex matrix for each application. The essential oil was spiked with the standard compound at different ppm and ppb levels. All the samples were stored at + 4 °C, and taken at room temperature before each analysis.

- ***GC-O-FID/MS analyses***

GC-O-FID/MS analyses were carried out on a Shimadzu GCMS-QP2010 Ultra system mass spectrometer, equipped with an AOC-20i series auto injector (Shimadzu Europa, Duisburg, Germany). Additionally, the system was equipped with a Deans switch transfer device. Helium was supplied at constant pressure by AFC and APC units as the carrier gas (60 kPa head pressure and 40 kPa auxiliary pressure). Capillaries exploited were SLB-5ms, 30 m × 0.25 mm i.d., 0.25 μm film thickness (Merck Life Science, Darmstadt, Germany), Equity-5, 30 m × 0.53 mm i.d., 5 μm film thickness (Merck Life Science, Darmstadt, Germany).

Aiming a simultaneous FID/MS detection, the end of the third capillary column was connected to a Deans switch device and the effluent was transferred via a deactivated fused silica capillary (20 cm × 0.25 mm) to a split system. The latter, consisted of a zero dead volume union equipped with a double hole graphite ferrule. Thus, two different capillaries diverted the effluent to both the detectors FID and MS: 150 cm × 0.20 mm, and 80 cm × 0.25 mm i.d. were used as retention gap respectively. Similarly, for carrying out a GC-O application the effluent was transferred via an uncoated fused silica capillary to the sniffing port (80 cm × 0.25 mm i.d.). The sniffing port consisted of a cylindrically shaped aluminum device with a beveled top and a central drill hole (2 mm) housing the capillary. During a GC-O run, the nose of the panelist was placed closely above the top of the sniffing port and the odor of the effluent was evaluated. If an odor was recognized, the retention time was marked in the chromatogram, and both the odor quality and intensity was assigned. The injection conditions differed depending on the capillary column used: in the case of the narrower one the injection volume was 1.0 μL in split mode (10:1), while 3.0 μL in splitless mode were injected when a wide bore column was employed.

Analyses were performed under the following conditions: oven temperature program from 50 °C to 250 °C, at 3 °C min^{-1}; split/splitless injector, 250 °C. For GC-FID analyses, helium was used as carrier gas, at a constant linear velocity of 30.0 cm s^{-1}, and the inlet pressure was set to 75 kPa; APC 40 kPa. FID (280 °C) gases were H_2 at 40.0 mL min^{-1} and air at 400 mL min^{-1}; the sampling rate was 80 msec. Data were acquired by the LabSolutions software ver. 5.82 (Shimadzu Europa, Duisburg, Germany). GC-MS analyses were carried out as follows: inlet pressure, 75 kPa; APC 40 kPa; carrier gas, He at constant linear velocity of 30 cm s^{-1}; source temperature, 220 °C; interface temperature, 250 °C; EI energy, 70 eV; mass scan range, 40-400 *m/z*; scan speed, 10 Hz. Data were acquired by the GCMSsolution software ver. 4 (Shimadzu Europa, Duisburg, Germany). Identification was achieved by searching the experimental data into the FFNSC 4.0 mass spectral library database (Shimadzu Europa, Duisburg, Germany), exploiting a double filter approach based on spectral similarities and Linear Retention Index (LRI) values.

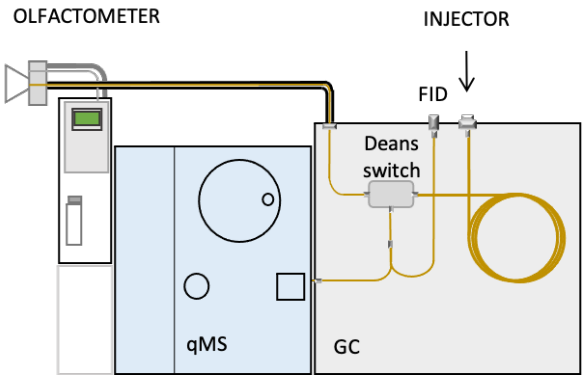

Figure 5.1.a. **Scheme of the GC-O-MS/FID system.**

- ***TDGC-O-MS/FID analyses***

A multidimensional heart-cut approach was carried out by using three Shimadzu GC 2010 Plus coupled to a mass spectrometer (GCMS-QP2010) and to an olfactometric port (Phaser OP-275). As displayed in Figure 5.1.b, each dimension is equipped with a Deans switch transfer device; the third one alternatively diverted the effluent to a simultaneous FID/MS detection, or to the olfactometer as explained above. Additionally, three different auxiliary pressure control provided a constant carrier gas flow.

GC1 was equipped with a split/splitless injector (250 °C); the column (^{1}D) was an Equity-5 [poly (5% diphenyl/95% dimethylsiloxane)], 30 m × 0.53 mm i.d. × 5 µm d_f (Merck Life Science, Darmstadt, Germany), preceded by a 1 m segment of an uncoated column of the same

I.D. FID1 was connected to Deans 1 *via* 1 m × 0.22 mm i.d. segment of uncoated column. Carrier gas pressure was maintained constant at 100 kPa, while a constant pressure of 90 kPa was applied to APC1. The oven temperature program in ^{1}D was: 50 °C to 250 °C, at 3 °C min^{-1}; the transfer line between GC1 and GC2 was maintained at 200 °C. GC2 column (^{2}D) was a Supelcowax-10 (100% polyethylene glycol, PEG), 30 m × 0.53 mm i.d. × 1.0 µm d_f (Merck Life Science, Darmstadt, Germany). FID2 was connected to Deans 2 *via* 0.8 m × 0.22 mm i.d. segment of uncoated column. The oven temperature program in ^{2}D was: 50 °C to 250 °C, at 3 °C min^{-1}; the transfer line between GC2 and GC3 was maintained at 200 °C. APC2 pressure was maintained constant at 75 kPa. GC3 column (^{3}D) was an SLB-IL59 (custom-made ionic liquid) 30 m × 0.53 mm i.d. × 0.8 µm d_f (Merck Life Science, Darmstadt, Germany). Deans 3 was connected both to the split as described for the mono-dimensional system, and to the olfactometric port. The oven temperature program in ^{3}D was: 50 °C to 240 °C, at 3 °C min^{-1}. APC3 pressure was 40 kPa. Detector gases for FID1, 2, and 3 were H_2 at 40.0 mL min^{-1} and air at 400 mL min^{-1}; the temperature was 280 °C and sampling rate was 80 msec. Data were collected by the MDGCsolution software (Shimadzu Europa, Duisburg, Germany).

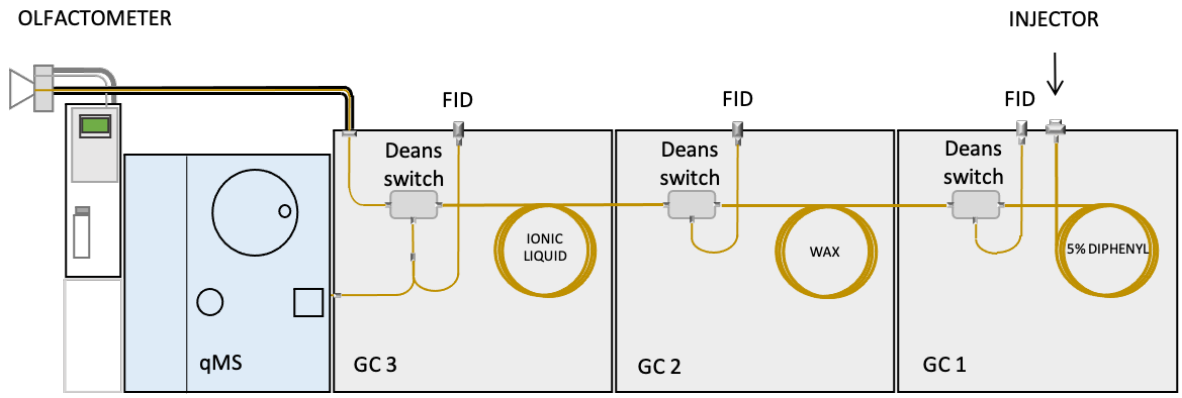

Figure 5.1.b. **Scheme of the TDGC-O-MS/FID prototype.**

5.3 Results and discussions.

The odour character of some compounds is not always directly related to their concentration in a sample. It is well known as trace components could greatly influence the odour impact and be considered as characteristic of a natural sample. Mostly in the case of compounds with a very odour impact in trace amounts, their isolation exploiting a GC-O analysis might become tricky if co-elutions arose with other sample components. Highly complex chemical composition may lead to extensive co-elutions resulting in inaccurate identification of odour-active compounds. Moreover, the possible hiding of odour-active trace-level compounds by major interferences due to the olfactive impressions overlapping could result in an unreliable olfactive characterization. Depending on the complexity of the sample, monodimensional GC techniques could not be able to provide accurate results, thus, in this study, a multidimensional GC-O approach was developed with the aim to overcome these issues. To compare the capabilities of conventional and multidimensional GC-O approaches, a sulphur compound with a low-odour threshold was used, namely, p-mentha-8-thiol-3-one, characterised by a tenacious sulphurous odour type, which can be described as catty and black currant [8, 9]. The fruity, berry and tropical characteristics of this compound with raspberry and minty nuance make it great for flavours such as peach, berry, and grape. Nevertheless, recommended levels range from 10 to 100 ppb as consumed [10] increasing the risk of peak/odour hiding when a complex sample is investigated. With this aim, a sweet orange essential oil was used, spiked with the sulphur compound at different levels (from 10 ppm to 10 ppb). Obviously, depending on the on-column amount injected, these relative concentrations could correspond to very small or higher absolute compound amounts. Firstly, as in each conventional GC-O analysis, a narrow bore column was selected, equipped with an apolar stationary phase (see Figure 5.2). The column outlet was connected to a Deans switch device allowing the diversion of the eluate either to the olfactometric port (O) or to a FID/MS simultaneous detection. As usually performed in a GC analysis, only a limited volume (1 μL) of a diluted sample (1:10) was injected, in split mode (10:1). To determine the sulphur compound retention time a 10 ppm solution of the latter was used. Although the highly efficient separation, a sensorial limit of 10 ppm, corresponding to 100 pg of the sulphur compound, was obtained due to the low on-column sample amount introduced due to the sample dilution and split not to overload the chromatographic column. At this stage, the requirement for a low absolute amount to be introduced appeared as the main limitation for the odour evaluation of a trace component.

Thus, taking advantage of the higher sample capacity, a wide bore column equipped with the same apolar stationary phase was exploited with the same system configuration. Beside the advantage to increase the absolute sample amount injected, on the other hand these columns are well known for a reduced chromatographic efficiency, often providing an insufficient peaks resolution. In fact, even if 3 µL of neat sample were injected in splitless mode, the odour perception of the target compound at 10 ppm resulted hidden due to the unresolved peak coelutions (see Figure 5.3).

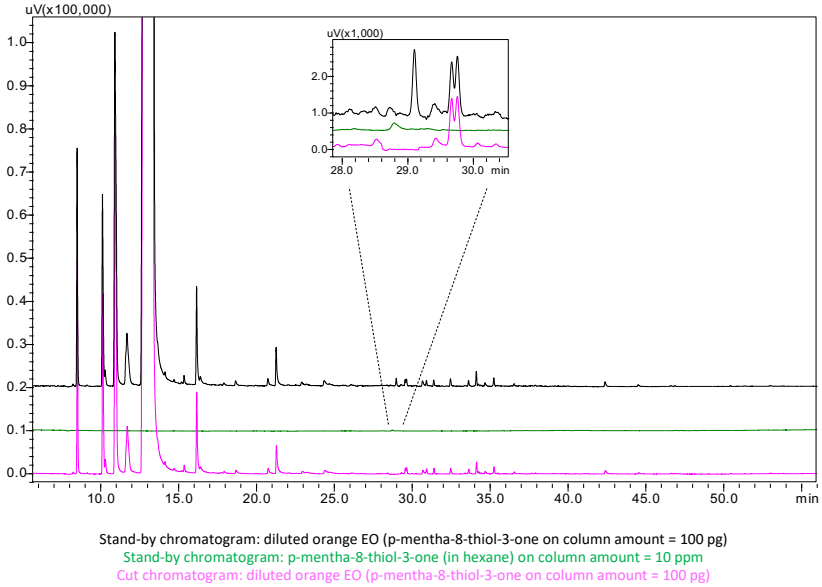

***Figure 5.2*. GC-O-MS/FID Stand-by and cut chromatogram: narrow bore column.**

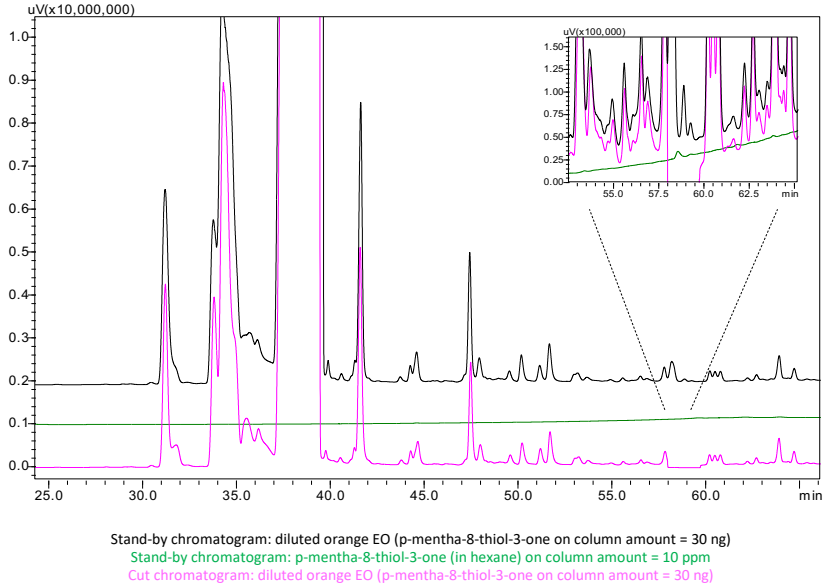

***Figure 5.3*. GC-O-MS/FID Stand-by and cut chromatogram: wide bore column.**

To combine the advantages of both the previous approaches a three-dimensional GC system (TDGC) was developed, coupling the higher efficiency of the MDGC approach to the higher sample capacity of the wide bore column. The aim of the system was to allow the injection of very high sample amounts, overloading the first dimension wide-bore column, exploiting the heart-cut mode to reach a complete peak purification in the next two chromatographic steps before the sniffing port. The system was equipped with three Deans switch devices located between the first and second columns (DS1), between the second and third columns (DS2) and at the third column outlet (DS3), respectively. While DS1 and DS2 in the stand-by mode were connected to two FIDs, DS3 was connected either to the olfactometric port (O) or to the MS/FID as in the monodimensional applications. Figure 5.4.a shows the ^{1}D stand-by and cut analyses of the orange sample on the same apolar stationary phase containing the lower concentration used of 10 ppb. Once operated the first heart-cut the fraction was transferred to the ^{2}D column (mid-polar stationary phase) where the same approach was again used according to the 10 ppm sulphur compound standard solution analysis. Figure 5.4.b shows the ^{2}D separation of the two sulphur compound isomers on the PEG stationary phase: comparing the relative amounts of the two isomers in the standard solution with those of the orange sample it was clear as some interference was still present. By selecting two consecutive heart-cuts the two peaks were transferred to the third dimension equipped with an ionic liquid stationary phase. Thanks to the different selectivity of the latter, despite the similar polar degree, the peaks were completely purified as demonstrated by the high MS similarity achieved, 96% and 98%, respectively. A further run selecting the olfactometric port after the ^{3}D column allowed us to smell a very low concentration of the target peak due to the higher on-column amount injected. A sensorial limit of 10 ppb (30 pg) was obtained: it is important to highlight that such an absolute amount was only three times lower than those observed in monodimensional GC-O (100 pg) due to the injection of 3 μL instead of 1 μL, while was 1000 times lower in relative concentration thanks to the use of a neat sample. Moreover, thanks to the fact that the odour lasts for tens of seconds, as visible in Figure 5.4 c, the odour perception resulted extremely enhanced compared to conventional approaches where the sensation is very short.

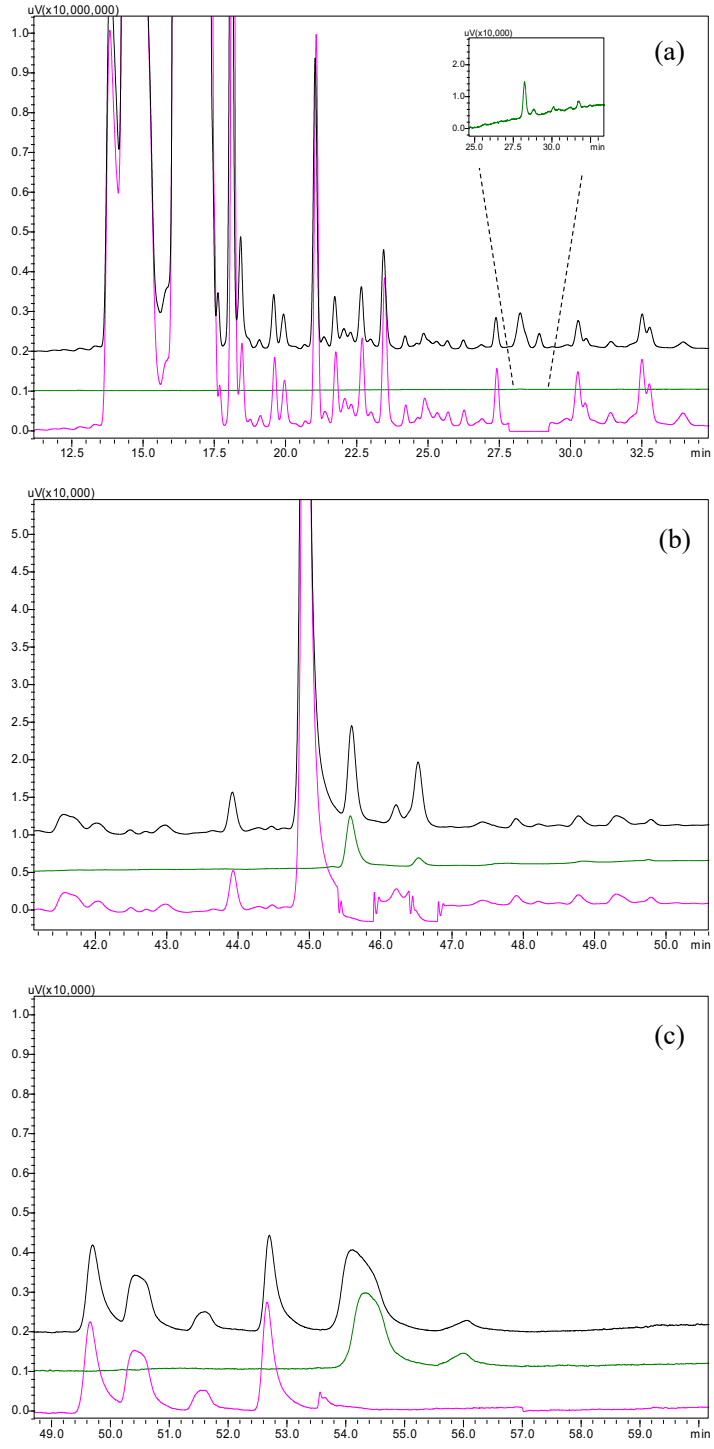

Stand-by chromatogram: neat orange EO (p-mentha-8-thiol-3-one on column amount = 30 pg)
Stand-by chromatogram: p-mentha-8-thiol-3-one (in hexane) on column amount = 10 ppm
Cut chromatogram: neat orange EO (p-mentha-8-thiol-3-one on column amount = 30 pg)

Figure 5.4. **TDGC-O-MS/FID analysis: (a) ^{1}D Stand-by and cut chromatograms; (b) ^{2}D Stand-by and cut chromatograms; (c) ^{3}D Stand-by and cut chromatograms.**

5.4 Conclusions.

The reduced efficiency of a conventional monodimensional GC-O system often avoids reliable odour evaluation, especially for trace components. On the contrary, the use of the TDGC-O system, combining the heart cut method and the use of wide-bore columns, represents an effective approach and guarantees an enhanced odour evaluation. Moreover, the TDGC-O allowed to focus on key fractions of the entire sample allowing to achieve fully resolved peaks, thus the characteristic molecule odour. Furthermore, the prototypal approach provides an extremely simplified odour evaluation for the panellists improving a user-friendly approach to the GC-O technique.

5.5 References.

1. S. M. van Ruth, *Biomolec. Eng.*, 17 (2001) 121-128.
2. W. Berstsch, *J. High Resol. Chromatogr*., *22*, (1999) 12, 647-665.
3. M. Steinhaus, in Food Chemistry, Function and Analysis, Royal Society of Chemistry (2020) 9, pp. 337-399.
4. B. d'Acampora Zellner, P. Dugo, G. Dugo, L. Mondello, *J. Chromatogr. A* 1186 (2008) 123-143.
5. C. Cordero, J. Kiefl, P. Schieberle, S. E. Reichenbach, C. Bicchi, *Anal Bioanal Chem* (2015) 407:169–191
6. Eyres G., Marriott P., Dufour J., *J. Chromatogr. A* 1150 (2007) 1-2, 70-77.
7. D. Sciarrone, S. Pantò, C. Ragonese, P. Q. Tranchida, P. Dugo, L. Mondello, *Anal. Chem*. 84 (2012) 7092-7098.
8. D. Lamparsky, P. Schudel, *Tetrahedron. Letters* 36 (1971) 3323-3326
9. http://www.thegoodscentscompany.com
10. https://www.perfumerflavorist.com

Final conclusions

As evidenced by the studies collected in this thesis, and as it was previously reported in the cited literature, multidimensional analysis has evolved into a key method for flavours and fragrances characterisation. Specifically, the research carried out during the PhD course was focused on the full exploitation of the multidimensional concept in gas chromatography (i.e., heart-cut MDGC) for preparative and analytical purposes, combined with different detection principles (e.g., FID, qMS, IRMS, FTIR, human nose by olfactometric port).

The higher efficiency and resolution power of the heart-cut method allowed the authenticity assessment of quality markers in premium F&F materials through IRMS detection, assuring reliable results. The multidimensional concept was also extended to preparative purposes, and a triple Deans switch system was designed adopting a wide bore column set in order to achieve the isolation of target compounds from complex matrices, with high purity degree and in reasonable time. Additional efforts were put into the optimization of trapping technology and related conditions to maximize the recovery of pure fractions operating in a wide range of volatilities. Finally, the studies were dedicated to develop a proof of concept model, capable of combining olfactometry, qMS and FID as complementary yet synergic detection systems for effective odorants analysis in complex fractions. Superior analytical power and information capabilities were achieved by designed prototypal systems, implementing fundamental techniques nowadays adopted in the flavour and fragrance industry for authenticity evaluation, novel compounds elucidation and quality assessment.